DEPARTMENT WATER AND SANITATION

CHIEF DIRECTORATE WATER ECOSYSTEMS

DIRECTORATE RESERVE DETERMINATION

APPLY RELEVANT METHODS FOR GROUNDWATER AND SURFACE WATER INTERACTION FOR PROTECTION OF THE WATER RESOURCES IN THE UPPER VAAL

Draft Groundwater, Surface Water and Numerical Modelling Components of the Study.

May 2016

water & sanitation

Department:
Water and Sanitation
REPUBLIC OF SOUTH AFRICA

DEPARTMENT: WATER AND SANITATION

Directorate: Reserve Determination

APPLY RELEVANT METHODS FOR GROUNDWATER AND SURFACE WATER INTERACTION FOR PROTECTION OF THE WATER RESOURCES IN THE UPPER VAAL

WP10941

REPORT NO.: INTERNAL DRAFT REPORTS.

MAY 2016

TABLE OF CONTENTS

CONTENTS

List of Figures

List of Tables

1. GROUNDWATER COMPONENT

1.1 GEOLOGY

The study area falls in the eastern parts of the main Karoo basin (viz. Karoo Supergroup) in southern Africa and is in-filled with sedimentary strata of up to 12 km thickness and capped by a 1.4 km thick layer of basaltic lava (Woodford and Chevallier, 2002). These sediments were deposited during the late Carboniferous (354 to 290 Ma) through to Mid Jurassic (176 to 161 Ma) times. Jurassic age Karoo basalt(s) extruded onto the surface of the Karoo sediments during a period of extensive magmatic activity (183±1 Ma, Duncan, et al, 1997) The same magmatic event has generated large volumes of hypabyssal dolerite dykes and sills that shaped the geomorphology and drainage system of the Karoo basin.

A generalized profile of the Karoo Supergroup sequence in the study area is illustrated in ***Figure 1***. The rock sequence include formations of the Beaufort Group, Stormberg Group and Drakensberg Basalt capping. The formations consist mainly of thick (~500 to 1000 m) of successions of homogeneous arenaceous and argillaceous deposits from various depositional environments varying from (i) lucastrine/deltaic (Normandien Formation), formations in the north, (ii) braided river system (north) to distal meandering river facies (Tarkastad subgroup), (iii) a combination of sedimentation in a braided river plain with a few coal seams accumulated in a alluvial-plain-swamp environment (Molteno Formation), (iv) a typical "red" bed fluvial deposition facies (Elliot Formation, multi-layered 5-100m thick mudrock and 6-15m sandstones thick layers), and (v) typical playa lakes and aeolian sand dune formation deposited in a drier climate (Clarens Formation, 100 to 300 m thick).

The aquifer system over the study area is classified as an "Intergranular (or Weathered) and Fractured" aquifer type. Most of the Borehole Yields Classes falls in the "low" category, i.e. 0.1 to 0.5 l/s range in the northern quaternary catchments (C83C-J). The southern parts of quaternary catchments C83C and C83D have borehole yield classes of 0.5 to 2.0 l/s. Only a small area in the C83C Quaternary Catchment is classified as a "moderate" borehole yield class, i.e. 2.0 to 5.0 l/s (as illustrated in ***Figure 2***).

The influence of dolerite dyke/sill contacts zones normally increases the borehole yields (i.e. specific targets for water supply production), however, it seems that the water bearing characteristics of the contact zones (i.e. contact aquifers) between the host rock formations and Karoo Dolerite intrusions have not been specifically studied in the upper Beaufort, Tarkastad and Stormberg Groups. The historic borehole information set reports borehole blow test yields in the order of 5-10 l/s where dolerite rock has been intercepted at depth.

Figure 1: Karoo Supergroup Stratigraphy Column (Woodford and Chevallier, 2002)

1.2 RIVER FLOOD PLAIN ALLUVIAL AQUIFERS

Observations made during the November 2015 Groundwater Hydrocensus and historical borehole log information indicate that river flood plain alluvial deposits are present in the area. This aspect has been high-lighted by the drainage channel elevation mapping done for the surface water modelling component of the study.

The presence of alluvial deposits along the drainage channels is obvious in the lower lying reaches of the major drainage channels in the study area and reach there widest development in the lower ⅔'s of the study area up north . Based on the November 2015 and historical borehole datasets, these alluvium deposits may reach depths of 5 to 10 m in some flood plain sections (up to ~900 metres wide).

A conceptual model of a river flood plain alluvium system is presented in ***Figure 3*** below.

The diagramme indicates the actual full flow or "flood" condition in the river channel (viz. the Liebenbergsvlei main stem) which is the case most of the year; unless when maintenance of the tunnel section is performed. The principle of flood plain "bank storage" is illustrated in the water level depths indicated ① or ② in a hypothetical distribution of water boreholes situated in the flood plain zone and on the sidewalls of the drainage channel.).

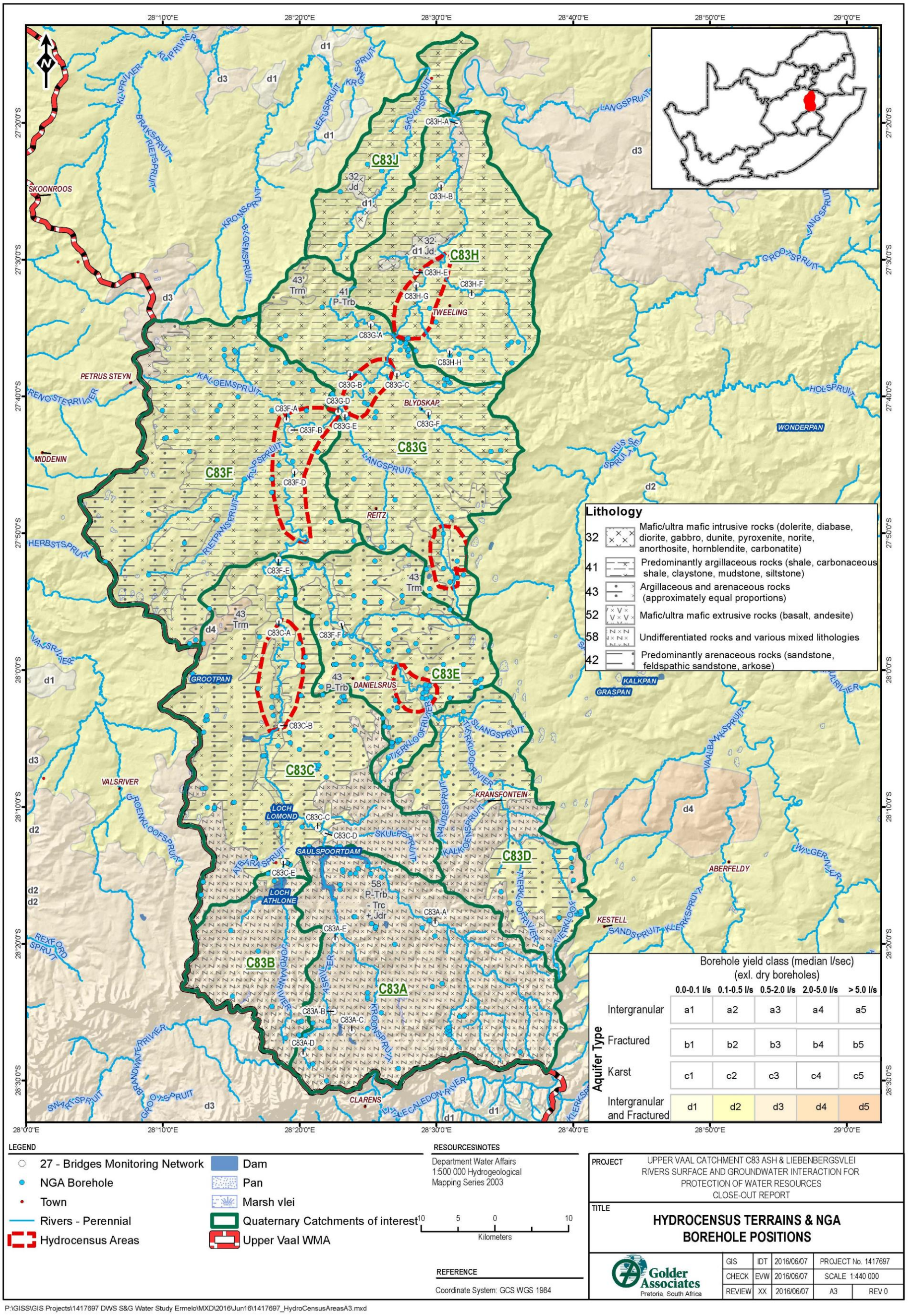

Figure 2: Hydrogeological Map of Upper Vaal Catchment C83 (QC's A to J) indicating the November 2015 Hydrocensus Terrains

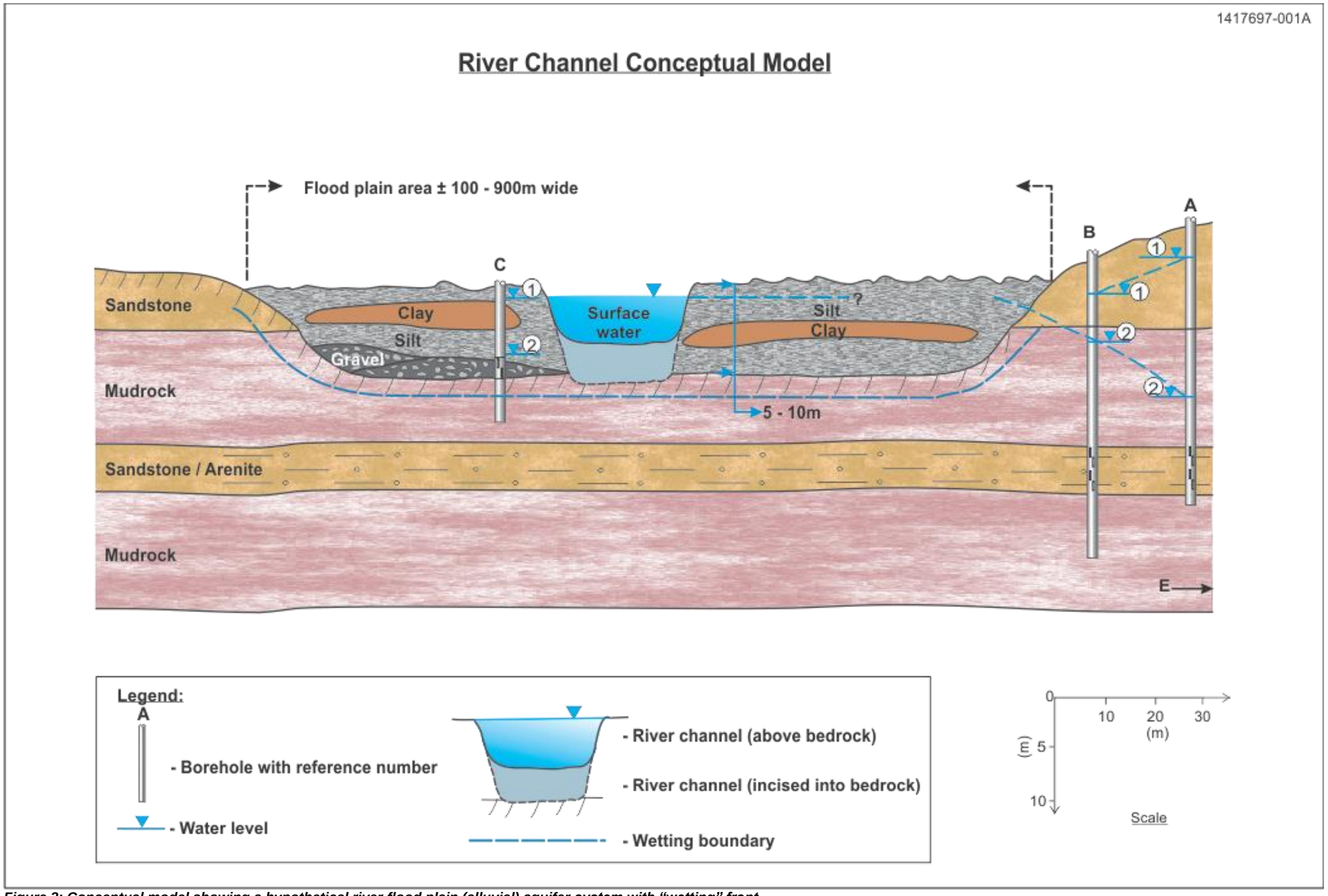

Figure 3: Conceptual model showing a hypothetical river flood plain (alluvial) aquifer system with "wetting" front.

The behavior of the groundwater level in the sidewall zone of the drainage channels predict whether the surface water system is a gaining or losing one.

Interpretations of historical water level data (DWS's National Groundwater Archive) indicate that the groundwater level elevations are following the natural ground elevations (see section 3.5); thus near the drainage channels the groundwater gradients are directed towards the drainage channels – i.e. condition A① – B① in ***Figure 3*** above. This condition has been noted during the November 2016 groundwater hydrocensus along the main stem system on the farm Violet No 660.

The above-mentioned observation, however, does not imply that this condition is value throughout the study area. There are areas where the river flood plain alluvium is not present, i.e. where the river channel flows directly on the basement rock formation whether it may be Karoo sediments or Karoo dolerite (i.e. remains of large andulating sills). This condition is illustrated in ***Figure 3*** (inset) showing the river channel cuts through the flood plain alluvial directly into the basement hard rocks.

The extent of the river flood plain alluvial deposits varies significantly throughout the study area as well as in thickness and lateral distance from the current drainage channel itself. There are areas, especially in the headwater regions of the Jordan, Ash and Liebenbergsvlei Rivers (QC's C83A and –B), where several stream rapids occur, and alluvial deposits are not present.

The occurrence of the river flood plain alluvial deposits is indicated in

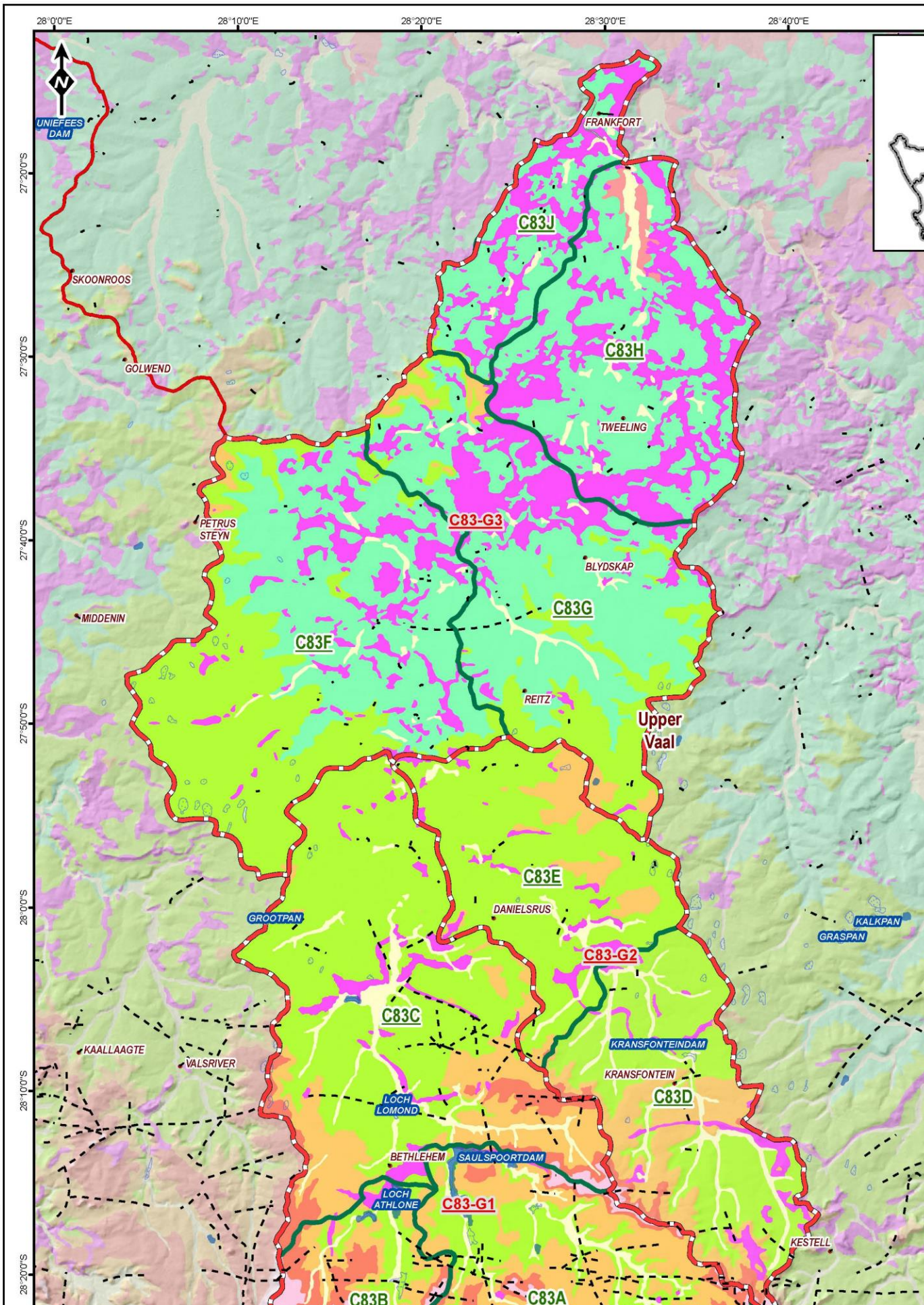

Figure** 4.**

It has been noted during discussions with the local members of the Project Steering Committee Meeting (November 2015) at Daniëlsrus (see ***Figure 2***) that significant scouring of the Ash River channel due to the high flow velocity since the LHTS came in operation, is resulting in fine sedimentary (probably silt) deposits piling up in the upstream parts of the Sol Plaatje Dam (Ash River branch) near Bethlehem. These fine, muddy sediments may cause build-up of an impermeable "liner" in the lower reaches of the Liebenbergsvlei River decreasing the hydraulic connectivity between local groundwater sources and surface water body.

1.3 GROUNDWATER MANAGEMENT UNITS

Due to the similarities between aquifer systems over large areas, they may be grouped together in resource units with a specific set of management protocols – these units are then regarded as groundwater management units or GMU's.

The northern part of the study area (QC's ½C83F-north, –G, –H and –J) is associated with the rocks (mudstones/sandstone) of the Normandien Formation (i.e. the Adelaide Subgroup), which shows a significantly higher density of dolerite intrusions (especially dolerite sill structures) in comparison to the central and southern parts (mostly sub-vertical dolerite dykes) of the study area associated with younger Karoo Supergroup rocks, see

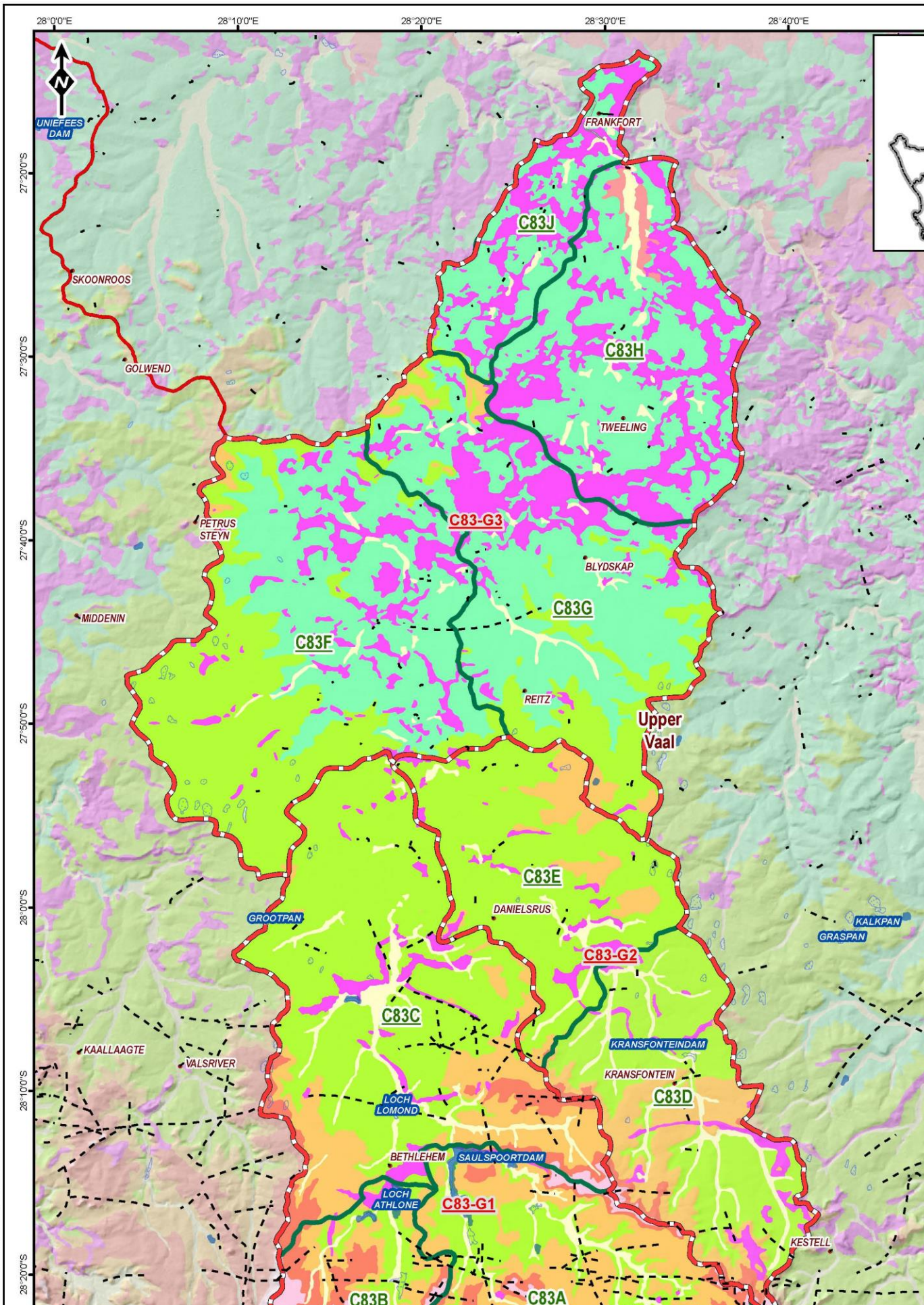

***Figure** 4*.

The central part of the study area (QC's ½C83F-south, –E, –C and –D) is associated with rocks (arenaceous sandstone and argillaceous mudstone) of the Katberg and Burgersdorp Formations (i.e. the Tarkastad Subgroup) with elevated areas (koppies) in the C83 QC capped by Molteno Formation rocks (viz. lower formation of the Stormberg Group: sandstone, conglomerate and mudstone).This part has much less dolerite rocks present although a few large dykes are present in the southern part (½) of QC C83C.

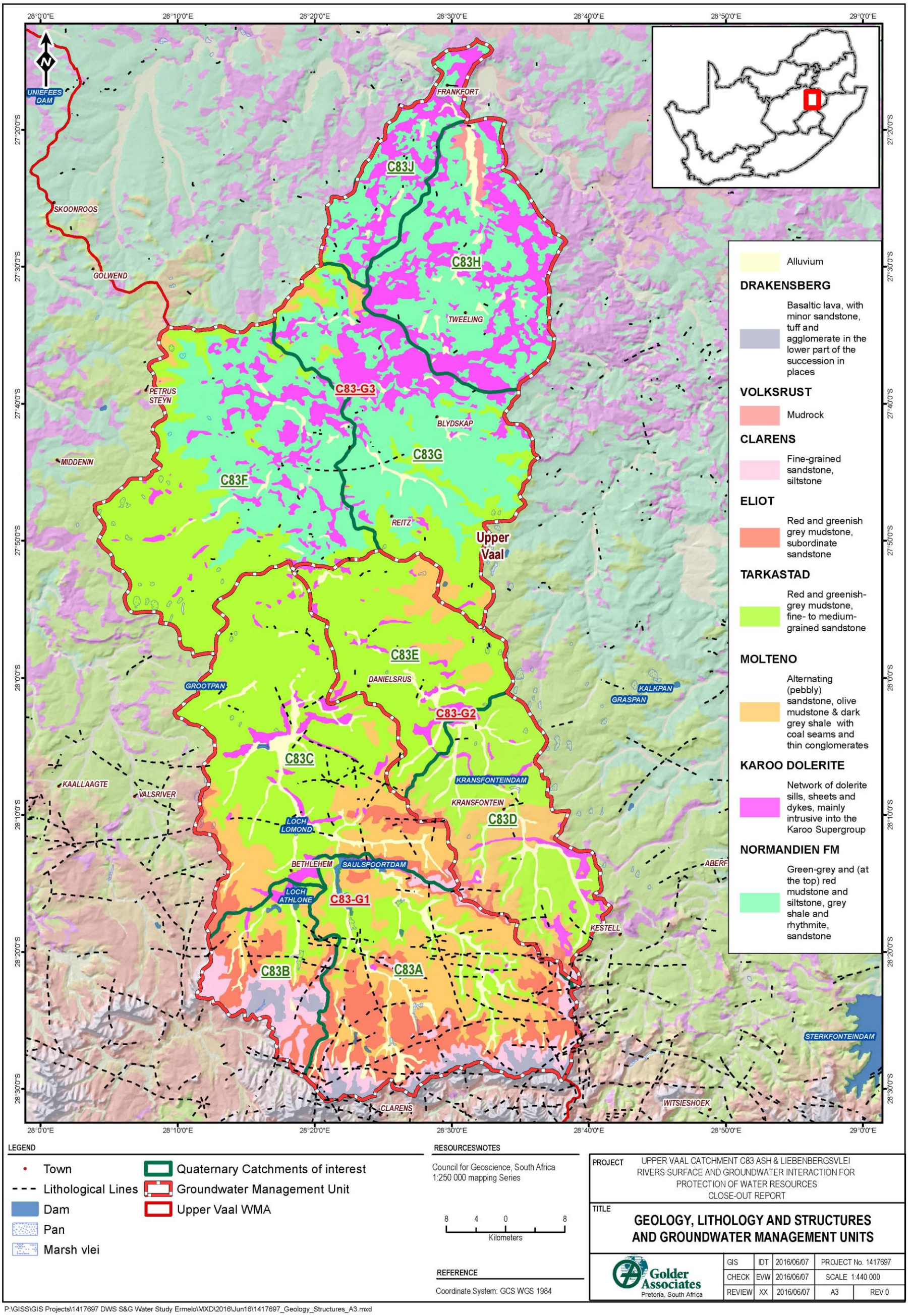

Figure 4: Occurrences of river flood plain alluvial deposits.

The southern part of the study area (QC's C83A and –B) is associated with rocks of the upper facies of the Karoo Supergroup and Karoo Basalt capping. The sequence is as follows: lower Molteno Formation (sandstone, conglomerate and mudstone), the middle Elliot Formation (mudstone and subordinate sandstone) and the upper Clarens Formation (massive, aeolian sandstone). Only the extreme elevated southern parts of the southern part is capped with basalt rocks (viz. Drakensberg Volcanics (see ***Figure 4*** above).

The rock formations throughout the study area profile consists mainly of similar primary hydraulic characteristics as classified by borehole yield classification (based on borehole yields logged during drilling operations). Thus, a hydraulic classification into groups of GMU's based on the primary hydro-lithological characteristics will not be feasible, however, based on the presence of secondary aquifer systems presented by the intrusive Karoo dolerite dykes and sills allows one to demarcated between three possible groundwater units as indicated in Table 1 below

Secondly due to the similarity between the different primary rock formations in the area (viz, multi-layered arenaceous sandstone and argillaceous mudrocks), hydraulic differentiation in the study area is not feasible. However, in terms of secondary aquifers as a result of the presence of Karoo dolerite intrusions in the study area, and thus the presence of contact aquifer systems especially in the contact aureole, a demarcation between three hypothetical GMU's could be drawn (see Table 1) and they are as follows:

- C83–G1: C83A, C83B and C83C – Stomberg Group - based on the presence of several regional dolerite dykes and virtually no Karoo dolerite sill features (BYC: Moderate);
- C83–G2: C83D and C83E – Mainly Tarkastad Subgroup (mudstone and sandstone) and limited Karoo dolerite sills (BYC: Low); and
- C83–G3: C83F, C83G, C83H and C83I – Mainly Adelaide Subgroup (Normandien Formation: mudstone, siltstone shale and sandstone) with high Karoo dolerite sill coverages (BYC: Low to Insignificant.)

The river flood plain alluvial aquifer system represents a forth hydrogeological unit (or possible GMU) in the study area and probably the most important link with the surface water resource. Based on the conceptual flood plain alluvial system (see section 1.2) interaction between a surface water source and the flood plain alluvial aquifer system can be based on six different scenarios, as illustrated in ***Figure 5*** below.

Based on the available geological information, the November 2015 hydrocensus survey and field reconnaissance in the study area, the hydrogeological conditions in the surface water – groundwater interface (viz. the river flood plain alluvial) can be correlated with Scenarios 1 and 3 as illustrated in *Figure **5***.

In the case of Scenario 1: The Regional Aquifer is a mixture between fine grained, arenaceous sandstones and mudrock with a moderate diffusivity (viz. the ration between aquifer media permeability and storativity, or T/S) based on the BYC values (low to insignificant yields). The "valley train" consists of a fine grained silt/mudstone filling with insignificant diffusivity, i.e. what we interpret as the river flood plain alluvial aquifer.

In the case of Scenario 3: The river flood plain alluvial aquifer is absent and the drainage channel lies directly on the regional aquifer system with moderate diffusivity. One special case here is where the main stem drainage channel runs over large dolerite sills, or barren basement rocks as visible in

QC C83F, –G and –H (see

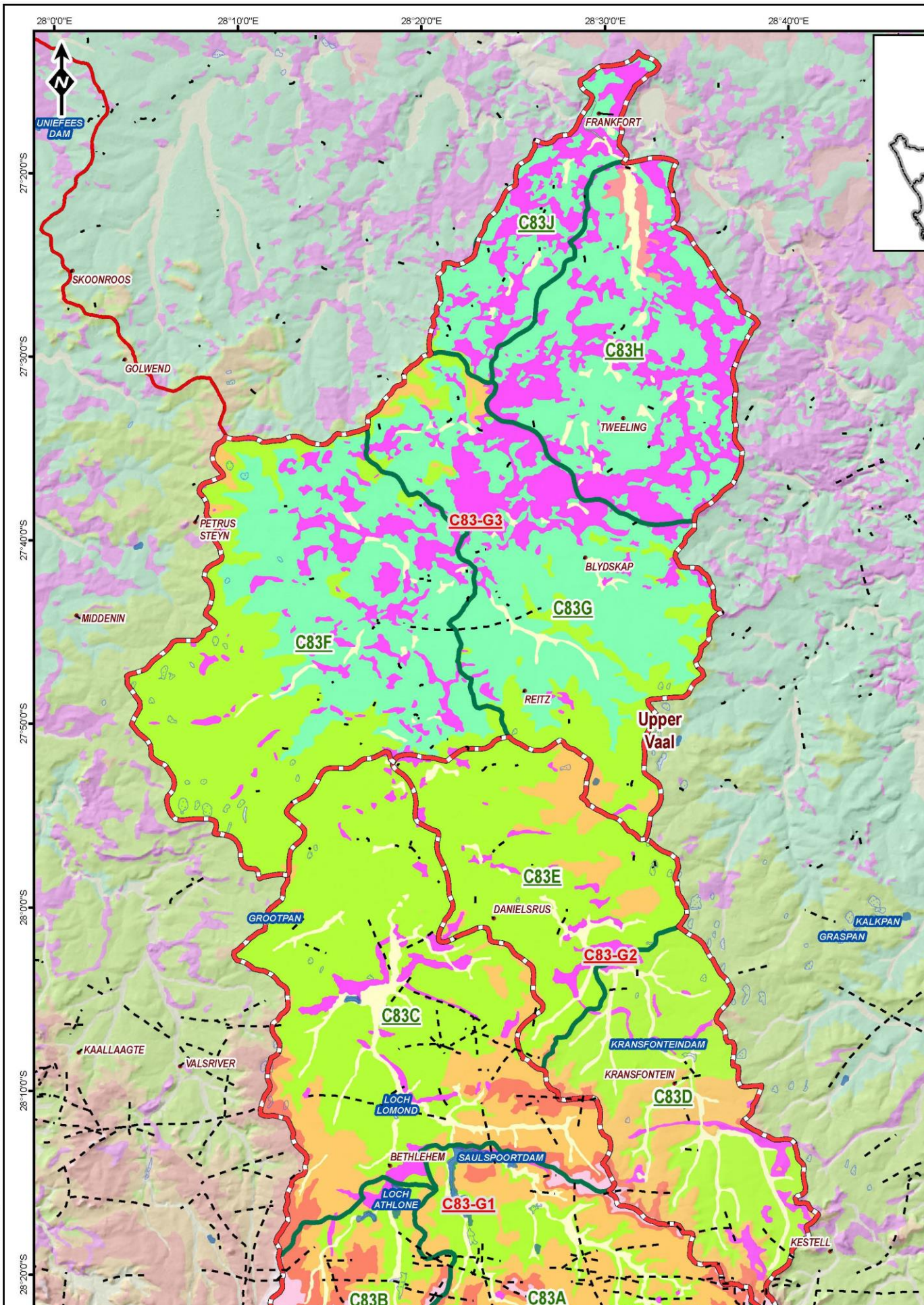

***Figure** 4*). This site will be earmarked for future investigations, viz. a specific monitoring network to investigate the interaction between the surface water and the groundwater involving an underlying "strip aquifer system". The number of such cases are actually limited in the study area.

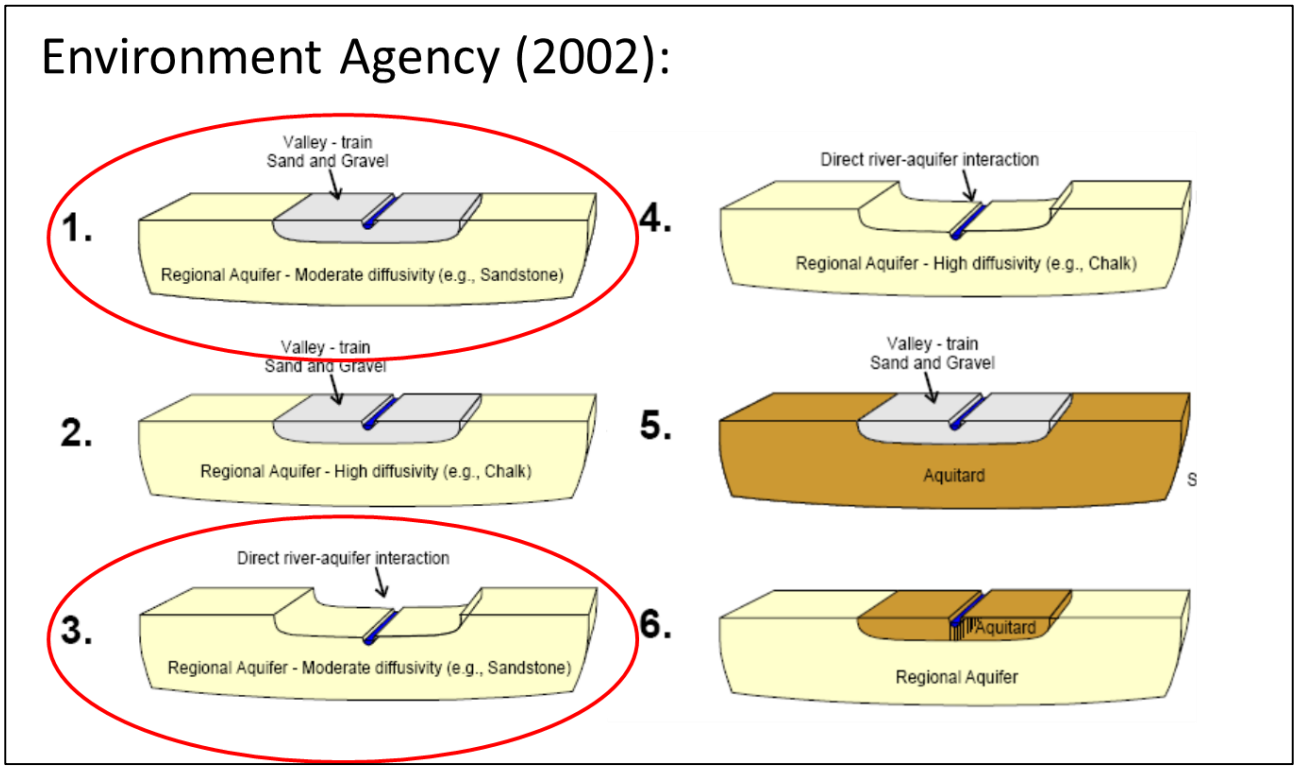

Figure 5: Six potential surface water – groundwater interaction scenarios.

1.4 LAND USE ACTIVITIES IN THE STUDY AREA

The major land use activities in the study area is listed in Table 1 below.

Most of the activities focus on dry land cultivations. Pivot driven irrigation schemes are present along the main stem, obviously using water. . It is especially in the downstream area of the C83F-A QC where pivot irrigation occurs (i.e.17 by 51 ha' size pivots).

The irrigation practices are probably in operation since the start of the L:HTS. Pre 1996 LHTS flows in the main stem would probably be too low to sustain long-term abstraction from the surface drainages.

Of particular importance is the moderate to high level of dry land cultivations, and stock farming. Several pivot irrigations systems are present in the study area, however the large majority (~95%) is supplied by surface water resources from the main stem and a small percentage from local dams and depressions (probably pans) containing surface water runoff.

Several local irrigations pivots are situated along the Main Stem system at the outflow area of Quaternary Catchment C83F (west of Reitz and with waste water discharges from the Reitz WWTW, could be ranked as probably the most critical stretch of the Liebenbergvlei River after the discharges from the Bethlehem area (specifically the Jordan River).

A large bank of waste water evaporation dams occur just north of Reitz which is also regarded as a waste treatment works, discharging to a small drainage system leading to the Langspruit where serious levels of organic pollution has been noted in the 27-Bridges Monitoring Programme, for

example at monitoring site C83G-E.

The WWTW at Tweeling is situated in a local drainage system which seems to "dry-out" long before it reaches the Main Stem Liebenbergsvlei River ~7.5 km further downstream.

Two waste water treatment facilities (probably of low level treatment status – removal of sludge) are present at Frankfort, both discharging directly into the Wilge River.

Not many high level water borne industrial activities occurs in the study area. Only two broiler chicken farms have been spotted from the satellite imagery and is situated close to Tweeling and Reitz. The former seems to discharge industrial water into a small "pooled" drainage running directly to the Main Stem Liebenbergsvlei River about 2.62 km towards the west. Although his is a potential threat for water quality of the main stem system; significant dilution of any local, poor quality discharges with large volumes of LHTS water, is taking place.

The most prominent chicken farm occurs just south of Reitz. No direct linked water discharge into local drainage could be noted here, although their discharges could be piped to the Reitz waste water evaporation dams discussed above.

To conclude in terms of land use activities, several small dams have been constructed in the tributaries of the study area. These constructions have an impact of the through flows during drier seasons preventing "natural flushing" of these drainages. Taking cognizance of the current high volume water release from the LHTS in the main stem, these dams are playing an important role in terms of controlling high catchment runoff events and subsequently protecting to main stem systems from severe flooding, especially in the low-lying northern region, i.e. QC's C83H, C83G and specifically C83E (e.g. the Tierkloof River catchment).

Table 1: Proposed Groundwater Management Units with Geological Formations, Hydrogeological Characteristics and Land Use Activities

GMU No. (*Quaternary Catchments*)	**Supergroup/Group/*Subgroup/Formation1-Formation2.***	**Formation**	**Aquifer Type**	**Hydrogeological characteristics and major land use activities.**
GMU C83-G1: *C83A and C83B*	**Karoo**/Drakensberg/*Clarens-Elliot-Molteno Formations/Tarkastad Sbgrp in major incised river channels* **Intrusive rocks**: Major Karoo Dolerite Dykes: ~10-15 km's long.	Basaltic lava/ Sandstone, siltstone-; Mudstone, (sandstone)-; Sandstone, mudstone and shale/; Mudstone, arenite.	Intergranular and fractured.	Gwater Quality: <70 mS/m; Borehole Yield Class: 0.5 to 2.0 l/s. **Major Land Use Activities:** **1. Irrigation downstream of Miemiesrust Dam;** **2. Various isolated irrigation practices from local depressions (Sw);** **3. Pivot irrigation upstream from Sol Plaatje Dam;** **4. Quarrying upstream of the Loch Athlone Dam (dry pits); and** **5. Intensive land irrigation upstream from Gerrands Dam upstream from Bethlehem.**
C83C	**Karoo**/*Clarens-Elliot-Molteno Formations/Tarkastad Sbgrp* **Intrusive rocks**: Major Karoo Dolerite Dykes, <10 km long.	Sandstone, siltstone-; Mudstone, (sandstone)-; Sandstone, mudstone and shale/; Mudstone, arenite.	Intergranular and fractured.	Gwater Quality: <70 mS/m; Borehole Yield Class: 0.1 to 0.5 l/s (~75%); Borehole Yield Class: 0.5 to 2.0 l/s (<20%); Borehole Yield Class: 2.0 to 5.0 l/s (<5%). **Major Land Use Activities:** **1. Bethehem with large local industries;** **2. Kromkloof North and Eden Small Holdings, probably with pit latrine sanitation;** **3. Pivot irrigation just west of the Loch Lomond Dam site – Return water concern via local aquifer systems;** **4. Isolated pivot irrigation systems (4) along the Main Stem below the Loch Lomond Dam;** **5. Moderate level (~50% of farm land area) of dry land farming; and** **6. Bethehem Waste Water Treatment Works discharging into Main Stem.**
GMU C83-G2: C83D	**Karoo**/*Molteno Formation/Tarkastad Sbgrp* **Intrusive rocks**: Minor Karoo Dolerite Sills: <5 km long.	Sandstone, mudstone and shale/; Mudstone, arenite.	Intergranular and fractured.	Gwater Quality: <70 mS/m; Borehole Yield Class: 0.1 to 0.5 l/s (~80%); Borehole Yield Class: 0.5 to 2.0 l/s (~20%). **Major Land Use Activities:** **1. Mainly dry land farming; and** **2. Stock farming.**

GMU No. (*Quaternary Catchments*)	Supergroup/Group/*Subgroup/Formation1-Formation2.*	Formation	Aquifer Type	Hydrogeological characteristics and major land use activities.
C83E	**Karoo**/*Molteno Formation/Tarkastad Sbgrp* **Intrusive rocks**: Minor Karoo Dolerite Dykes, <2.5 km long. Karoo Dolerite Sills become more prominent.	Sandstone, mudstone and shale/; Mudstone, arenite.	Intergranular and fractured.	Gwater Quality: <70 mS/m; Borehole Yield Class: 0.1 to 0.5 l/s. **Major Land Use Activities:** **1. High level >75% of farm area) dry land farming;** **2. Isolated pivot irrigation from local water filled depressions; and** **3. Irrigation activities along the Tierkloof River from local water filled depressions.**
GMU C83-G3: C83F	**Karoo**/*Tarkastad Sbgrp/Normandien Formation.* **Intrusive rocks**: Major Karoo Dolerite Sills: ~15% 0f area.	Mudstone, arenite/; Mudstone and siltstone, shale, rhythmite and sandstone.	Intergranular and fractured.	Gwater Quality: <70 mS/m; Borehole Yield Class: 0.1 to 0.5 l/s. **Major Land Use Activities:** **1. Several (~10) irrigation pivots below the main stem confluence with the Kaloemspruit and the Klipspruit – irrigation return water concern;** **2. High level (>75% of dry land farming on farm areas);** **3. Isolated pivot irrigation systems in the upstream areas near local dams in the surface water drainages;** **4. Intensive irrigation system (viz. apples) near Main Stem, i.e. on the farm Violet 660;** **5. Reitz WTW next to Main Stem and DWS Gauging Station; and** **6. Several pools of standing water in the non-perennial drainages.**
C83G	**Karoo**/*Molteno Formation/* Beaufort Spgrp/*Tarkastad Sbgrp./Normandien Formation.* **Intrusive rocks**: Large Karoo Dolerite Sills become more prominent (~20% of the area).	Sandstone, mudstone and shale/; Mudstone, arenite/; Mudstone and siltstone, shale, rhythmite and sandstone.	Intergranular and fractured.	Gwater Quality: <70 mS/m; Borehole Yield Class: 0.1 to 0.5 l/s. **Major Land Use Activities:** **1. Town of Reitz/Petsana;** **2. Chicken Broiler Farm;** **3. Several local dams in the Langspruit;** **4. Waste water dams just north of Reitz discharging into local drainage system;** **5. Mostly dry land cultivations at < 75% of farm land area; and** **6. Several irrigation systems along the main stem just south of DWS Gauging Station C8H020 – this is an concern for the level of irrigation return flows into the local groundwater and altimately into the main stem drainage.**

GMU No. (*Quaternary Catchments*)	Supergroup/Group/*Subgroup/Formation1-Formation2.*	Formation	Aquifer Type	Hydrogeological characteristics and major land use activities.
C83H	**Karoo**/Beaufort/*Adeliade & Escourt Spgrp/Normandien formation*/Ecca/*Volksrust Formation.* **Intrusive rocks**: Regional Karoo Dolerite Sills become more prominent (~20% of the area).	Mudstone and siltstone, shale, rhythmite and sandstone/; Mudrock.	Intergranular and fractured	Gwater Quality: <70 mS/m; Borehole Yield Class: 0.1 to 0.5 l/s (~97%); Borehole Yield Class: 0.5 to 2.0 l/s (~3%). **Major Land Use Activities:** **1. Town of Tweeling (WWTW);** **2. Several irrigation pivot systems just above the Main Stem confluence with the Wilge River – obtaining water from the main stem channel;** **3. Dry land cultivation <50% of farm land area; and** **4. A few small dams in local drainages and may have a local impact of catchment runoff..**
C83J	**Karoo**/Beaufort/*Adeliade & Escourt Spgrp/Normandien formation*/Ecca/*Volksrust Formation.* **Intrusive rocks**: Regional Karoo Dolerite Sills become more prominent (~20% of the area).	Mudstone and siltstone, shale, rhythmite and sandstone/; Mudrock.	Intergranular and fractured	Gwater Quality: <70 mS/m; Borehole Yield Class: 0.1 to 0.5 l/s (~97%); Borehole Yield Class: 0.5 to 2.0 l/s (~3%). **Major Land Use Activities:** **1. Town of Frankfort, along the Wilge River System;** **2. Significant industrial developments, probably linked to local waste water reticulation systems;** **3. Cemetery and waste water dams/outlet into Wilhge River upstream of town lands (seems to be limited aeriation treatment);** **4. WWTW just north of the town with discharges into small drainage leading into the Wilge River 1.25 km downstream – this is a concerned situation.** **5. Several small dams were constructed in the Skulpspruit – limited impact on local catchment runoff.;** **6. Pivot irrigation taking water from the Wilge River developed between the confluences of the Liebenbergsvlei-Wilge River and the Skulpspruit-Wilge River; and** **7. >75% dry land farming**

1.5 WATER RESOURCES QUALITY COMPARISONS

Water quality analyses of the water resources in the study area are limited to bi-weekly analysis at four (4) of the DWS Gauging Stations along the main stem at the following stations:

- C8H036 Upper Ash River @ LHTS Tunnel Outfall site;
- C8R004 Liebenbergsvlei@ Sol Plaatje Dam discharge site;
- C8H020 Liebenbergsvlei @ Roodekraal gauging site; and
- C8H026 Liebenbergsvlei @ Frederiksdal gauging site.

No water quality analyses were available from the tributaries in the study area. Due to the possibility that the base flows in the tributaries could derive from local groundwater resources, a monitoring programme was initiated right at the start of the study to capture the surface water quality component.

Two sample runs (6-9 July'15 and 17-19 August'15) were conducted at sixteen surface water points along the Ash and Liebenbergsvlei Rivers and selected tributaries. The analyses results are illustrated on Piper Diagramme plots in *Figure **6***.

The surface water samples suggest generally a fresh, calcium-magnesium-bicarbonate (Ca-Mg-HCO3) water facies (left quadrant of the "diamond" field plot). Such water type indicates a dominance of rainwater chemistry (recently recharged), with limited weathering reactions and CO_2 equilibrium with the atmosphere and soil vapour (elevated CO_2 due to decomposition of organic material) to form the dominant bicarbonate anion. In other words, the surface water chemistry is not significantly influenced by deeper groundwater contributions – probably a much lower contribution or not linked due to the fine – ultra-fine sediment types (thick mudrock layers).

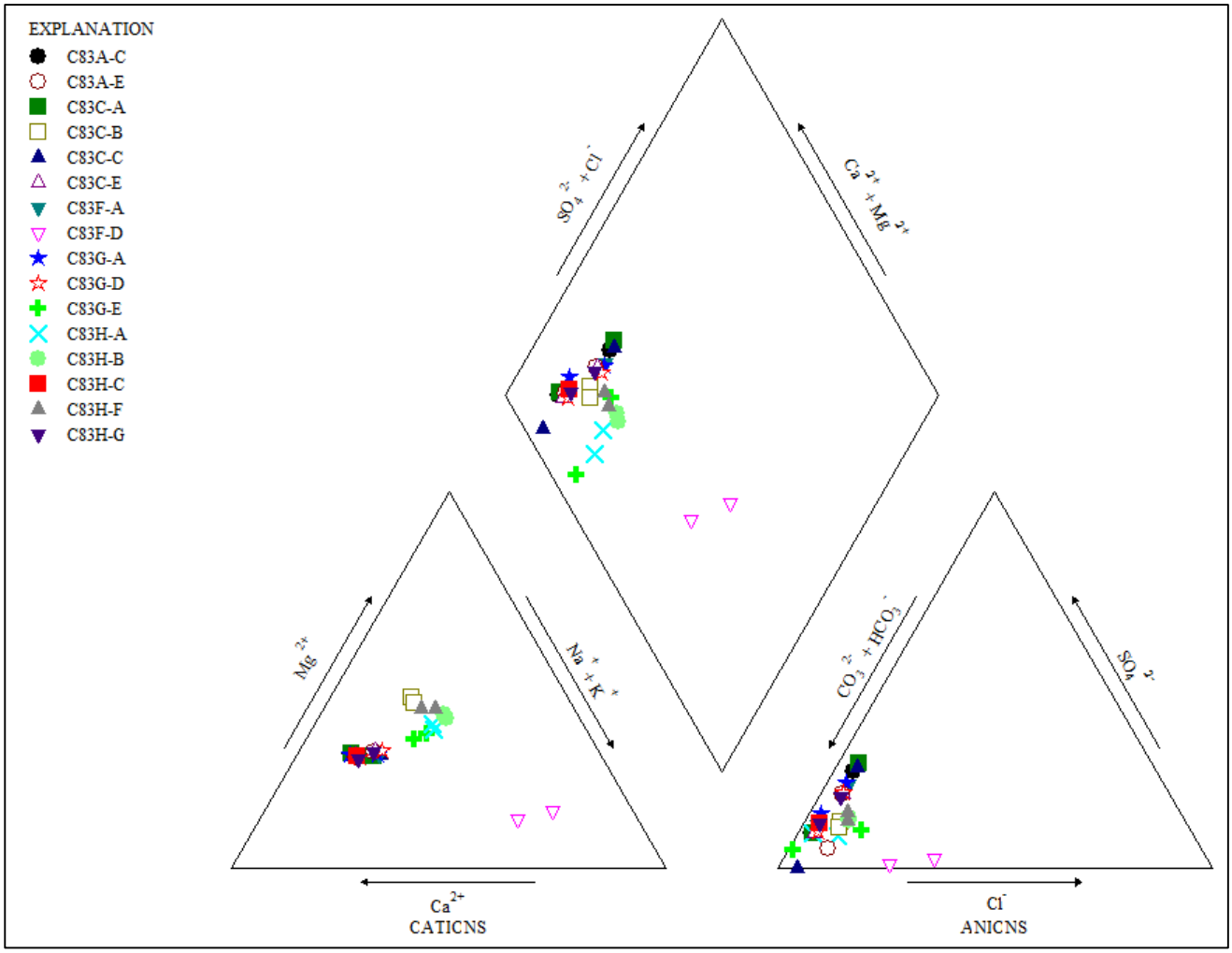

Figure 6: July and August 2015 surface water Piper Diagramme plots.

The plot positions of monitoring site C83G-E, however, falls towards a more saline water type– this is a sample from the surface water at the time of monitoring in the Langspruit downstream of the town of Reitz (QC C83G). The water quality at this specific site shows relatively elevated levels of Sodium (75mg/l Na) and Chloride (78 mg/l Cl) whereas these concentrations in the other tributaries are much lower, viz. mean values for Sodium = 27.0 mg/l and Chloride = 15.7 mg/l. Surface water quality in the Landspruit is a concern as elevated concentrations of dissolved Iron (583 µg/l), dissolved Manganese (1977 µg/l) and dissolved Phosphorus (15870 µg/l) have been noted in the August 2015 water quality analysis .

Piper Diagramme plots of the groundwater chemistry from the November 2015 hydrocensus survey (18 boreholes) is illustrated in ***Figure 7*.**

While generally higher mineralised than the surface water samples, most groundwater samples can still be described as an Ideal to Good quality (ground)water, which had limited time to equilibrate with the aquifer material along its flow path. The dominant calcium-magnesium-bicarbonate (Ca-Mg-HCO_3) water facies shown in the Piper plot might be a result of:

- The recently recharged groundwater chemistry (driven by infiltrating rainwater), limited weathering reactions and CO_2 equilibrium with the atmosphere and soil vapour for boreholes

within the weathered aquifer further away from surface waters (mostly on the flood plain slopes), or

- Hydraulic interaction with surface water for boreholes located in the alluvial aquifer next to the river.

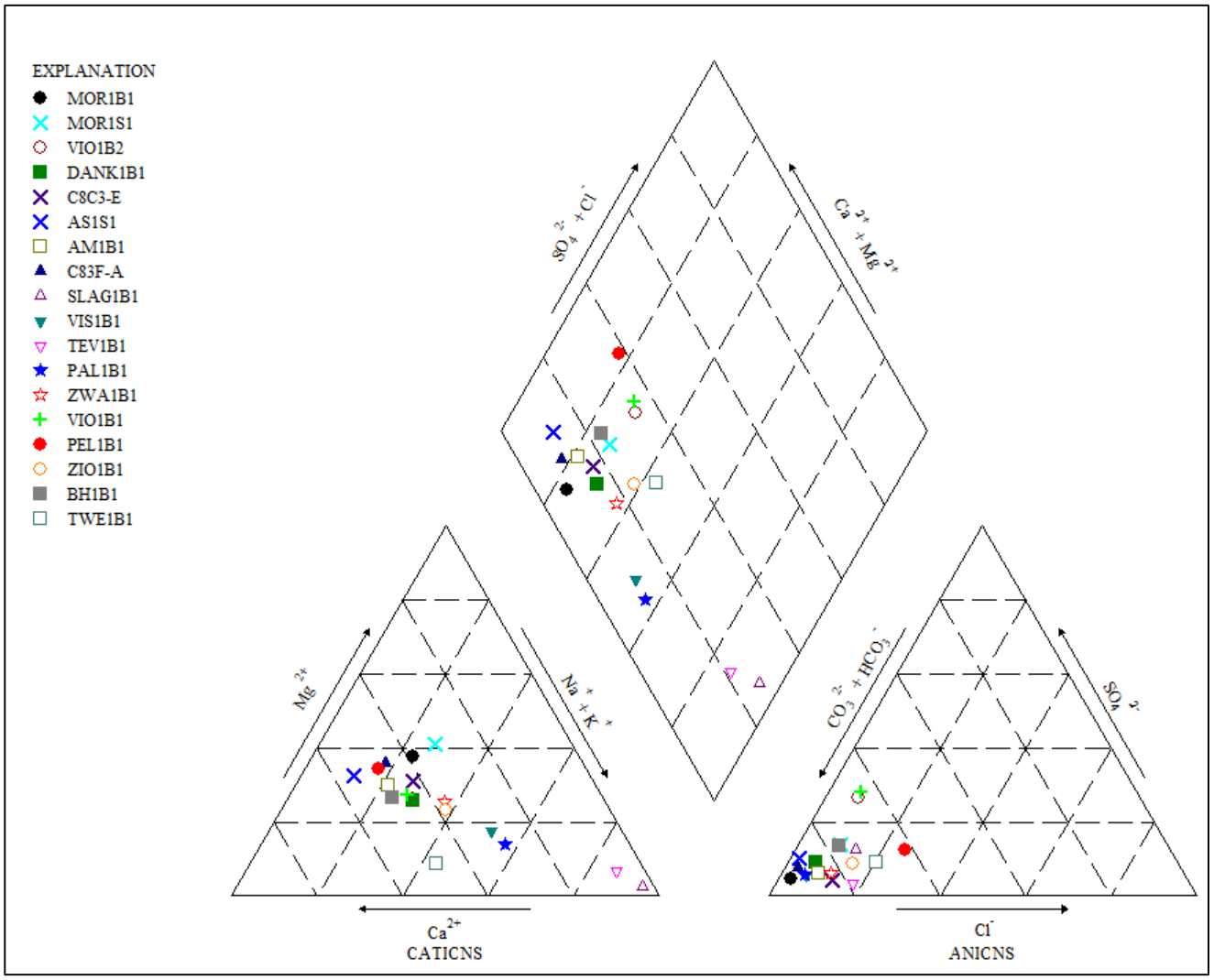

Figure 7: November 2015 groundwater hydrocensus boreholes Piper Diagramme plots.

The distance between the current river channel and the hydrocensus borehole position has no relevance to the plot position on the Piper Diagramme. Most of the boreholes that plot on the left side of the "diamond" field plot varies between 13 m (borehole VIO1B1) and ~800 m (borehole DANK1B1) from the main stem of the Liebenbergsvlei River.

The four boreholes plotting in the lower section of the "diamond" field varies between 90 m (borehole TEV1B1) and ~400 m (boreholes SLAG1B1 and VIS1B1) and 1700 m (borehole PAL1B1). There are therefore no definite hydrochemical correlations between surface water and groundwater at distances >50 m from the river channel. The reason is probably due to different groundwater stratification in the basement rock types and limited natural interaction between the surface and distant groundwater resources (viz. <50 m) from the river flood plain.

To conclude, the variation between the surface water quality (fresh mountain water from the LHTS) and the local groundwater is insignificant to apply the analytical modelling approach. Due to the

diurnal water quality (TDS, salinity as per the Diurnal Monitoring Dataset) changes in the main stem channel being larger than the observed water quality variation (as per the 27 Bridges Monitoring Network), application of the analytical modelling method could therefore not be used in identification of significant groundwater contributions to the surface water component.

Several of the 27 Bridges Monitoring Network's sites were revisited during a short monitoring run in April 2016, which should have been under the final "wet cycle" of the 2015-2016 Hydrological Cycle (Oct_{2015} to $September_{2016}$) under "normal" climate conditions.

The monitoring results indicated the following aspects of the system (reference used August 2015 datasets):

- No change in the EC-TDS values of the Main Stem Liebenbergsvlei (LHTS) between the LHTS Outfall and the Liebenbergsvlei-Wilge River Confluence (viz. 10 vs 9 mS/m);
- Minor changes in the EC-TDS values on the main tributaries, however, some degree of dilution were noted in Langspruit (~87 down to 64 mS/m), but others such as deteriorated slightly (viz. 56 to 62 mS/m).
- Water levels in the November 2015 Hydrocensus Survey boreholes have slightly risen (i.e. ~0.50 to 1.0 m); and
- Groundwater quality changes between Nov'15 and Apr'16 are highly variable, but it should be noted that on the farm Violet, it seems that the water quality has deteriorated in two boreholes situated close to the Main Stem Liebenbergsvlei – although the resulting quality (April 2016) is still classified as Ideal to upper Good Quality water.

To conclude, the overall water resources quality in the study area falls in the Ideal and Good quality water category, however, during the study, it has been noted that those tributaries linked with towns and their waste water treatment works, are causing specific dissolved constituents (viz. PO_4) to rise to unacceptable levels, i.e. Langspruit System.

2. SURFACE WATER ASSESSMENT: QUARTER 4/'16

2.1 SURFACE WATER FLOWS

To support the surface water modelling work required for the surface-groundwater interaction study along the Liebenbergsvlei, a large amount of data was collated and analysed. The initial analysis of the data was performed to identify any gaps as well as improve the understanding of the raw data. This data was further applied when calibrating the surface water numerical model, which was developed using the HEC-RAS (River Analysis System) software. This software was developed by the US Army Corps of Engineers and is freely available for download.

2.2 FLOW MONITORING STATIONS

A number of active and inactive flow monitoring stations within the catchment were identified and the raw data sourced from the DWS Hydrology website (DWS, 2015). The metadata for these stations are provided in Table 2 below and the locations are indicated in ***Figure 8***.

Table 2: Flow Monitoring Stations

Station ID	Name	Start Date	End Data	Updates of Rating Table
C8H036	Ash River (Tunnel @ Outlet from Katse)	Dec 1997	Active	Sept 1997
C8R005	Jordaan River @ Loch Athlone	Dec 1971	May 2015	Jun 1971
C8R004	Liebenbergsvlei @ Sol Plaatje Dam	Jun 1971	Nov 2009*	June 1971, Nov 2009
C8H007	Liebenbergsvlei @ Vogelfontein	Dec 1964	Mar 1978	Dec 1964
C8H037	Liebenbergsvlei @ Reward	Jun 1998	Active	Jun 1998
C8H004	Liebenbergsvlei @ De Molen	Mar 1957	Jan 1996	Mar 1957, Oct 1965
C8H020	Liebenbergsvlei @ Roodekraal	Oct 1974	Active	Oct 1974, Jul 1987
C8H026	Liebenbergsvlei @ Frederiksdal	Mar 1985	Active	Mar 1985, April 1998
C8H001	Wilge River @ Frankfort	Oct 1913	Active	Jun 1962 (last update)

*Rating unreliable thereafter

Discharge from the Katse Dam Tunnel started in January 1996. It was decided to analyse the data after this change thus the period analysed starts in October 1998 (beginning of the next hydrological year) and runs through to September 2009, where after the data for the Sol Plaatje Dam discharge becomes unreliable. Photos of the weirs used were sourced from the DWS website and are provided in ***Figure 9***.

The stations at the Tunnel outlet, Reward and Frederiksdal all have fairly recent rating curves that should ensure relative accurate measurements over the time period analysed. Sol Plaatje Dam, Roodekraal and the Wilge River station should have their rating curves re-assessed; for the purpose of this analysis the measurements are assumed to be sufficiently accurate.

2.3 FLOW DATA ANALYSIS

2.3.1 FLOW STATISTICS

Monthly average flow rates were sourced for each station from the DWS Hydrology website (https://www.dwa.gov.za/Hydrology) for the period October 1999 to September 2009. These average flow rates are shown in Table 3 and presented graphically in ***Figure 10*****.** As expected the flow rates in the Wilge River follow a season pattern with increased run-off being generated during the wet season and reduction of flow taking place over the dry season.

The flow rates in the Ash River and Liebenbergsvlei do not follow this pattern due to the significant discharge from the tunnel outlet. It is interesting to note the increase in flow rate as you move downstream during the wet season, caused by the catchment runoff, compared to the fairly constant flow rate along the river during the dry season.

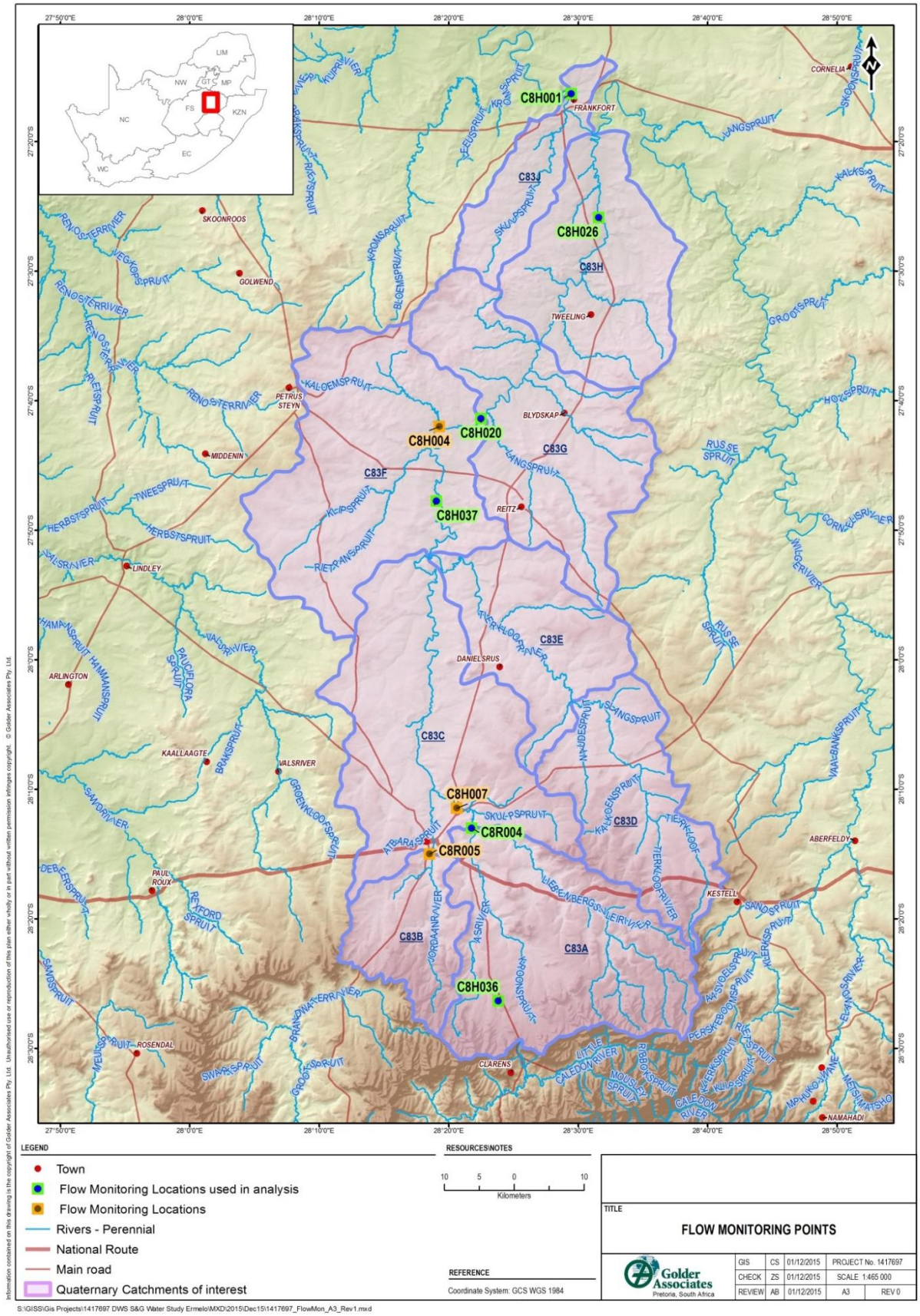

Figure 8: Flow Monitoring Locations

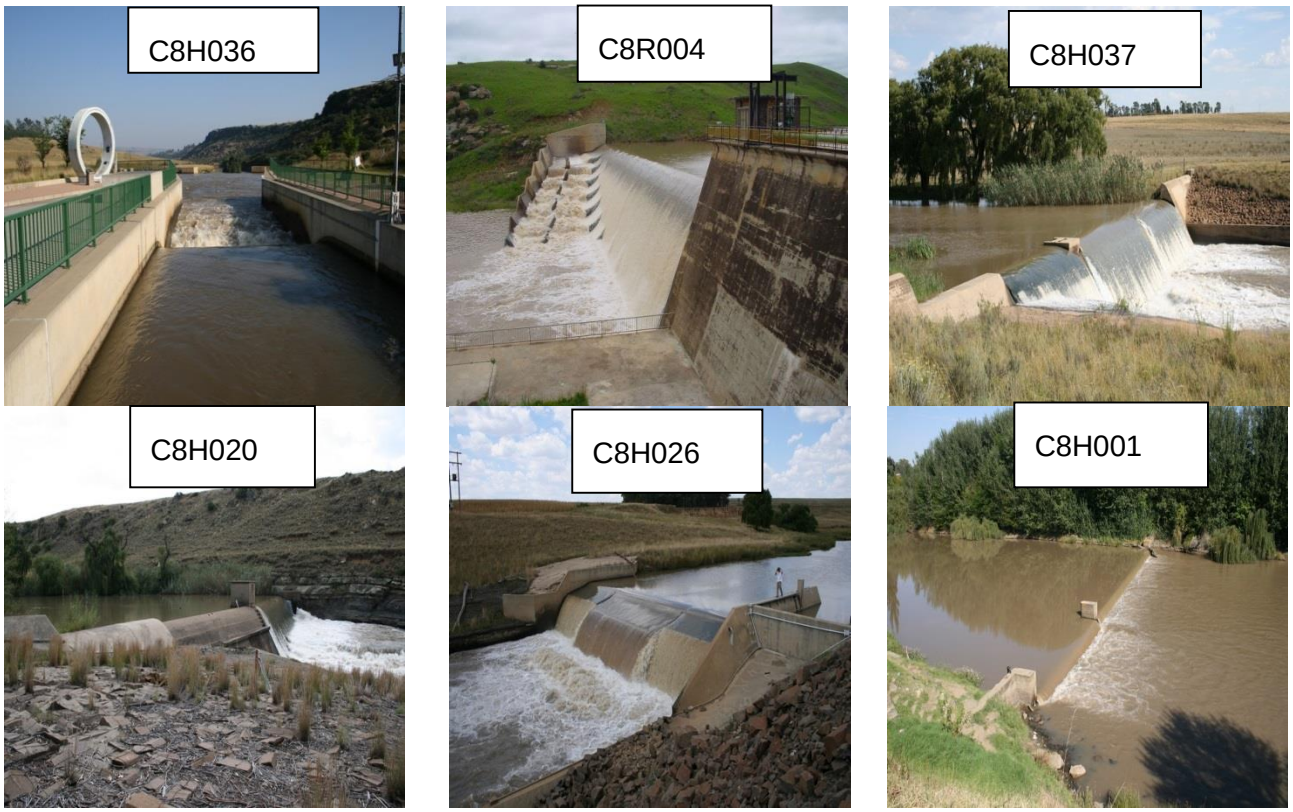

Figure 9: Flow Monitoring Stations Used

Table 3: Average Monthly Flows (Mm^3/month) 1999-2009

Station Name	ID	Oct	Nov	Dec	Jan	Feb	Mar	Apr	May	Jun	Jul	Aug	Sep
Tunnel Outlet	C8H036	50	47	48	51	42	51	50	66	70	73	71	62
Sol Plaatje	C8R004	57	53	56	59	51	57	55	72	74	77	74	64
Loch Athlone	C8R005	1.6	1.3	1.6	1.8	2.2	1.3	0.9	0.8	0.6	0.5	0.5	0.6
Reward	C8H037	60	56	64	65	57	65	56	73	76	79	77	69
Roodekraal	C8H020	60	57	66	74	65	64	56	74	73	75	73	66
Frederiksdal	C8H026	60	59	71	79	69	69	57	75	72	75	73	66
Wilge, Frankfort	C8H001	75	91	117	148	156	151	81	94	77	74	71	69

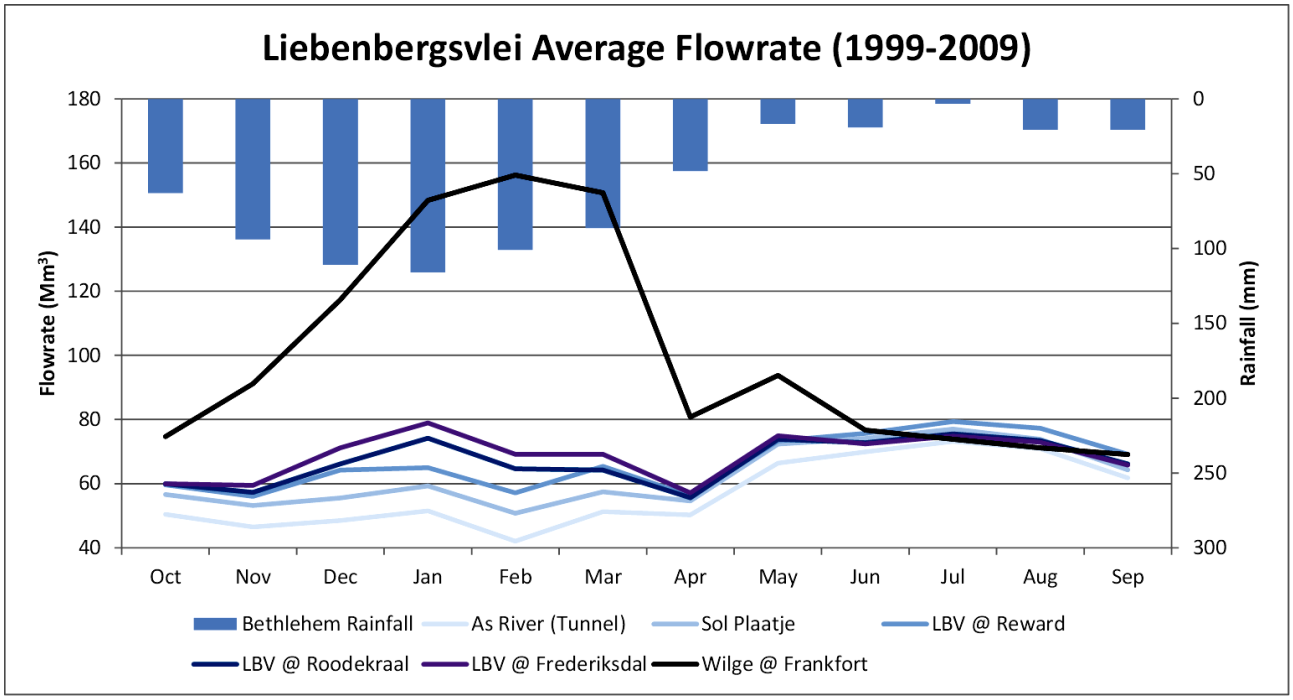

Figure 10: Liebenbergsvlei Average Monthly Flow Rates (1999-2009)

The annual stream flow volumes over this period were also analysed and are presented in Table 4. These results indicate that on average 143 Mm^3 of water is added to the system between the Tunnel discharge (683 Mm^3) and Frederiksdal, with a further 378Mm^3 added between Frederiksdal and Frankfort, primarily via the Wilge River. This addition along the Liebenbergsvlei varies between 4Mm^3 (2002) and 440Mm^3 (1999) per annum during the analysis period.

Table 4: Annual Stream Flow Statistics (Mm^3) 1999-2000

Station Name	ID	5th Percentile		Average		95th Percentile	
		Mm^3/yr	m^3/s	Mm^3/yr	m^3/s	Mm^3/yr	m^3/s
Tunnel Outlet	C8H036	538	17	683	22	803	25
Sol Plaatje	C8R004	624	20	749	24	887	28
Loch Athlone	C8R005	0	-	13	0	33	1
Reward	C8H037	626	20	798	25	933	30
Roodekraal	C8H020	606	19	804	25	970	31
Frederiksdal	C8H026	636	20	826	26	995	32
Wilge, Frankfort	C8H001	725	23	1204	38	2008	64

2.3.2 NATURAL RUNOFF

Natural monthly runoff data was sourced from the WR2012 datasets for all the quaternary catchments within the study area. The monthly averages over the October 1999 to September 2009 period are provided in Table 5. A number of very wet October's and January's significantly influence the total average annual runoff volume, which is estimated at 190Mm^3. This is in line with the average annual volume contribution measured along the river as noted in Table 4 above (143Mm^3). The discrepancy is partly due to the location of the final monitoring station (upstream of catchment C83J and half of C83H) but potentially also due to irrigation and other abstractions along the river reach.

Table 5: Average Monthly Natural Runoff (mm^3/a) from Quaternary Catchments (1999-2009)

	Oct	Nov	Dec	Jan	Feb	Mar	Apr	May	Jun	Jul	Aug	Sep	Annual
C83A	4.2	2.0	1.5	6.8	5.4	3.7	1.6	0.9	0.8	0.6	0.6	0.5	29
C83B	2.2	0.8	1.0	3.3	1.9	1.2	0.5	0.2	0.2	0.2	0.2	0.1	12
C83C	7.2	2.8	3.2	10.7	6.2	4.0	1.5	0.7	0.7	0.6	0.6	0.5	39
C83D	0.5	0.6	0.6	0.7	1.0	1.0	0.9	0.7	0.6	0.5	0.5	0.4	8
C83E	3.4	1.3	1.5	4.8	2.8	1.7	0.7	0.3	0.3	0.3	0.3	0.2	18
C83F	6.3	2.4	2.7	8.2	4.6	2.8	1.2	0.7	0.6	0.6	0.5	0.5	31
C83G	6.6	0.0	0.0	18.3	1.3	0.8	0.0	0.0	0.0	0.0	0.0	0.0	27
C83H	3.2	0.0	0.0	10.9	0.6	0.0	3.6	0.0	0.0	0.0	0.0	0.0	18
C83J	1.3	0.5	0.1	4.0	1.5	0.2	1.3	0.4	0.1	0.0	0.0	0.0	10
Total	**34.9**	**10.5**	**10.5**	**67.8**	**25.3**	**15.4**	**11.2**	**4.0**	**3.3**	**2.9**	**2.7**	**2.3**	**191**

2.3.3 WATER ABSTRACTIONS/RETURN FLOWS

Abstraction and return flow data was sourced from the WR2012 Land/Water Use information dataset for the catchment. Two abstractions (non-irrigation) are registered; the supply requirements for Bethlehem and Reitz are indicated in Table 6 below. A single return flow from the Bethlehem sewage treatment plant is also indicated at an average annual flow rate of approximately 150l/s or 12.3Ml/d, 60% of the abstraction. The net non-irrigation related abstraction from the river over this reach is estimated at 4.15Mm^3 per annum.

Table 6: Registered Abstraction & Return Flows (WR2012)

Catchment	Annual Abstraction (Mm^3)	Annual Return (Mm^3)	Comment	Upstream of
C83A	7.69		Bethlehem Town Supply 2009	Sol Plaatje Dam
C83C		4.50	Bethlehem Discharge 2009	Reward
C83G	0.96		Reitz Abstraction	Roodekraal

According to the WR2012 dataset the abstraction and return volumes do not vary significantly during the year as indicated in Table 7.

Table 7: Monthly Abstraction and Return Volumes (Mm3)

	Oct	Nov	Dec	Jan	Feb	Mar	Apr	May	Jun	Jul	Aug	Sep	Yr
Beth Abstraction	0.62	0.60	0.62	0.62	0.56	0.62	0.60	0.62	0.60	0.62	0.62	0.60	7.3
Beth Return	0.38	0.38	0.38	0.38	0.38	0.38	0.38	0.38	0.38	0.38	0.38	0.38	4.5
Reitz Abstract	0.08	0.08	0.08	0.08	0.08	0.08	0.08	0.08	0.08	0.08	0.08	0.08	0.96

A number of water abstractions for irrigation purposes within the catchment have been registered in the WARMS database (March 2013). The largest portion of the abstractions take place from the rivers/streams (88%) within the catchment as indicated in Table 8.

Table 8: Irrigated Areas per Quaternary (WARMS, 2013)

Catchment	Total Irrigated Area (km²)	Split by Source (km²)					
		Dam	Borehole	River/Stream	Lake	Wetland	Spring/Eye
C83A	19.1	0.84	0.02	18.2	0	0	0
C83B	0.8	0.7	0	0.11	0	0	0
C83C	19.7	1.95	0.26	16.6	0.3	0.55	0
C83D	0.6	0.24	0.05	0.3	0	0	0
C83E	17.9	0.58	0	17.0	0	0.26	0
C83F	15.3	4.3	0.02	11.0	0	0	0
C83G	23.4	3.25	0.01	20.2	0	0	0
C83H	20.8	0.35	0.31	19.9	0	0	0.21
C83J	5.0	0.3	0.5	4.2	0	0	0
Total	**122.6**	**12.5**	**1.2**	**107.5**	**0.3**	**0.8**	**0.2**
Percentage of Total		**10%**	**1%**	**88%**	**0%**	**1%**	**0%**

2.3.4 ANALYSIS OF VOLUMETRIC CHANGES ALONG THE RIVER REACH

The dry winter months were analysed separately to identify if there are any significant increases or decreases in flowrate as the water flows downstream (which may be caused by groundwater-surface water interaction). This reduces the data noise generated by surface runoff between the monitoring locations. A graph showing the change in flow rate along the river for each of the winter months, is provided in *Figure **11***.

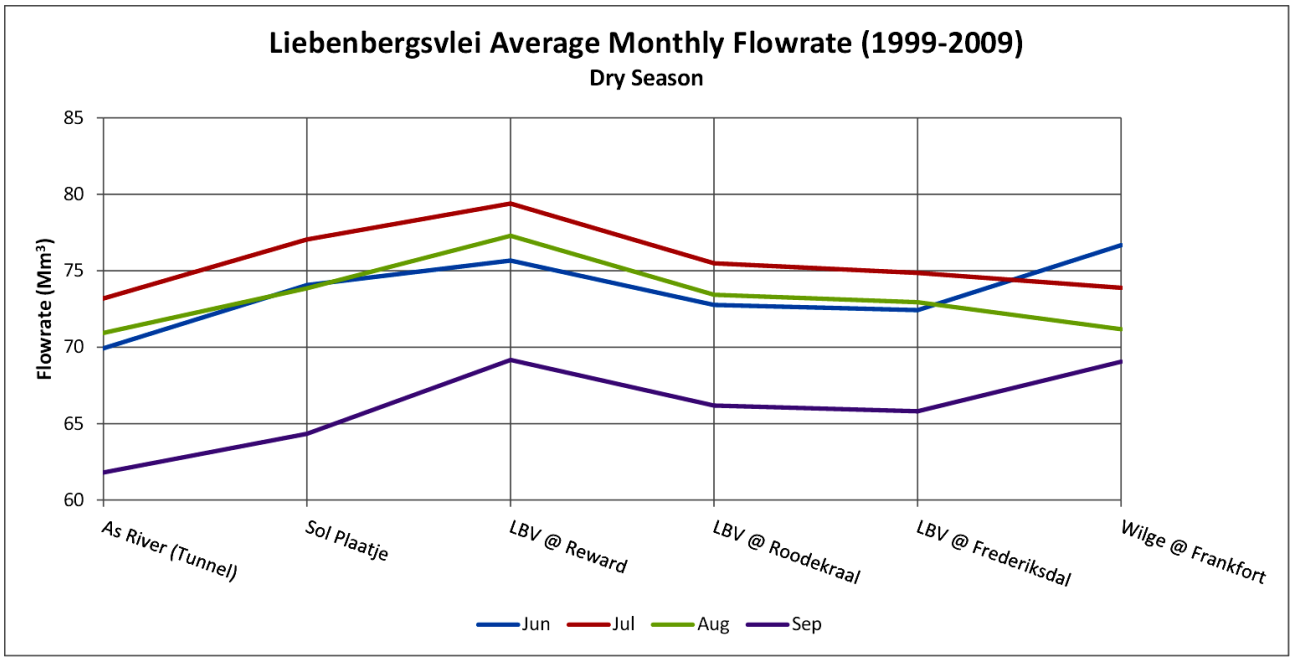

Figure 11: Liebenbergsvlei Average Monthly Flow Rates (1999-2009) – Dry Season

All four of the driest months seem to follow the same pattern as one moves downstream - an initial increase from the tunnel outlet to Reward and thereafter a decrease in flow rate. A decrease over the entire river stretch would have been expected due to limited runoff, continued evaporation and abstractions. On average this initial increase is around 6.4Mm^3 per month or 2.5m^3/s, the driest month (September) shows an increase of 7.4Mm^3 or 2.8m^3/s.

To rule out the possibility of the increase in observed flow being a result of runoff over this period, the quaternary runoff volumes were sourced from the WR2012 online dataset. These average runoff volumes were added systematically to the observed flow rates to estimate the expected flow rates at the next monitoring locations as shown in *Figure **12***. Even after taking the assumed runoff into account, the estimated flow rates remain significantly higher than expected.

The average daily flow rates for all the September months within the period were analysed and are indicated in *Figure **13*** through *Figure **16*** for the three stations indicating the increased flow rates during September.

Variations in daily flow rates are expected when comparing the Tunnel outlet flow to the release from Sol Plaatje dam as the storage within the dam can impact the pattern. An example of this is seen during the September of 2000 where a significant peak is observed in the dam release flows even though no such peak was observed for the tunnel release. It is likely that additional water was released from dam storage during this time thus resulting in a dam level decrease.

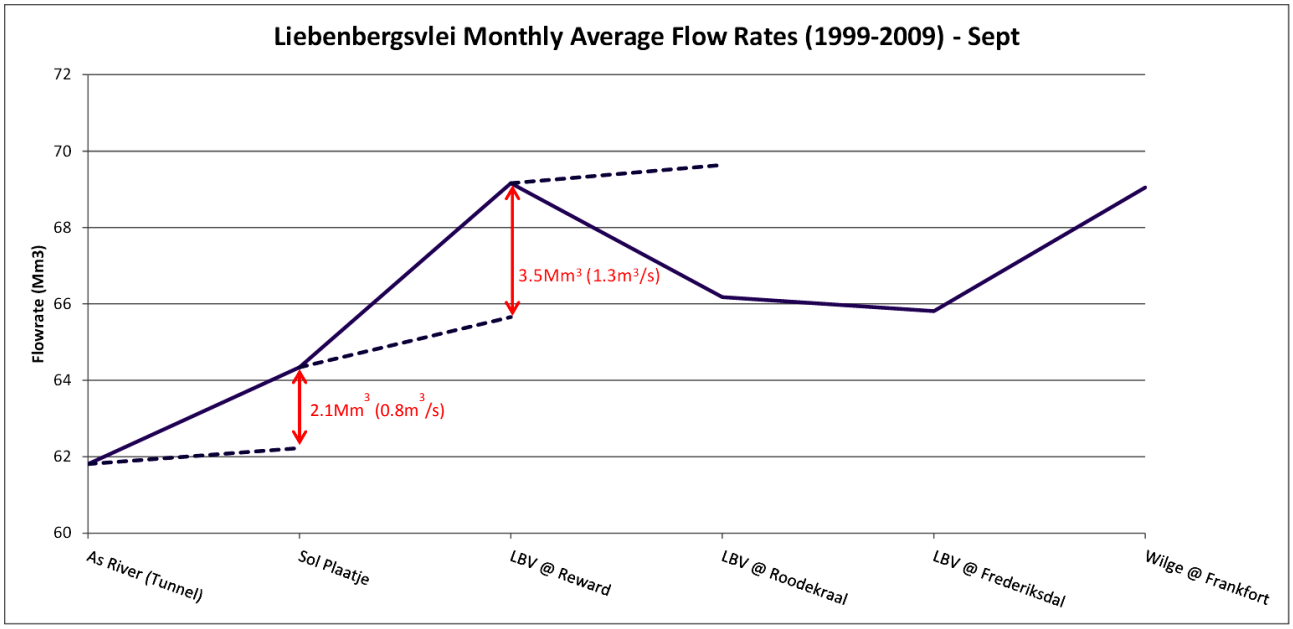

Figure 12: Liebenbergsvlei Average September Flow Rates (1999-2009) – Observed vs. WR2012 Estimates

The pattern seems to remain consistent during the period with the release from Sol Plaatje slightly higher than the discharge from the tunnel until September 2009. September 2009's flow rates indicate a different pattern with the Sol Plaatje flow rate consistently below the Tunnel outlet flow rate (***Figure 13***).

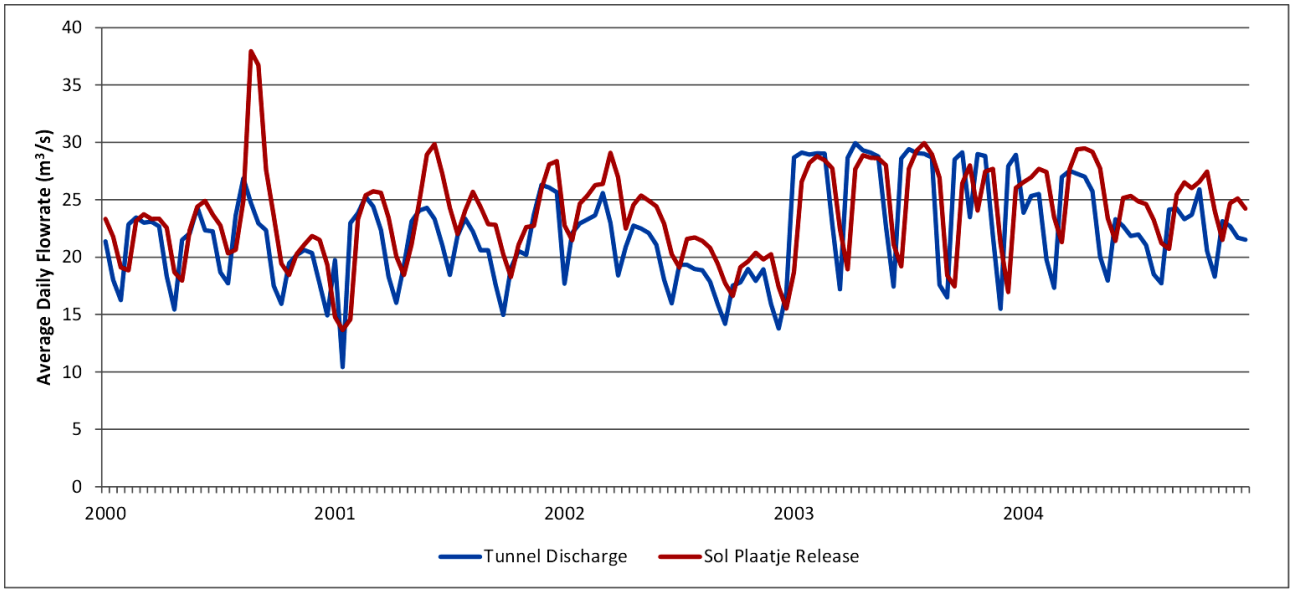

Figure 13: September Daily Average Flow Rates (Tunnel Outlet & Sol Plaatje Release) - 2000 to 2004

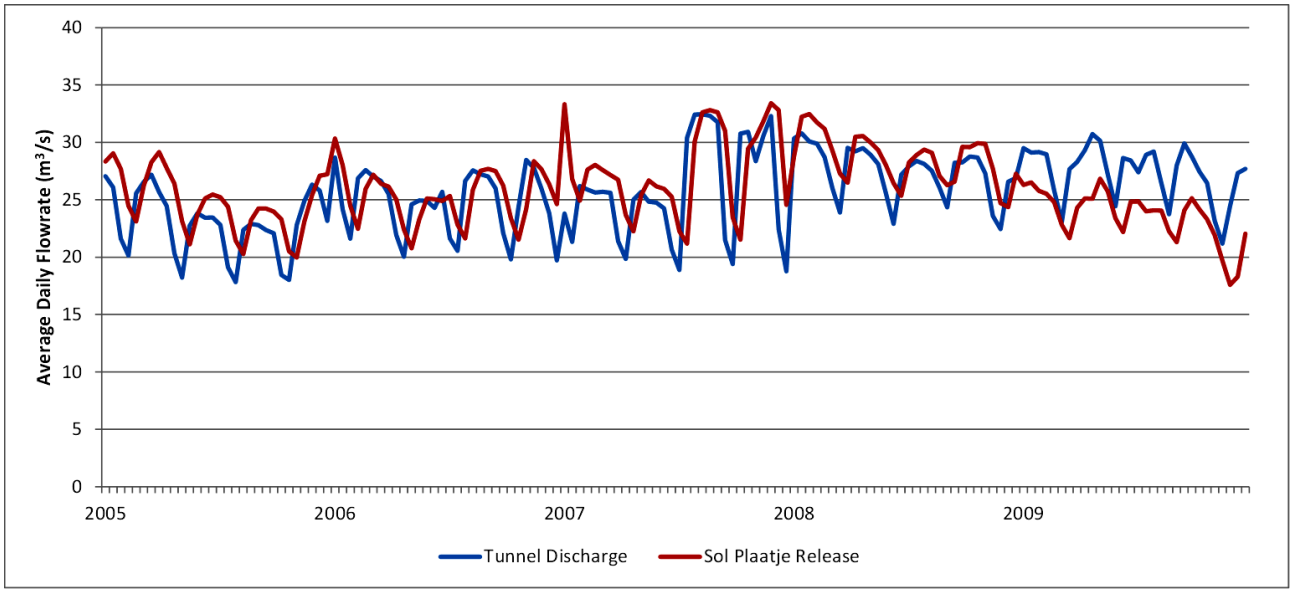

Figure 14: September Daily Average Flow Rates (Tunnel Outlet & Sol Plaatje Release) - 2005 to 2009

The Sol Plaatje daily flow rates are compared to the downstream Reward flow rates in *Figure **15*** and *Figure **16***.

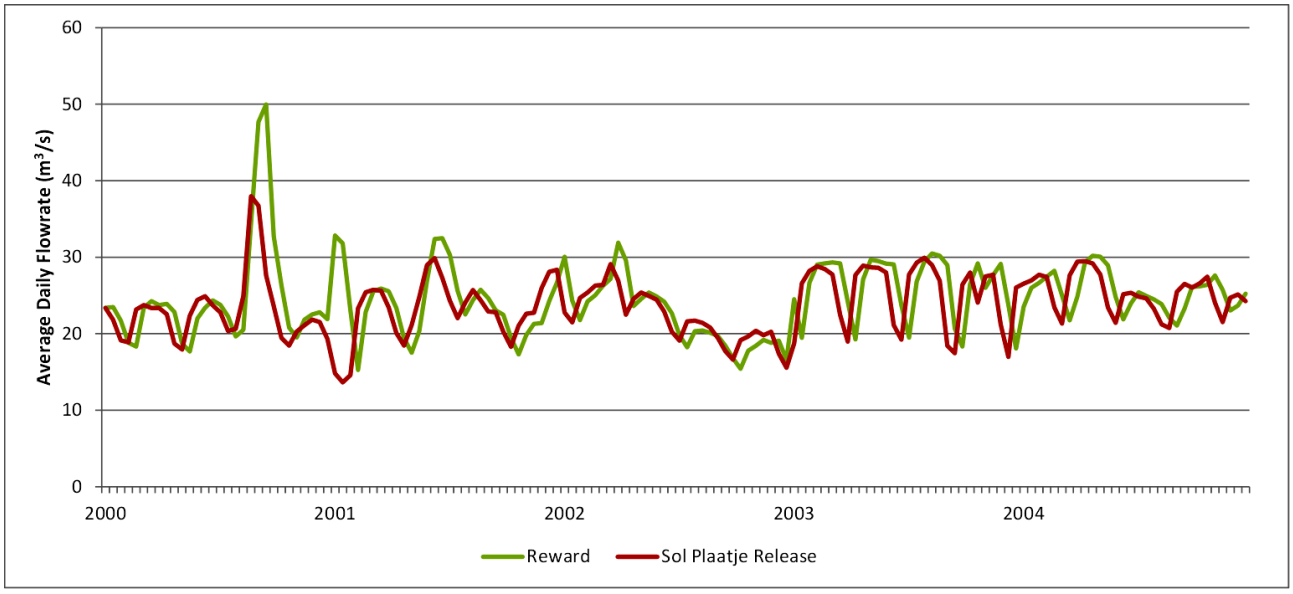

Figure 15: September Daily Average Flow Rates (Sol Plaatje Release & Reward) - 2000 to 2004

As with the comparison above the pattern seems to remain consistent for the first couple of years, from 2005 onwards there seems to be greater variance between the two monitoring stations. This could not be caused by storage changes along the river reach as no major dams are located between these two stations.

From September 2009 onwards the difference between the two stations' records seems to increase. It was noted in Section 2.2 that the Sol Plaatje Dam rating curve was updated in November 2009 and all data subsequent to this date was discarded by DWS. It seems likely that the rating or calibration of the weir was already affected before November 2009.

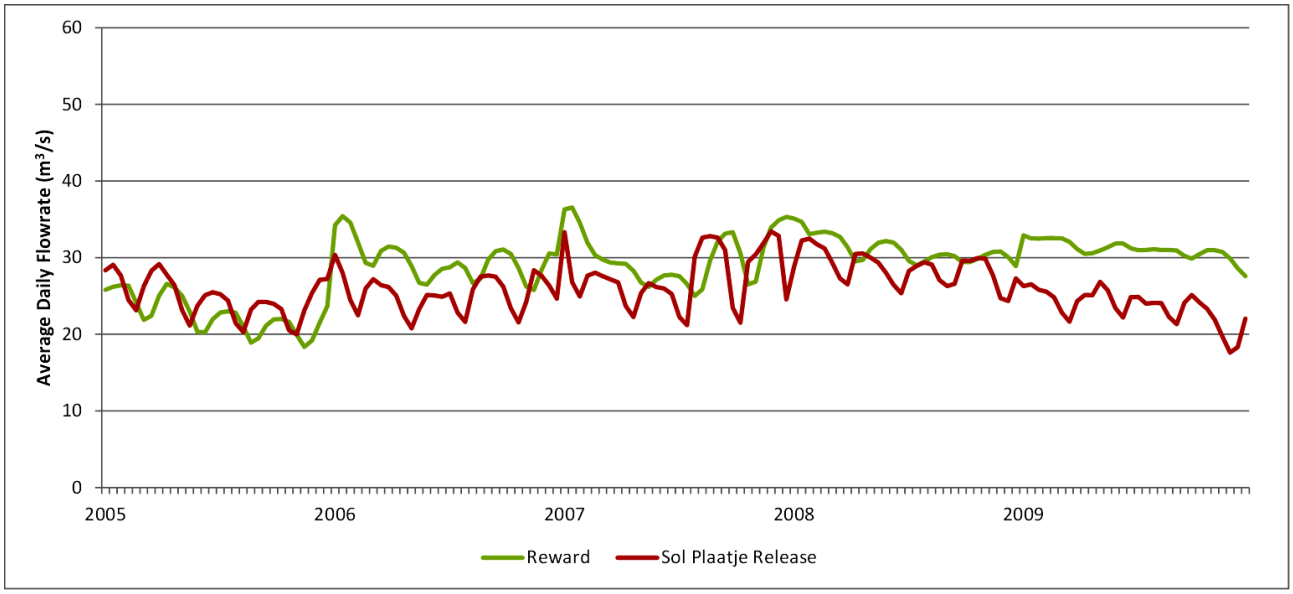

Figure 16: September Daily Average Flow Rates (Sol Plaatje Release & Reward) - 2005 to 2009

2.4 SURFACE WATER QUALITY

2.4.1 WATER QUALITY MONITORING STATIONS

A number of active and inactive water quality monitoring stations within the catchment were identified and the measured data sourced from the DWS Hydrology website (DWS, 2015). The metadata for these stations are provided in Table 9 below and the locations are indicated in *Figure **17***.

Table 9: Water Quality Monitoring Stations

Station ID	Name	Start Date	End Data	Comments
C8R004	Liebenbergsvlei @ Sol Plaatje Dam	Mar 1975	May 2015	
C8R005	Jordaan River @ Loch Athlone	Nov 1975	Jul 2015	
C8H007	Liebenbergsvlei @ Vogelfontein	Nov 1975	Mar 1978	1 Sample in Nov 1996
C8H037	Liebenbergsvlei @ Reward	May 2012	May 2015	
C8H004	Liebenbergsvlei @ De Molen	Nov 1975	Jul 2015	No samples in 1999, 2013
C8H020	Liebenbergsvlei @ Roodekraal	Jan 1978	Jul 2015	
C8H026	Liebenbergsvlei @ Frederiksdal	Mar 1985	Jul 2015	
C8H001	Wilge River @ Frankfort	Nov 1975	Jul 2015	2 Samples in 1971 & 1974

Discharge from the Katse Dam Tunnel started in January 1998. It was decided to analyse the data after this change thus the period analysed starts in October 1998 (beginning of the next hydrological year) and runs through to September 2014.

2.4.2 WATER QUALITY DATA ANALYSIS

Water quality monitoring data was sourced from the "Resource Quality Information Services water quality data exploration tool" using Google Earth for the stations listed above. A number of the available parameters were identified as potentially significant to the understanding of the groundwater-surface water interaction, these are:

- Dissolved Sulphate (SO_4);
- Dissolved Major Solids (DMS);
- Dissolved Chloride (Cl);
- Electrical Conductivity (EC);
- Dissolved Sodium (Na);
- Dissolved Silicon (Si); and
- Total Alkalinity as Calcium Carbonate (TALK).

The average measured concentrations for each of these parameters for each month over the period analysed (October 1998 to September 2014) are presented in *Figure **18*** through to *Figure **24*** below. As a reference, the concentrations observed at the Vaal Barrage over the same period are also indicated. Other than Silicon and Total Alkalinity, the concentrations observed in the Liebenbergsvlei are significantly lower than the concentrations at the Vaal Barrage.

Excluding the water in Loch Athlone, available data shows that the water quality along the river reach is consistent and minimal seasonal variability is observed. Loch Athlone seems to have elevated DMS, EC, Sodium and Total Alkalinity compared to the main stem of the river.

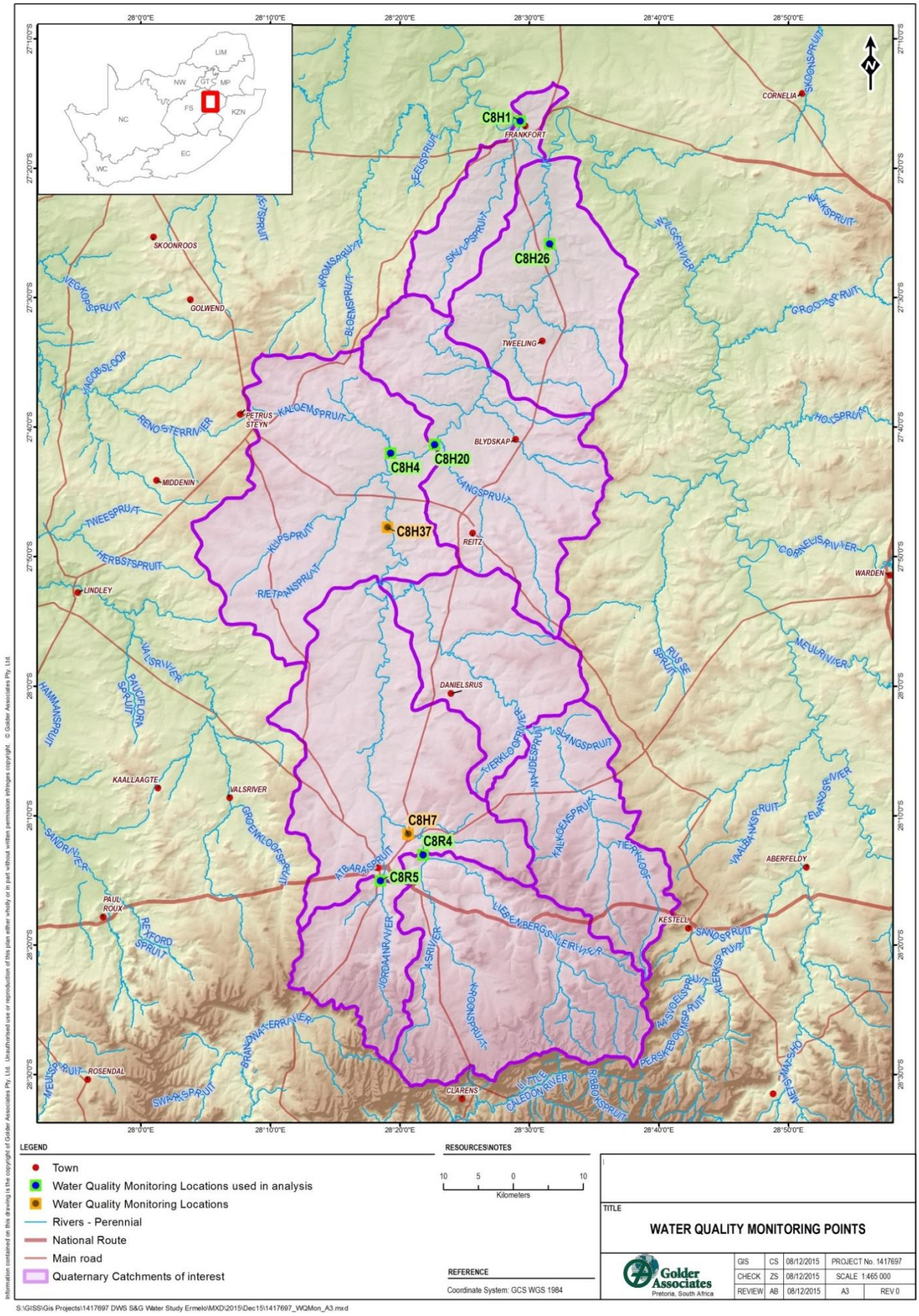

Figure 17: Water Quality Monitoring Locations

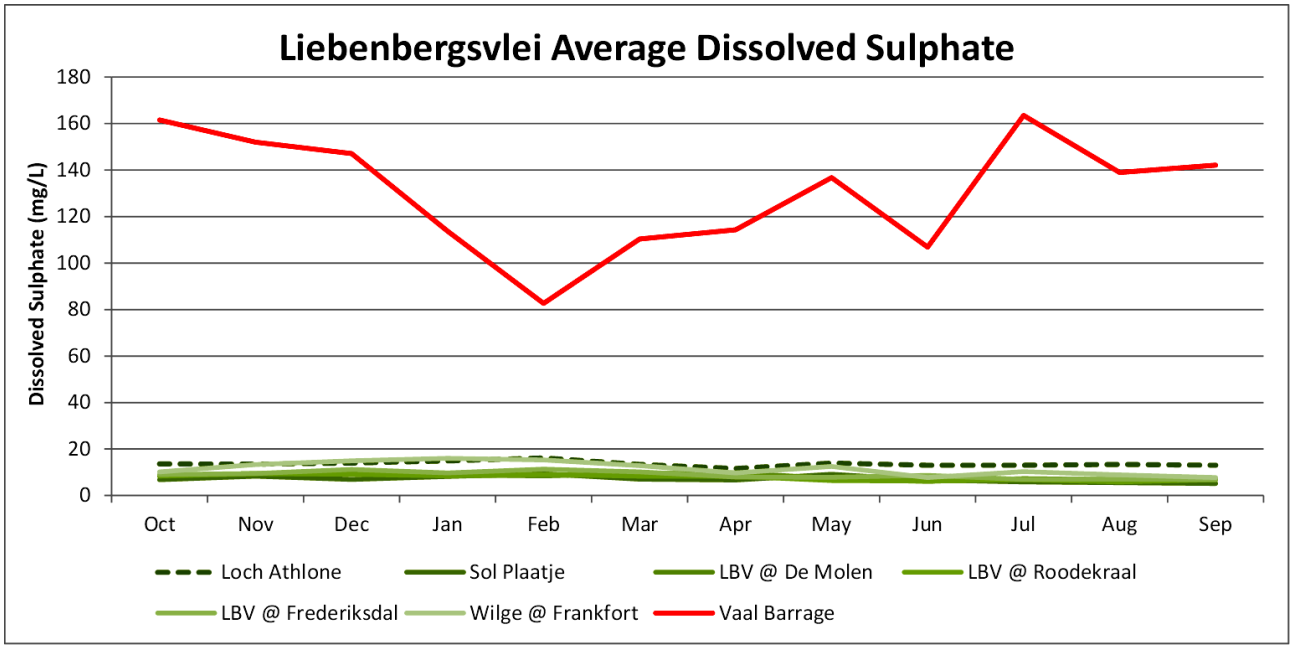

Figure 18: Dissolved Sulphate

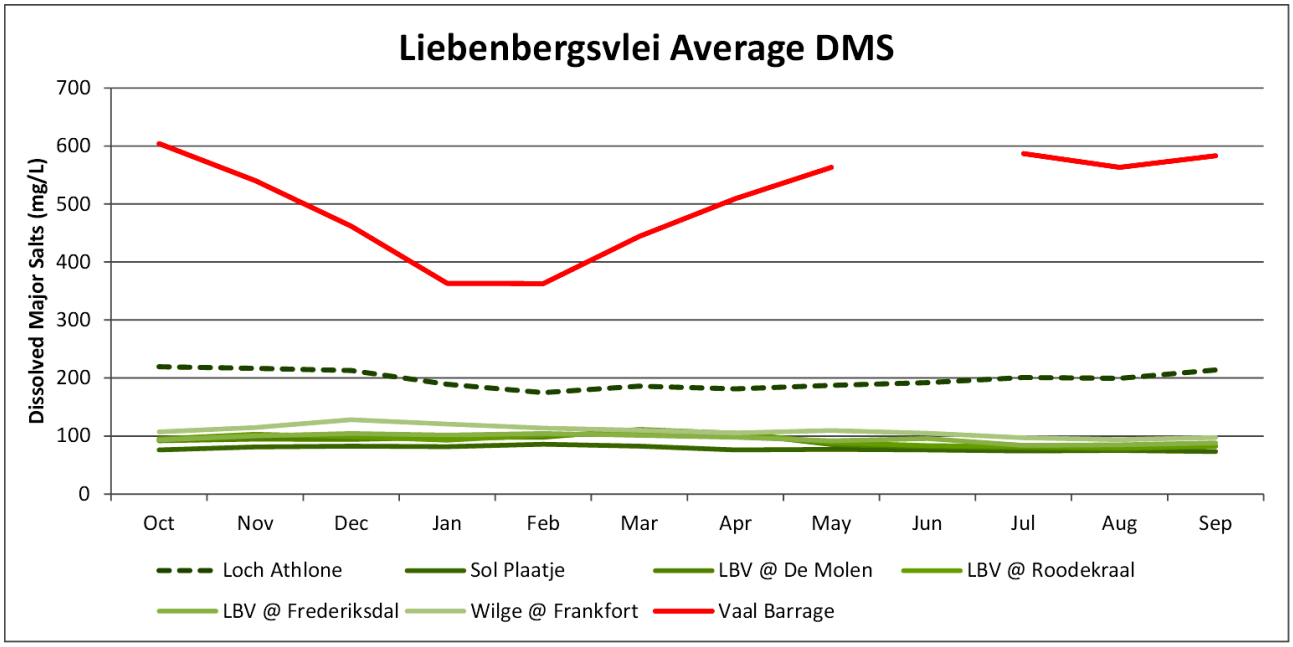

Figure 19: Dissolved Major Salts

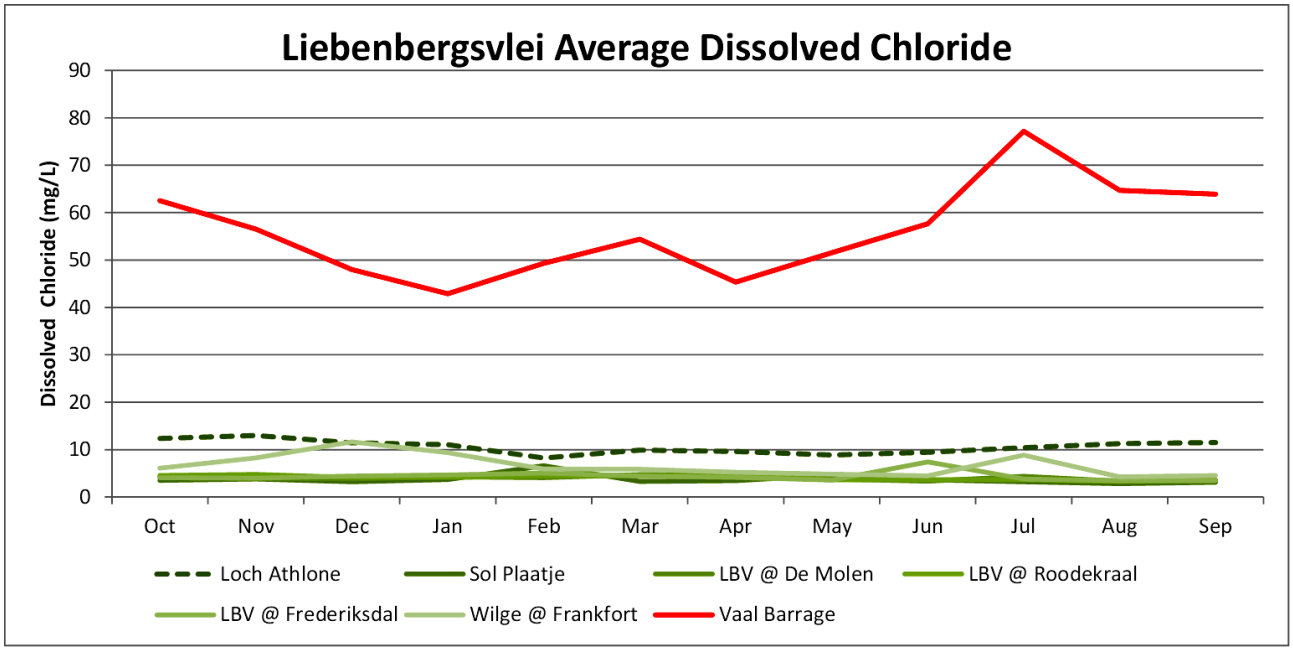

Figure 20: Dissolved Chloride

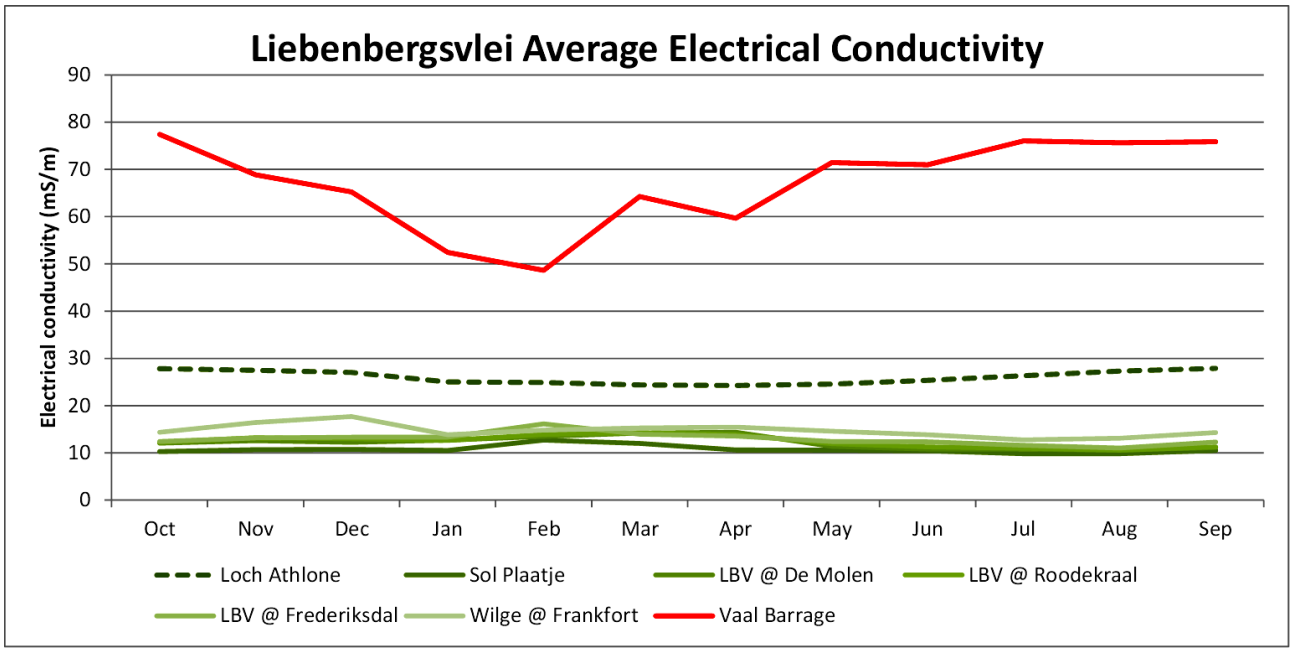

Figure 21: Electrical Conductivity

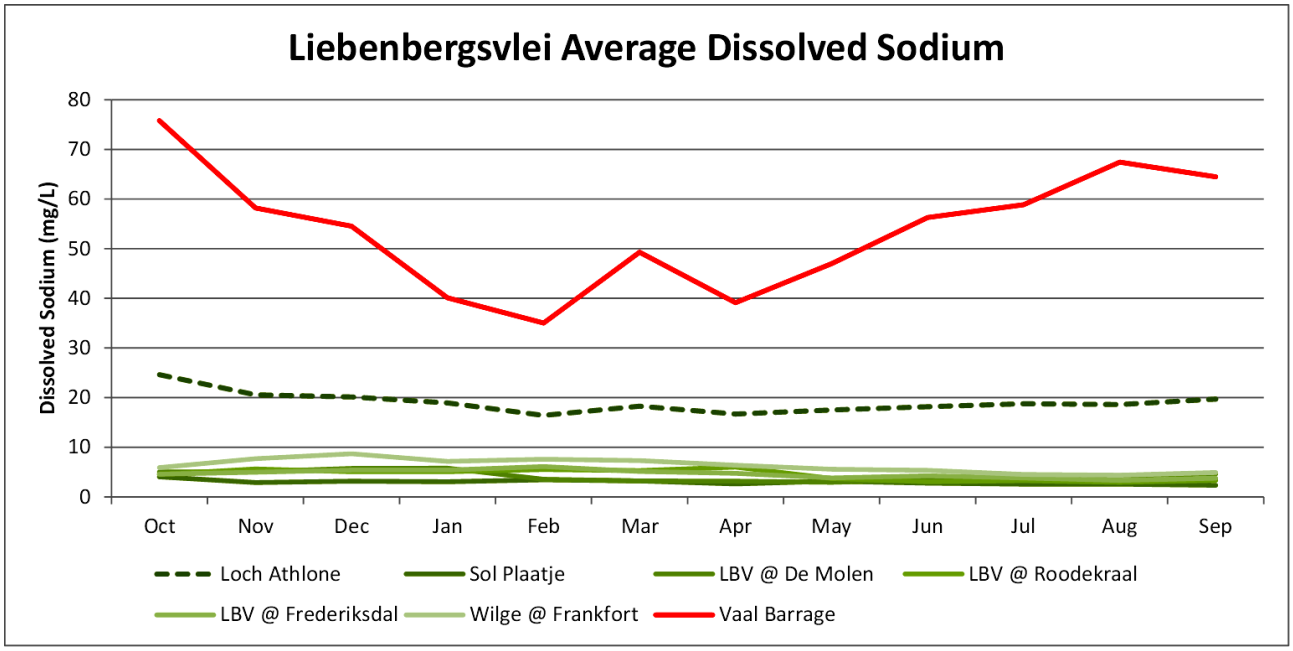

Figure 22: Dissolved Sodium

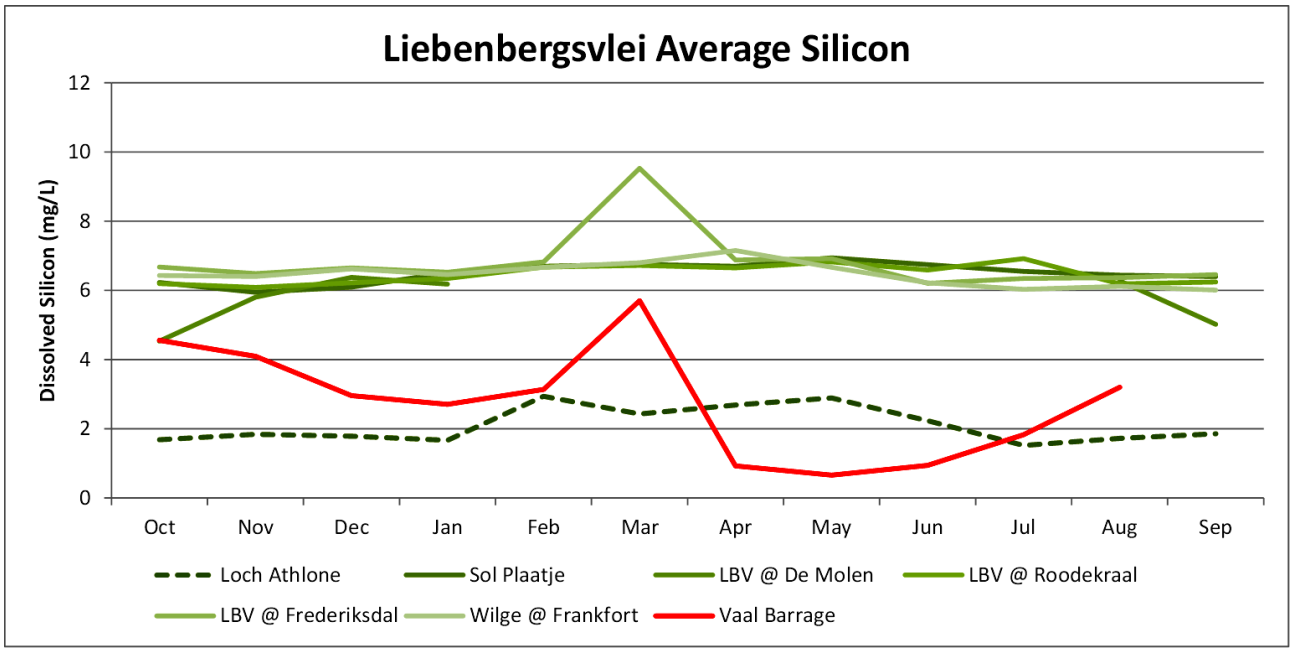

Figure 23: Dissolved Silicon (Limited Samples Analysed)

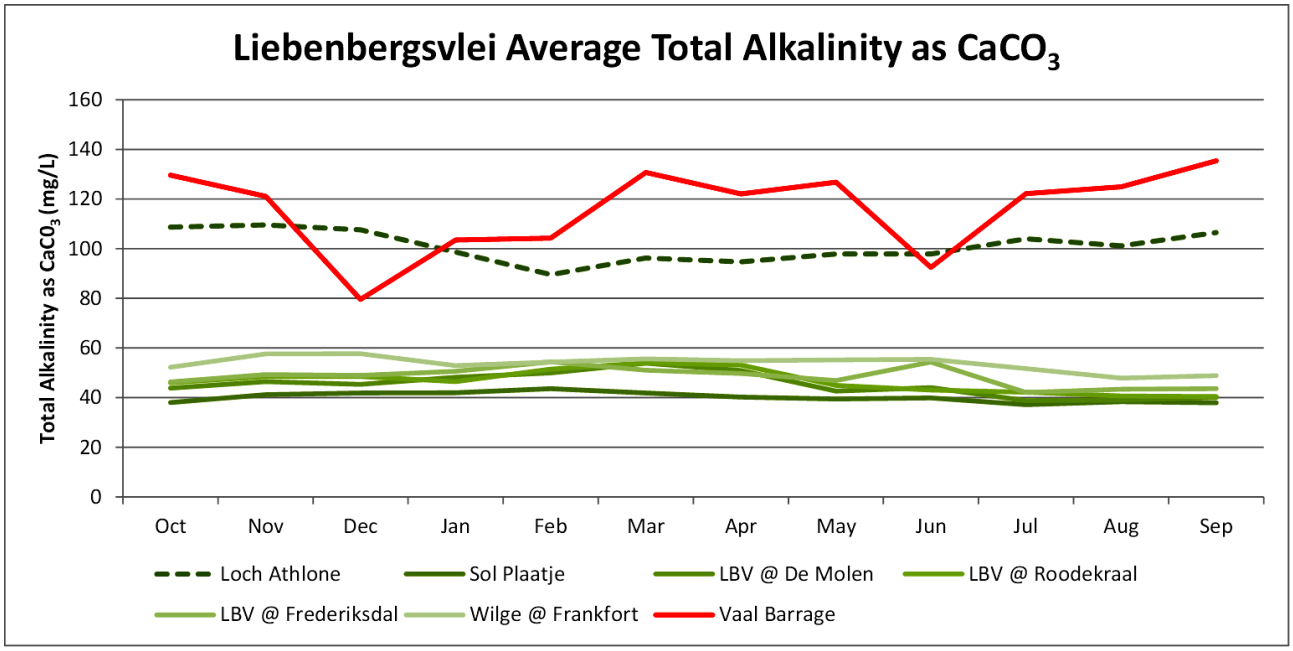

Figure 24: Total Alkalinity as $CaCO_3$

2.5 DATA REVIEW CONCLUSION

It was concluded that data from the following active flow monitoring stations located on the Liebenbergsvlei and the Wilge River will be used to calibrate the surface water model: C8R004, C8H037, C8H020, C8H026 and C8H001. Data over a 10-year period, October 1999 through September 2009, will be used for all the stations except C8R004. The analysis of the flow data measured at C8R004 (discharge from the Sol Plaatje Dam) indicates that the data could be inaccurate from October 2008, thus data for the last year will also be excluded.

The water quality observed along the stretch of the river is similar for the different stations and is indicative of the good quality water being transferred from the Lesotho Highlands via the tunnel. Any seasonal variation of the water quality was shown to be insignificant. The data does not suggest any noteworthy changes along the river reach and does not indicate any surface/groundwater interaction.

The contribution from the Jordaan River which drains the populated area of Bethlehem is a concern in terms of poor water quality impacts and releases. However, the current impact on the main stem water quality is significantly diluted below the confluence with the Liebenbergsvlei River.

The same argument counts for the Langvlei River tributary. Although the macro-salinity is a fraction of magnitude (i.e. 0.5) higher, the impact on the water quality (i.e. salinity) is completely diluted downstream from the confluence between the main stem and the tributary containing the poor water quality.

2.6 SURFACE WATER FLOW MODELLING

2.6.1 METHODOLOGY

The water surface elevations and corresponding flowrates at the weirs along the Liebenbergsvlei running from the Sol Plaatje discharge point to the weir located at Frederiksdal were analysed. The following method was used for this study:

- Strategic points located along the project area were visited to assess the site specific hydrological and hydraulic conditions;
- The catchment areas of the tributaries for the Liebenbergsvlei located within the project area were delineated based on the 1:15 000 scale topographical maps;
- A digital elevation model (DEM) was prepared based on available contour data and used as an input to the US Army Corps of Engineers' Hydrologic Engineering Center's River Analysis System model (HEC-RAS model);
- The flow monitoring data was analysed and used as inputs to the 2D HEC-RAS backwater programme to determine the water elevations for different scenarios;
- The HEC-RAS model was evaluated for unsteady and steady flow conditions;
- The water extent, depth and maximum velocities were plotted on the available mapping.

A base case scenario was set up to check the model calibration. The inputs for the base case is as follow:

- Discharge into river is limited to the tunnel;
- Average daily discharge values for the months where low rainfall are measured (June, July, August and September) were used;
- A manning roughness coefficient of 0.03 was used for the river, this value was based on the assumption that the channel is clean with limited riffles or deep pools (having been scoured out due to the high velocity of the water being transported via this conduit).

The results of this model were compared to the actual measurements taken at monitoring points for the same time period

2.6.2 TOPOGRAPHY

A digital elevation model (DEM) used within the numerical model was generated using the available contour data for the region (5m intervals). The potential extent of the river's floodplain was identified and is shown in *Figure **25***. From this image, the smaller river cross-sections are present in the top reaches of the system with floodplains increasing as you move further downstream. Thus in these areas (during the winter months, with minimal additional runoff contributing), the flow velocities are likely to be less but spread over a larger surface area

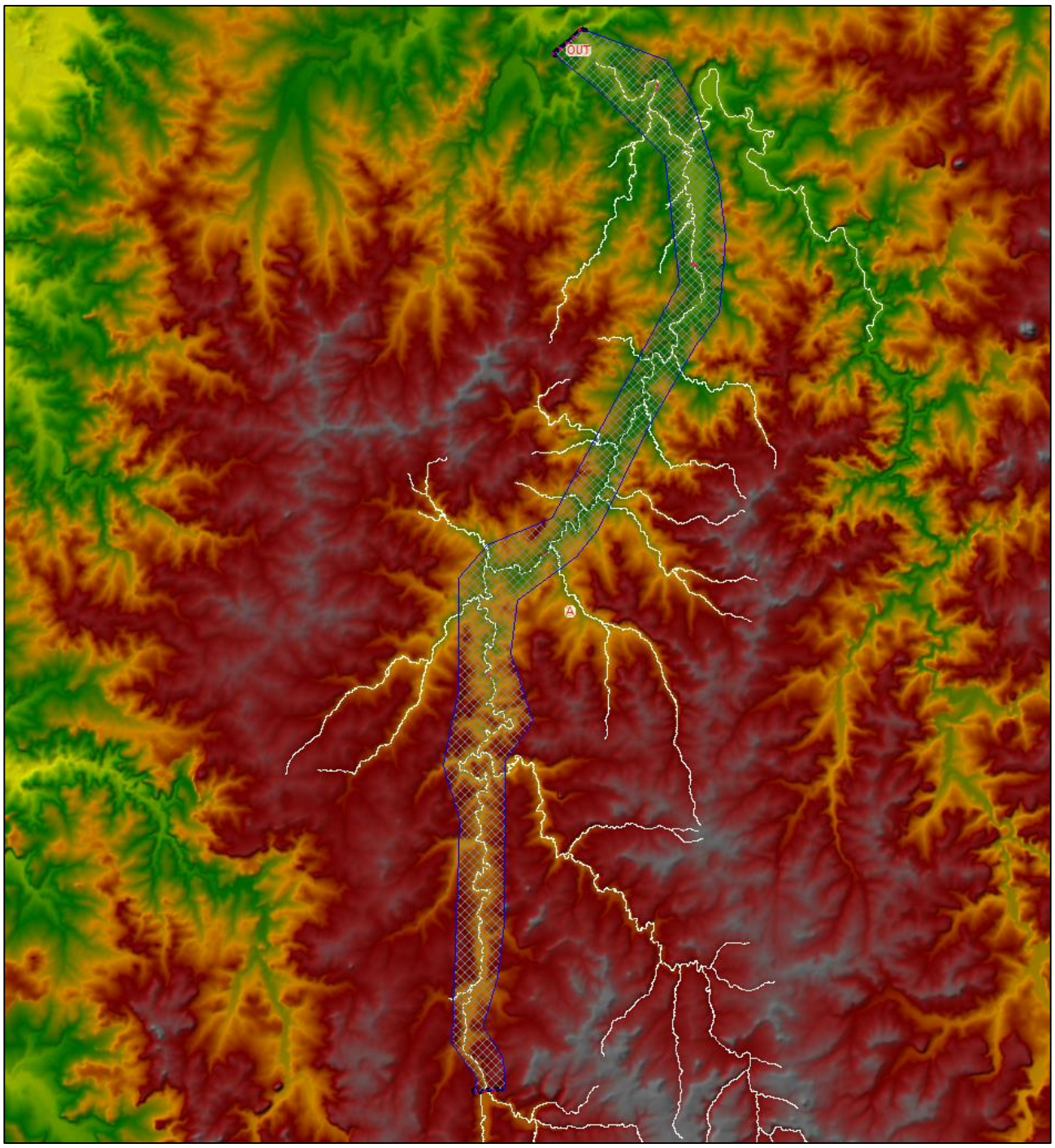

Figure 25: Catchment Topography and Extent of Numerical Model

2.6.3 SURFACE COVER

The flow pattern and velocity of the water within the river system is influenced by the topography but also by the surface cover and the vegetation along the banks. To be able to select an appropriate Manning's coefficient (roughness coefficient), which is required when setting up the model, a visual assessment of the river reach was performed. Photos along the river reach are provided in ***Figure 26*** and ***Figure 27***.

Figure 26: Ash river between C8H036 and C8R004

Figure 27: Liebenbergsvlei between C8R004 and C8H037

The catchments' vegetation cover is primarily characterized by veld type grasslands with a number of bigger trees scattered along the river banks. A manning's coefficient of 0.03 was selected (see *Figure **28***), as the analysis was performed during the winter months and the length of the grass in the grasslands would be significantly reduced during this period.

Channel Description	Average Value of *n*
Grassland	
Short grass	0.030
Tall grass	0.035
Cultivated ground	
Bare ground	0.030
Mature row crops	0.035
Mature field crops	0.040
Brushy areas	
Dense weeds and sparse brush	0.050
Brush-covered with some trees (winter)	0.050
Brush-covered with some trees (summer)	0.060
Dense brush (winter)	0.070
Dense brush (summer)	0.100
Forested	
Densely covered with willows (summer)	0.150
Cleared land with stumps; no new growth	0.040
Cleared land with stumps; dense new growth	0.060
Dense stands of large trees; flood stage below branches	0.100
Dense stands of large tress; flood stage reaching branches	0.120

Figure 28: Values of Manning's n to be used for overbank areas along streams or rivers

2.6.4 INITIAL HEC-RAS MODEL RESULTS

The model first needed to be evaluated based on the travel time between the monitoring stations, to ensure the base velocity/flowrate is within range. This was done by comparing the hydrographs observed between two stations (C8R004 and C8H037) over a short time interval (September 2000). The comparison of data measured at Sol Plaatje and Reward is shown in ***Figure 29***.

The two dashed red lines in ***Figure 29*** and ***Figure 30*** indicate the start of water level rise for a single peak flow event – approximately one day delay. This lag period is likely to fluctuate somewhat during wetter and dryer periods, however due to the flowrate within the river system primarily being controlled by the tunnel discharge (relatively constant) this fluctuation should be negligible in the winter months.

The first HEC-RAS scenario analysed, using a Manning's coefficient of 0.03 resulted in lower velocities (longer time delay between monitoring stations) compared to the measured data. The Manning's coefficient was adjusted to 0.01 in order to achieve a similar time delay as seen in ***Figure 30***.

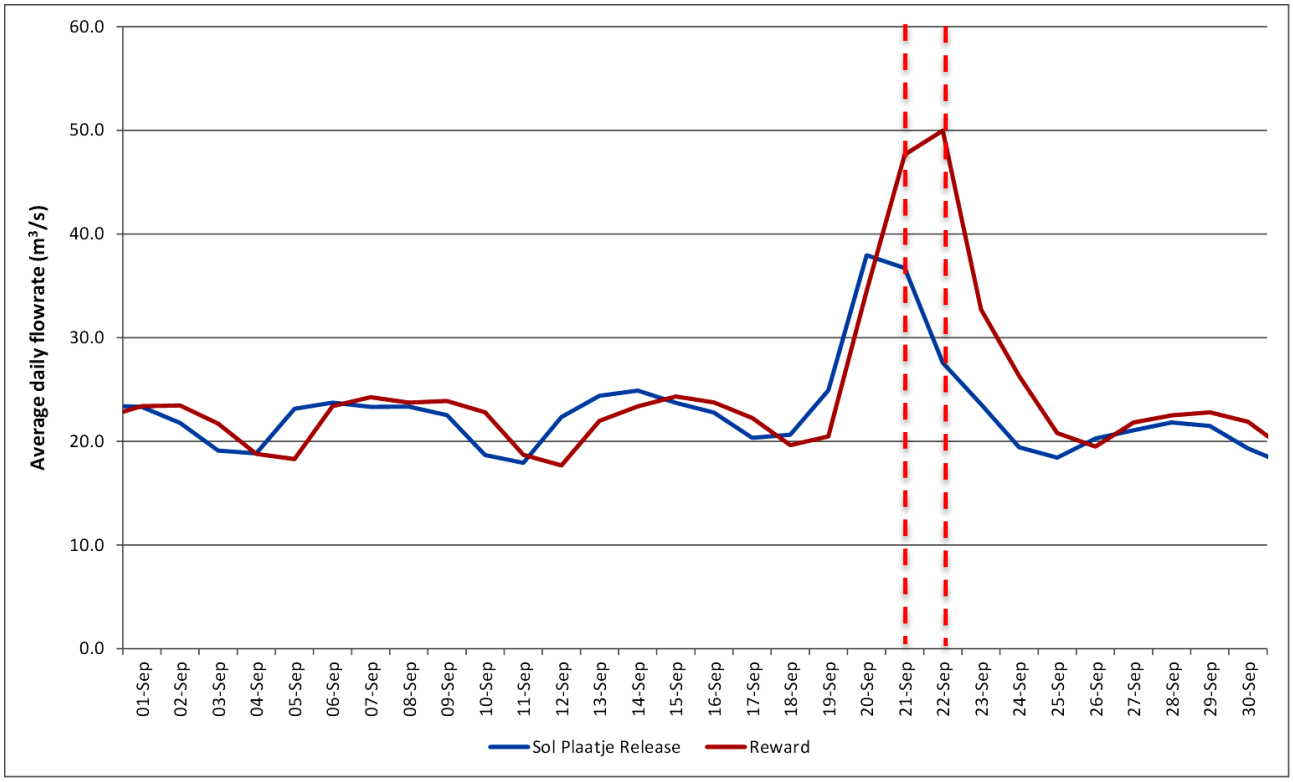

Figure 29: Recorded average daily flowrates (September 2000)

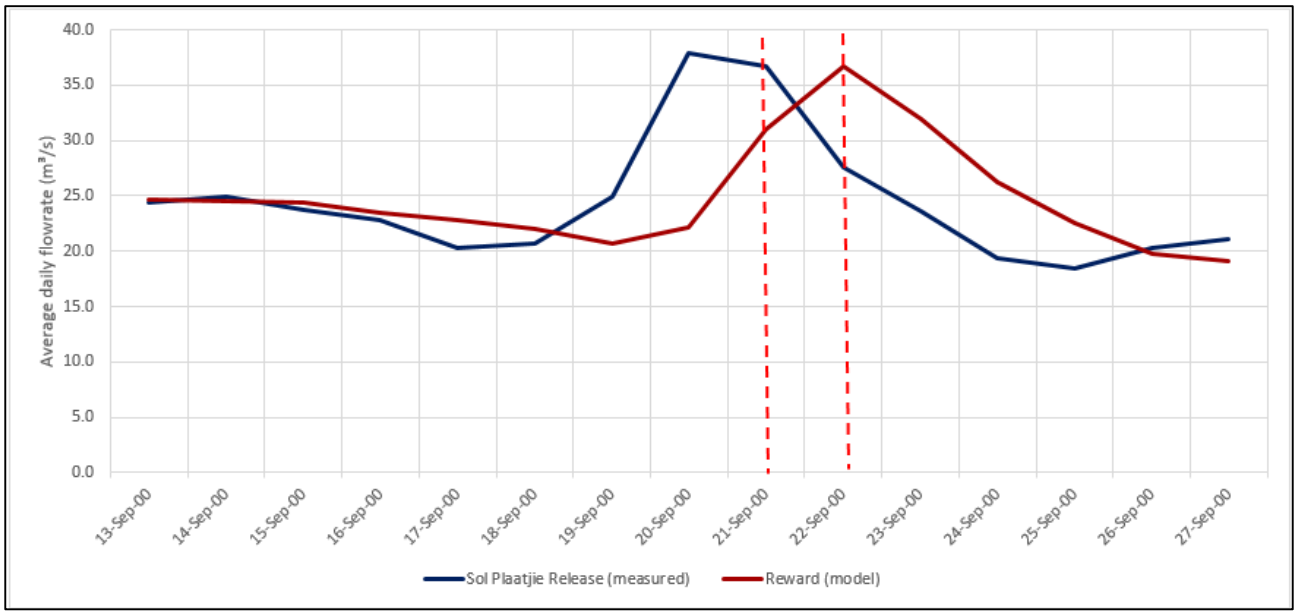

Figure 30: Measured vs modelled average daily flowrates (September 2000)

Once the model input setup was complete the June-August 2000 Sol Plaatje measured discharge volumes (***Figure 36)*** were used to generate a flow hydrograph used as an input for the HEC-RAS model as an upstream boundary condition.

The downstream boundary condition was set to a normal depth with a friction slope of 0.01. The model was run using the "unsteady-flow" computational framework and applying a daily time step. Initial calibration of the model was done to ensure the lag between the Sol Plaatje and the Reward

monitoring stations was approximately 1 day. The resulting maximum surface extent of the water in July-August 2000 are shown in ***Figure 31*** and ***Figure 32*****.**

The daily depth records that were measured upstream of the weirs and used by DWS to estimate the flowrates were compared to the modelled data. These graphs are provided in ***Figure 33*** through ***Figure 35***.

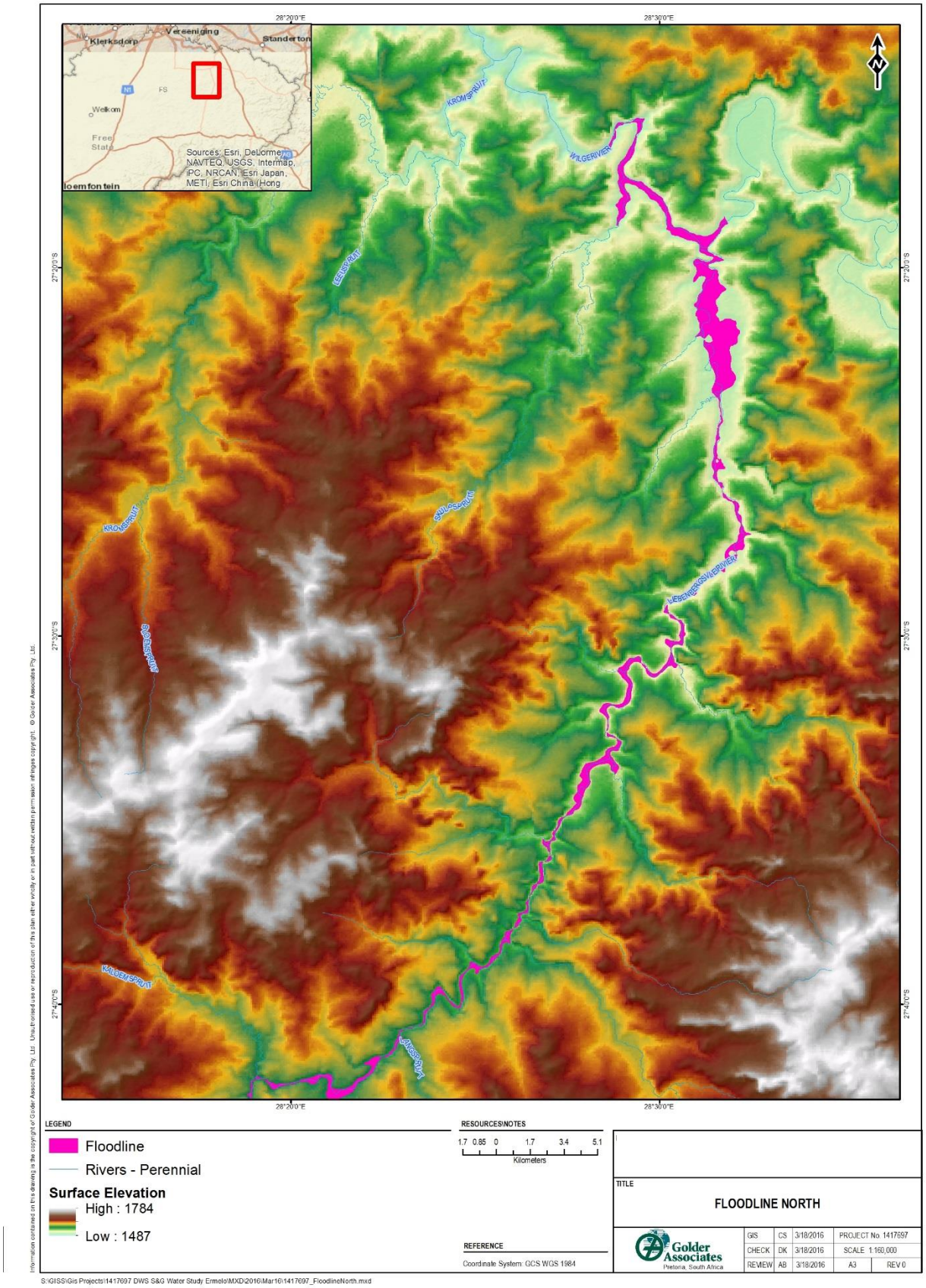

Figure 31: Maximum water depth- northern project area

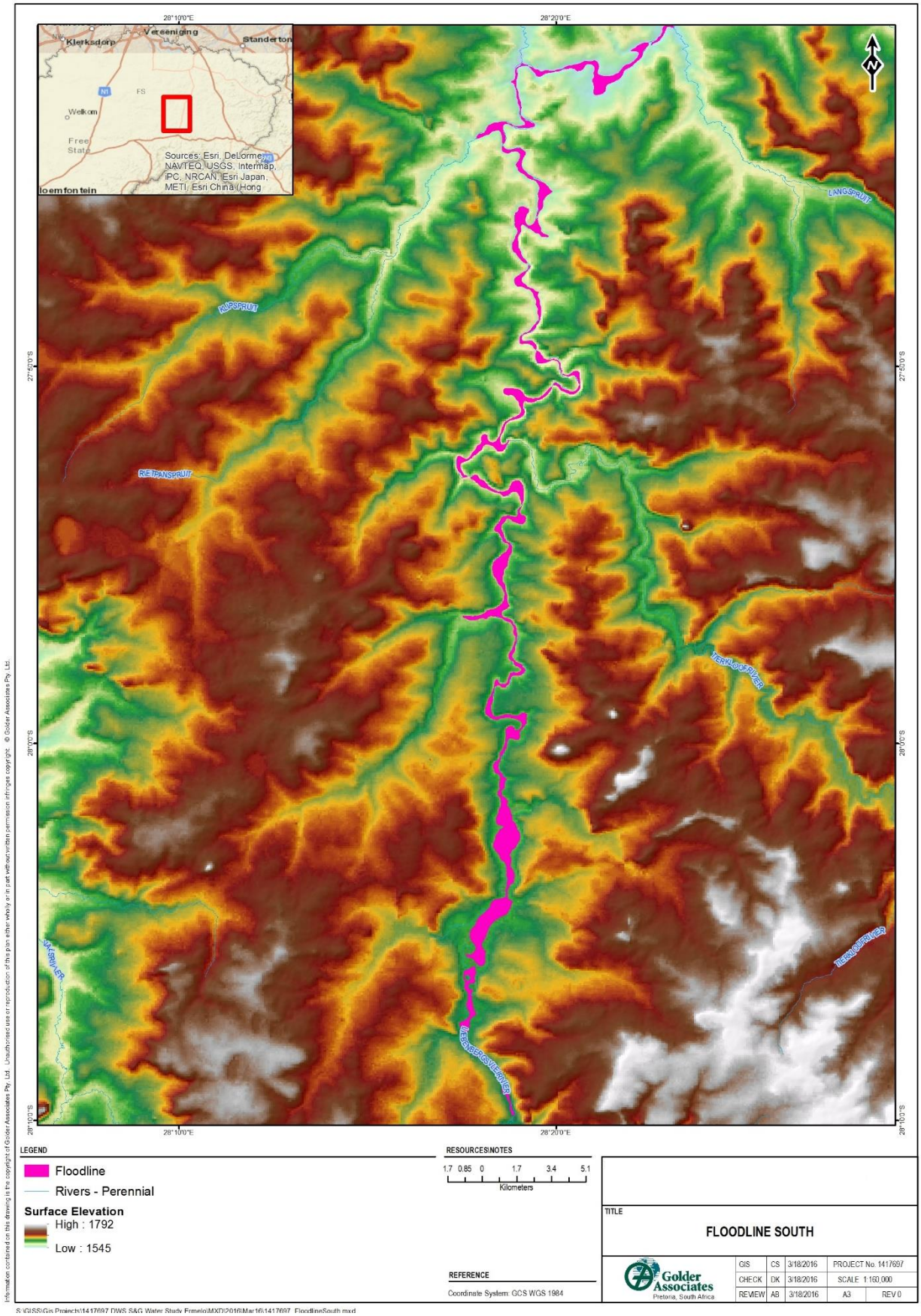

Figure 32: Maximum water depth – southern project area

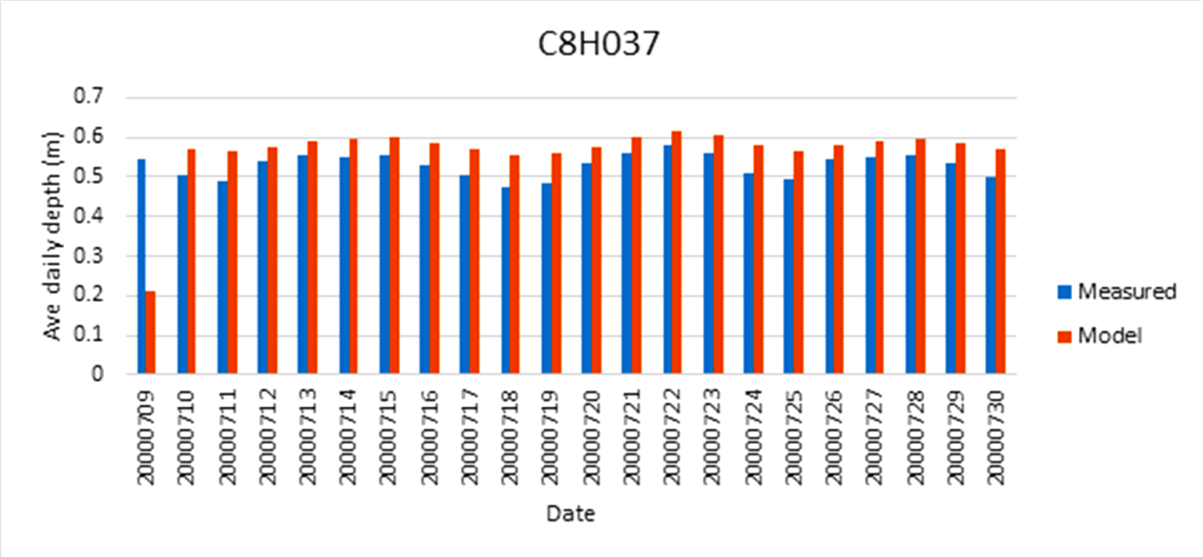

Figure 33: Modelled vs measured water elevations upstream of the Reward weir (C8H037)

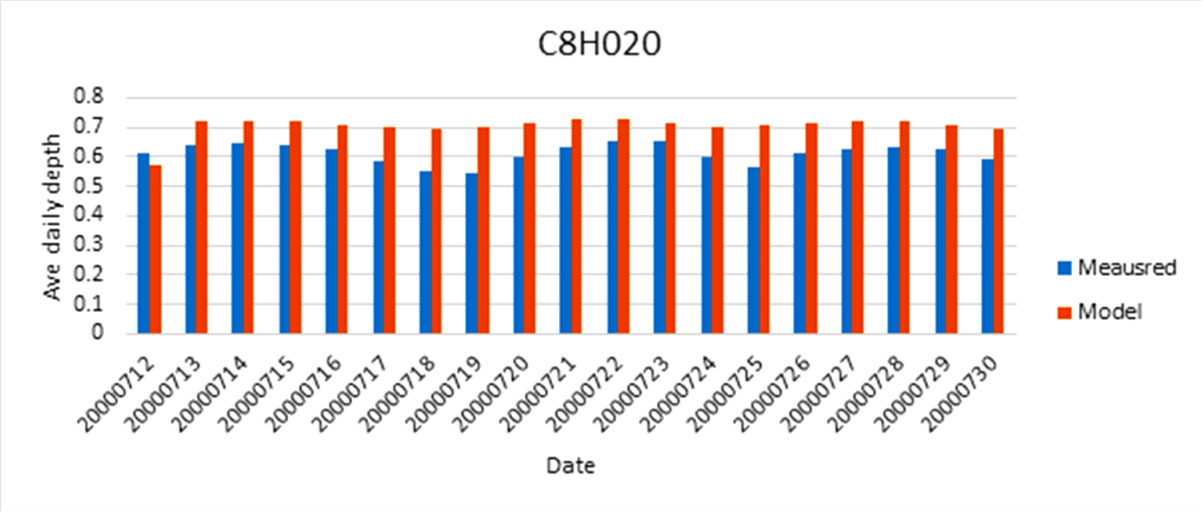

Figure 34: Modelled vs measured water elevations upstream of the Roodekraal weir (C8H020)

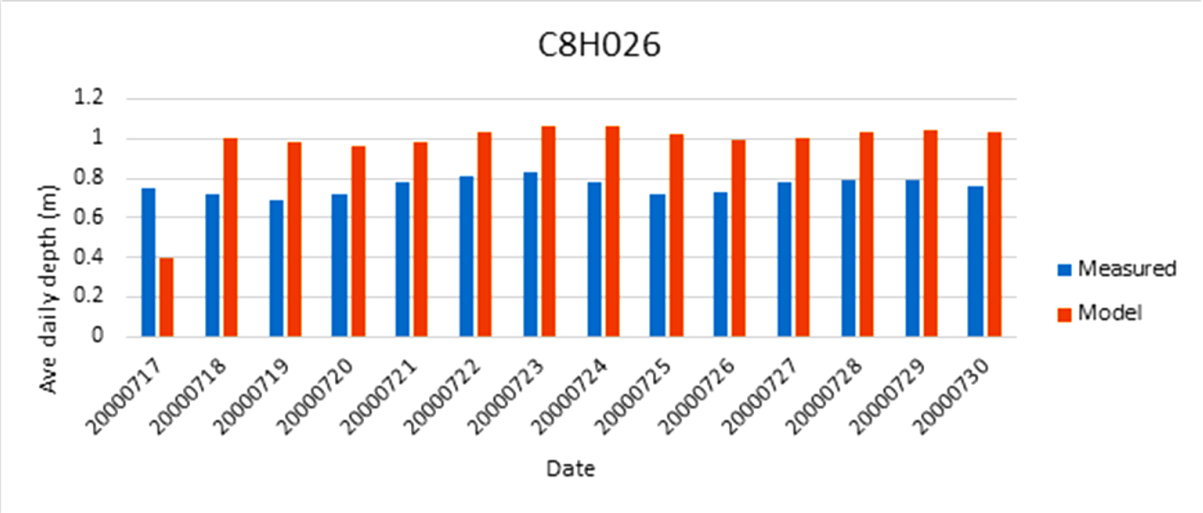

Figure 35: Modelled vs measured water elevations upstream of the Frederiksdal weir (C8H026)

2.6.5 SURFACE WATER MODELLING DATA ANALYSIS

A similar flow pattern observed at the Sol Plaatje release can be seen at the Katse Dam Tunnel (***Figure 36*** and ***Figure 37***). Hydropower generation at the Muela Dam is demand driven, and the volume of water released at the dam is directly dependant on the amount of energy generated. From ***Figure 37*** it can be seen that there is a clear increase in daily average flow during the week and decrease over the weekend, this is due to lower energy demands during weekends.

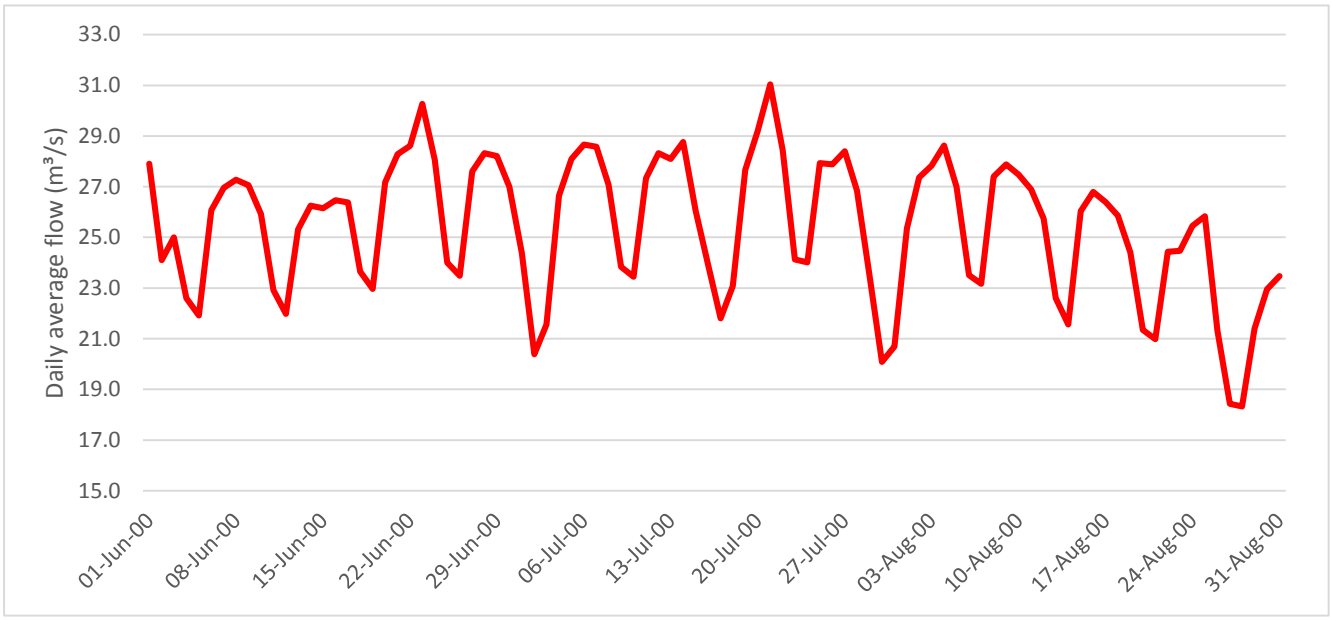

Figure 36: Daily average flow for the Sol Plaatje release (C8R004)

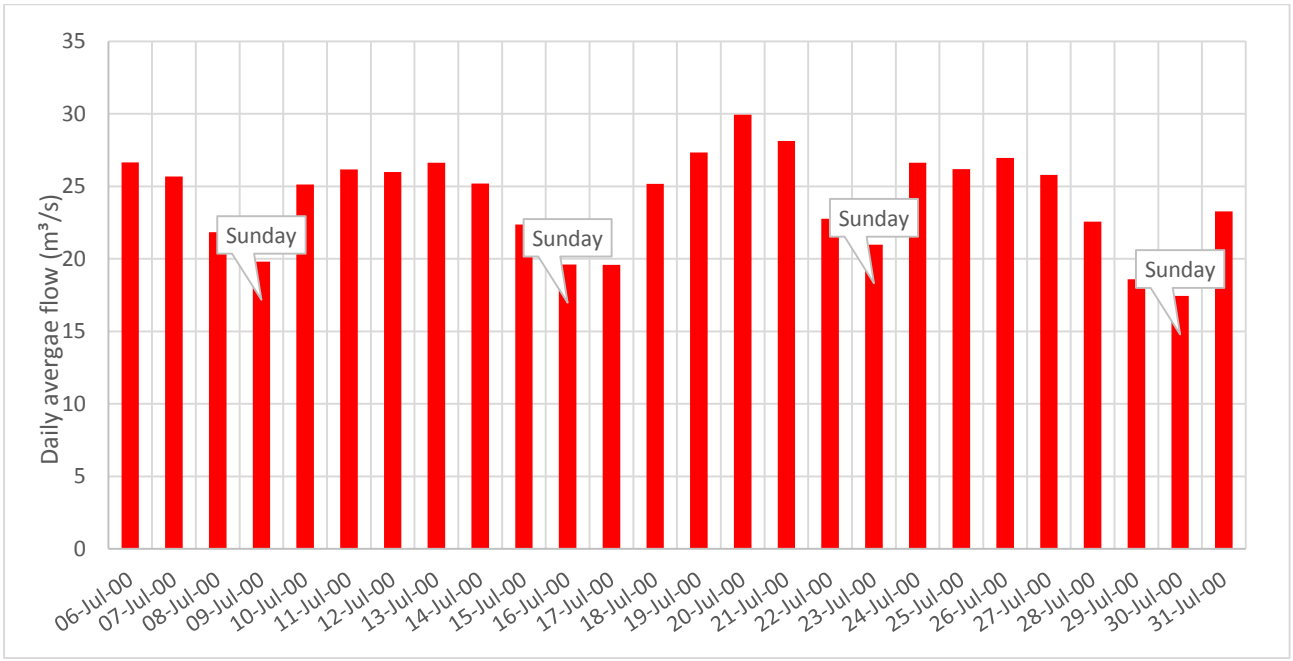

Figure 37: Daily average outlet at the Katse Dam Tunnel release (C8H036)

The volume of water released at the Katse Dam Tunnel is also influenced by the treaty between the government of the Kingdom of Lesotho and the government of South Africa. The agreement states that 680 million m³ water will be delivered to South Africa annually.

The water depth pattern within the river system was well represented however there is a clear discrepancy between the modelled and measured depths which increases downstream. This discrepancy is likely due to the limited and low-resolution survey data available at these locations. As discussed above the river bed spreads out further downstream, thus the water will cover a larger surface area.

Due to the discrepancy in the water elevation, the next step was to calibrate the model by analysing input and output flow patterns and volumes for the observed time period. The 2D flow area computation point spacing was set to 100x100m and the computation interval to a minute. The modelled and measured flow rates at the flow stations area provided in ***Figure 38***; ***Figure 39*** and ***Figure 40.***

The flow pattern within the river system is well represented in these graphs. There is a visible variance between the modelled and measured flows which increases as we move further downstream, this variance is however significantly small.

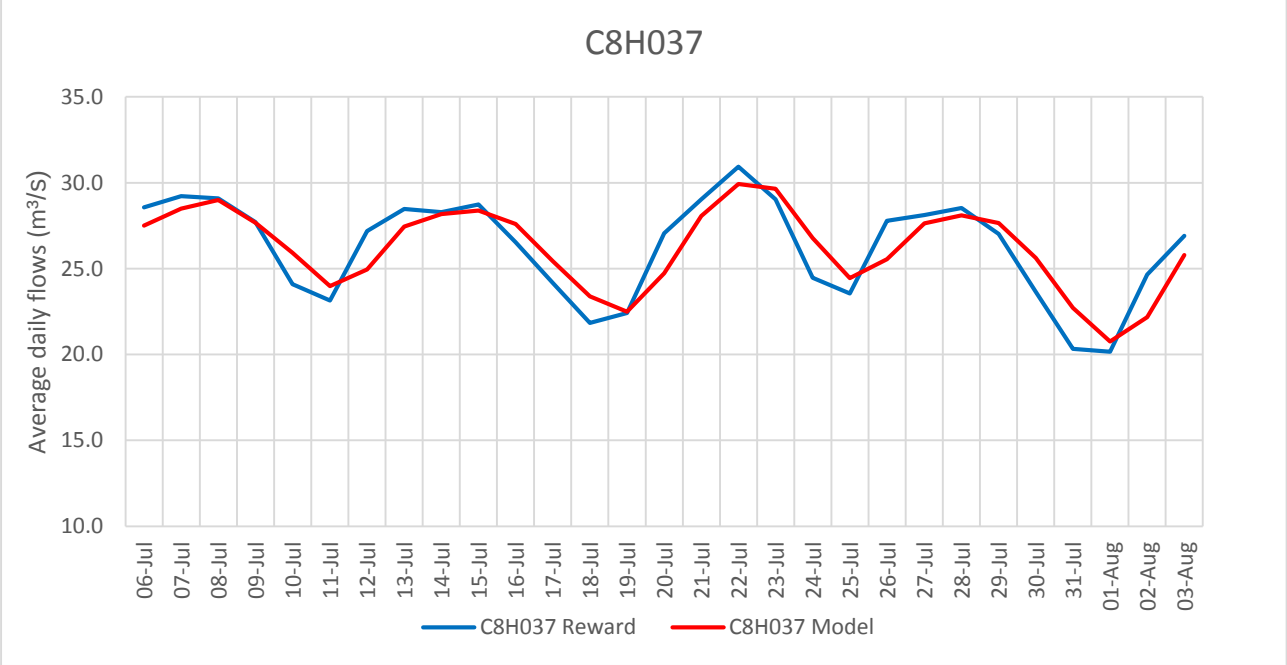

Figure 38: Modelled vs measured water volumes upstream of the Reward weir (C8H037)

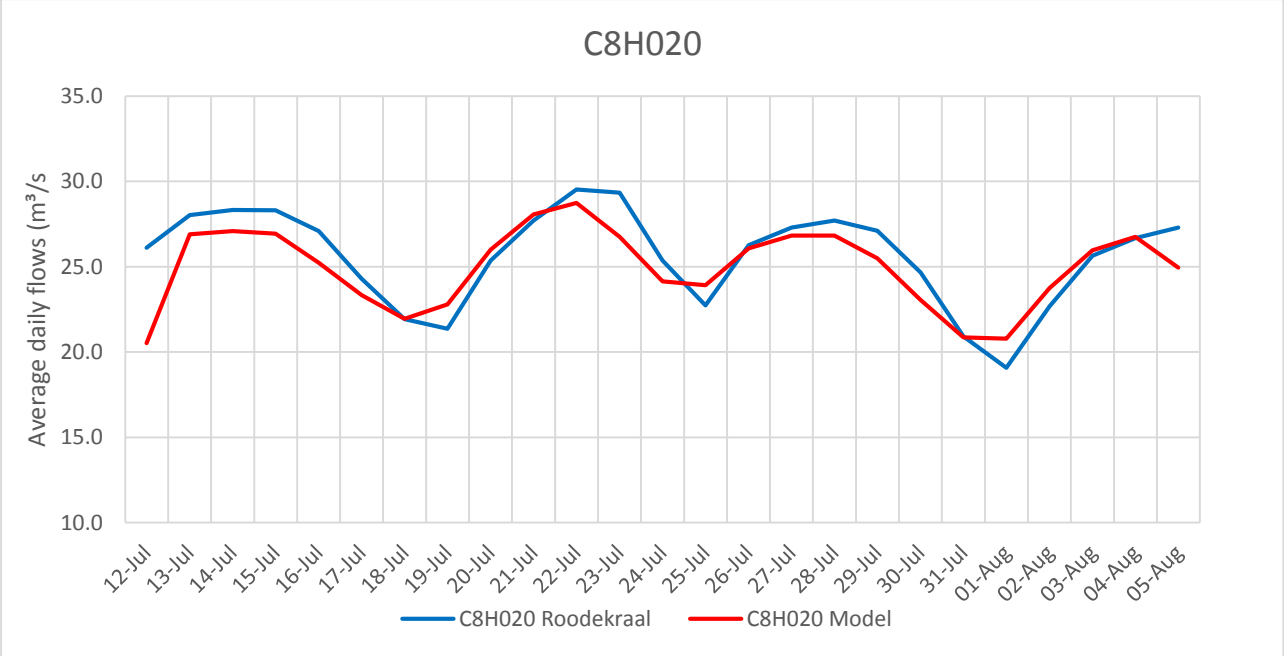

Figure 39: Modelled vs measured water volumes upstream of the Roodekraal weir (C8H020)

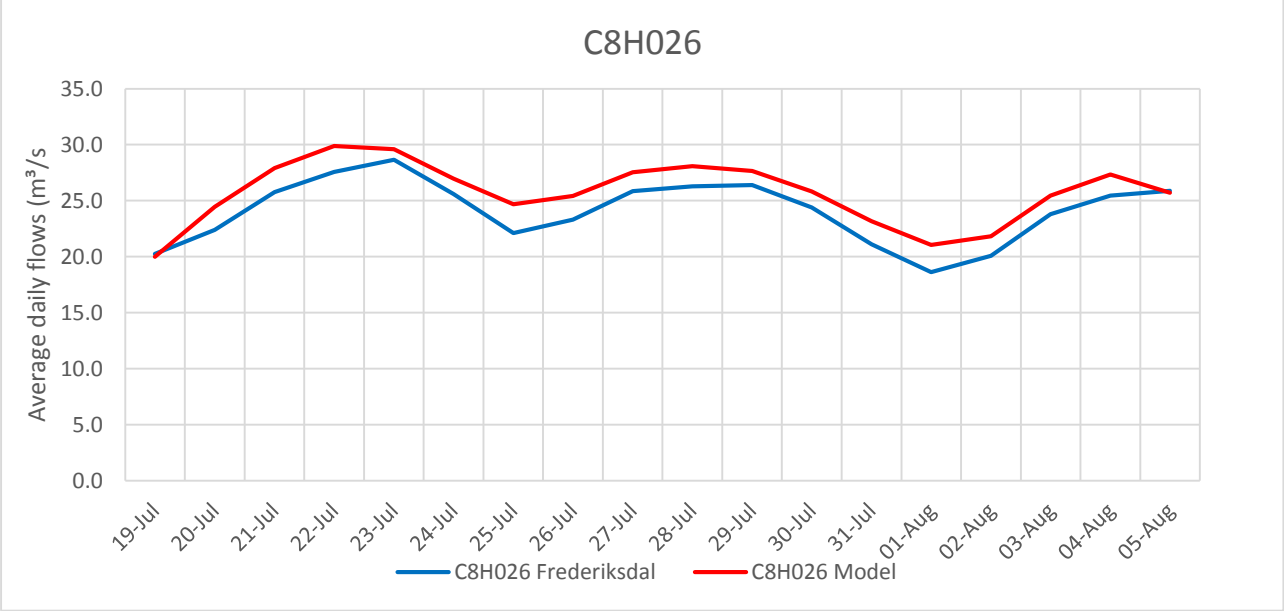

Figure 40: Modelled vs measured water volumes upstream of the Frederiksdal weir (C8H026)

The variance between September flowrates measured at Reward and Sol Plaatje that was identified in Section

2.6.6 SURFACE WATER MODELLING CONCLUSION

The results from the HEC-RAS model are showing that there is no significant gain or loss due to/from groundwater for the analysed period as seen in ***Figure 41***.

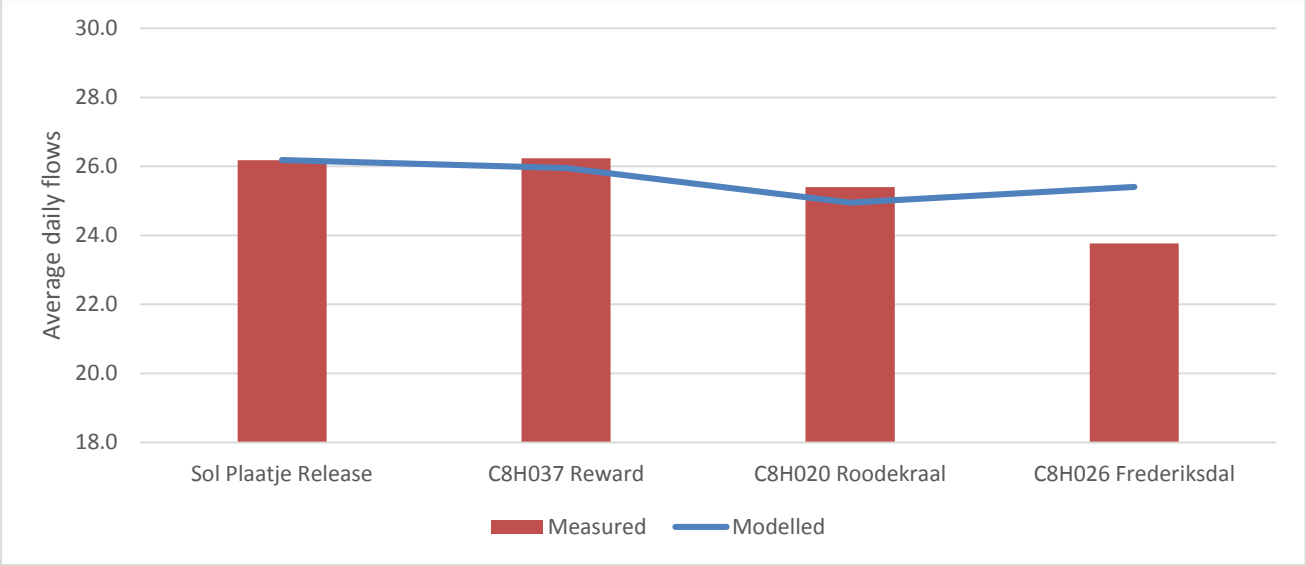

Figure 41: Modelled vs measured daily flows for the monitoring stations

It can therefore be concluded that the HEC-RAS model is suitable to determine the possibility of groundwater ingress and losses.

But the model is not limited to this application as it could have noteworthy operational benefits which include the following:

- Real time prediction of flood events;
- Prediction of floodplains based on a typical rainfall storm;
- Accurate water discharged requirements at the Ash River Tunnel and Sol Plaatje Dam;
- Analysing and or predicting water losses in the system due to abstractions;
- Analysing and or predicting water gains in the system due to runoff, sewage treatment plants etc.
- Management of environmental flows.

3. NUMERICAL MODELLING COMPONENT: SCENARIOS AND RESULTS

3.1 COMPUTER CODES

The software code chosen for the numerical finite-element modelling work was the 3D groundwater flow model SPRING, developed by the delta h Ingenieurgesellschaft mbH, Germany (König, 2011). The program, formerly known as SICK 100, was first published in 1970, and since then has undergone a number of revisions. The current saturated and unsaturated program module SPRING-SITRA is based on the well-known SUTRA model (Voss, 1984). SPRING is widely accepted by environmental scientists and associated professionals. SPRING uses the finite-element approximation to solve the groundwater flow equation. This means that the model area or domain is represented by a number of nodes and elements. Hydraulic properties are assigned to these nodes and elements and an equation is developed for each node, based on the surrounding nodes. A series of iterations are then run to solve the resulting matrix problem utilising a pre-conditioning conjugate gradient (PCG) matrix solver for the current model. The model is said to have "converged" when errors reduce to within an acceptable range. SPRING is able to simulate steady and non-steady flow, in aquifers of irregular dimensions.

3.2 GOVERNING EQUATIONS

SPRING solves the stationary flow equation independent of the density for variable saturated media as a function of the pressure according to:

$$-\nabla(K_{ij}\nabla h) = -\nabla\left(K_{perm}\frac{\rho g}{\mu}\nabla h\right) = q = -\nabla\left[\frac{K_{perm}\cdot k_{rel}}{\mu}(\rho g\nabla z + \nabla p)\right]$$

∇ $\left(\frac{\partial}{\partial x},\frac{\partial}{\partial y},\frac{\partial}{\partial z}\right)$

q Darcy flow
K_{ij} Hydraulic conductivity tensor
ρg Density · gravity
K_{perm} Permeability
μ Dynamic viscosity
k_{rel} Relative permeability
p Pressure

The relative hydraulic conductivity is hereby calculated as a function of water saturation, which in turn is a function of the saturation:

$$k_{rel}(S_r) = (S_e)^l\left[1-\left(1-(S_e)^{\frac{1}{m}}\right)^m\right]^2$$

$$S_e = \frac{S_r(p)-S_{res}}{S_s-S_{res}} = \left[1+\left(\frac{p_c}{p_e}\right)^n\right]^{\frac{1-n}{n}}$$

$S_r(p)$ Relative saturation dependent on pressure
S_e Effective saturation
l Unknown parameter, determined by van Genuchten to 0.5

m equal to $1-(1/\mathrm{n})$
n Pore size index
S_{res} Residual saturation

S_s Maximum saturation
p_c Capillary pressure
p_e Water entry pressure

Solving these equations for the relative saturation as a function of the capillary pressure $S_r(p_c)$ results in the capillary pressure- saturation function according to the Van Genuchten (1980) model as used in SPRING:

$$S_r(p_c) = S_{res} + (S_s - S_{res}) \cdot \left[1 + \left(\frac{p_c}{p_e}\right)^n\right]^{\frac{1-n}{n}}$$

The water entry pressure is a soil specific parameter and defined as the inverse of a = $1/p_e$ in the saturation parameters.

The density independent, transient flow equation for variable saturated media as a function of the capillary pressure is given as follows:

$$\rho\left(S_r(p_c)S_{sp} + \theta\frac{\partial S_r(p_c)}{\partial p}\right)\frac{\partial p}{\partial t} + \theta S_r(p_c)\frac{\partial \rho}{\partial t} - \nabla\left[\rho\frac{K_{perm}k_{rel}}{\mu}(\nabla p + \rho g \nabla z)\right] = q$$

The specific pressure dependent storage coefficient S_{sp} is hereby given as

$$S_{sp} = \alpha(1-\theta) + \beta\theta$$

α Compressibility of porous media matrix
β Compressibility of fluid (water)
θ Aquifer porosity

The transport equation for a solute in variably saturated aquifers is given as follows:

$$\theta S_r(p_c)\frac{\partial c}{\partial t} + \theta S_r(p_c) v\nabla c - \nabla\left(\theta S_r(p_c)\left(D_m\bar{\bar{1}} + D_d\right)\nabla c\right) = qc^* + R_i$$

qc^* Volumetric source/sink term with concentration c ∗
D_m Molecular diffusion
$\bar{\bar{1}}$ Unit matrix
D_d Hydrodynamic dispersion
R_i Reactive transport processes (sorption, decay, etc.)

The software is therefore capable to derive quantitative results for groundwater flow and transport problems in the saturated and unsaturated zones of an aquifer.

3.3 EQUATIONS DESCRIBING THE SURFACE – GROUNDWATER INTERACTION

Surface-groundwater interaction is in groundwater flow models commonly described with a third type or Cauchy boundary condition, whereby mathematically a relation between value of a function and its derivative (e.g. flow rate) is specified. In the case of surface-groundwater interaction, the value of the function represents the head whereas the derivative of the function represents the gradient, which in combination with Darcy's law gives a flow rate. The specific flux q (per unit area) is then directly proportional to the head gradient between a surface water course and groundwater.

$$q = -k\Delta h = \alpha\left(h_{WCL} - h_{GWL}\right)$$

Depending on the prevailing gradient, a river might receive (gaining stream or effluent groundwater conditions) or lose (losing stream or influent groundwater conditions) water from the aquifer
(*Figure* ***42***). While perennial streams are primarily effluent, ephemeral streams are primarily influent. Several other cases might be differentiated, like a disconnected or perched losing river (groundwater head falls below the base of the river) or a flow-through river which is simultaneously gaining and losing water due to different head gradients on either bank.

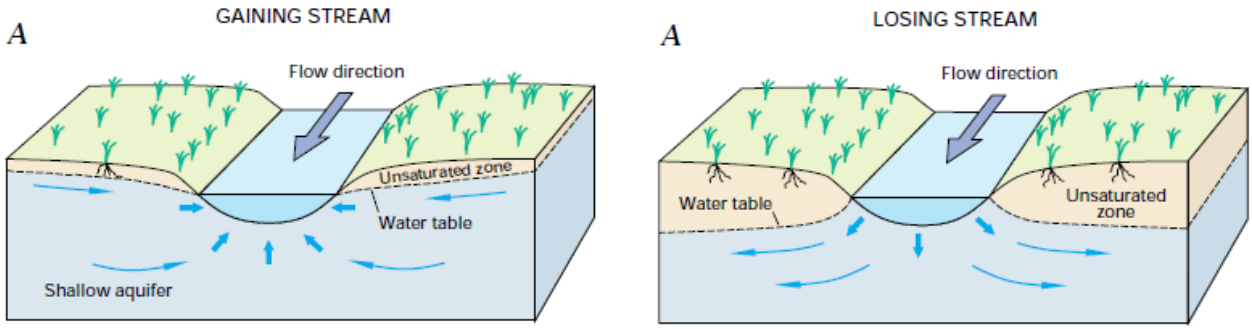

Figure 42: Conceptualisation of surface-groundwater interactions (Winter et al. 1998).

The rate at which a river gains or loses water is determined by the presence and conductivity of stream bed sediments or colmation layers. The vertical streambed leakage coefficient α [1/s] is hereby defined as the ratio of the hydraulic conductivity of streambed sediments k_f divided by its thickness *d*, and usually differs for effluent and influent conditions:

$$\alpha = \frac{k_f}{d}$$

In other words, the direction of the flow and the flow rate between a surface water body and the aquifer is determined by the mostly linear relation between the water course level h_{WCL} in the surface water and the groundwater level h_{GWL}, and the corresponding function called the leakage function (***Figure 43***).

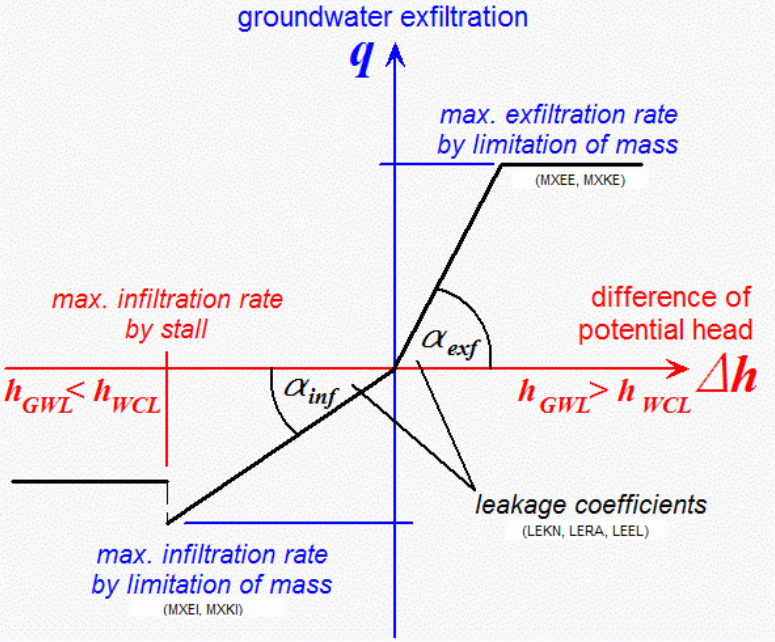

Figure 43: Schematic representation of the leakage function (König 2011).

Once the groundwater levels fall below the stream bottom and the stream becomes disconnected or perched, the river losses reach a maximum rate, which will not be exceeded regardless of further increases of the head difference. Bouwer and Maddock (1997) estimated that the losses from a losing river (influent conditions) reach already a maximum when the depth to the groundwater-table is greater than twice the river width. For certain situations, limiting the exfiltration rate might also be required.

While the chosen software code allows generally defining different leakage rates and limits for influent and effluent conditions, lack of data, especially for larger scale models, often precludes such detailed differentiation of the leakage function.

3.4 MODEL DOMAIN

The Upper Vaal groundwater model domain covers a surface area of around 4831 km^2 and entails eight quaternary catchments (***Figure 44***), namely C83A, C83B, C83C, C83D, C83E, C83F, C83G, and C83H.

Note that the Skulpspruit quaternary catchment C83J was excluded from the model domain, as its confluence with the Liebenbergsvlei is downstream of the last flow gauging weir in Frankfort (*Figure **44***). The catchment represents therefore an entirely separate surface and groundwater flow system from the other catchments listed above and was excluded from the numerical model domain to reduce computational efforts (CPU time).

A brief hydrological overview of the quaternary catchment based on the surface-groundwater assessment part of the GRAII project by the Department of Water Affairs and Sanitation is given in Table 10.

Table 10: Hydrological overview of the quaternary catchment (data source: GRAII by DWS)

Quat	Area	MAP	Baseflow after			Recharge	Baseflow	Aquifer Recharge	GW Baseflow	Interflow	GW outflow
			Schultz	Pittman	Hughes						
	km^2	mm/a	mm/a	mm/a	mm/a	mm/a	mm/a	mm/a	mm/a	mm/a	mm/a
C83A	746	691	4.89	10.9	17.45	18.33	16.94	11.08	9.44	7.50	0.10
C83B	251	667	4.56	9.2	14.83	15.94	14.53	11.08	9.05	5.47	0.29
C83C	828	662	4.20	9	13.23	14.28	12.91	10.70	8.65	4.25	0.09
C83D	465	649	4.22	8.1	13.14	14.22	12.83	10.75	8.68	4.15	0.16
C83E	426	653	4.08	8.5	12.42	13.57	12.24	10.64	8.46	3.77	0.17
C83F	875	636	2.58	8.6	12.27	13.42	10.67	8.85	6.53	4.12	0.08
C83G	695	646	2.71	9.1	13.42	14.46	11.60	8.96	6.75	4.83	0.11
C83H	547	646	2.69	8.9	13.37	14.04	11.47	8.74	6.41	4.93	0.13

The model boundaries follow generally the quaternary surface water catchment boundaries along topographical highs, which are considered to represent also groundwater divides or natural flow boundaries based on the observed correlation between water table and surface elevation (***Figure 44***).

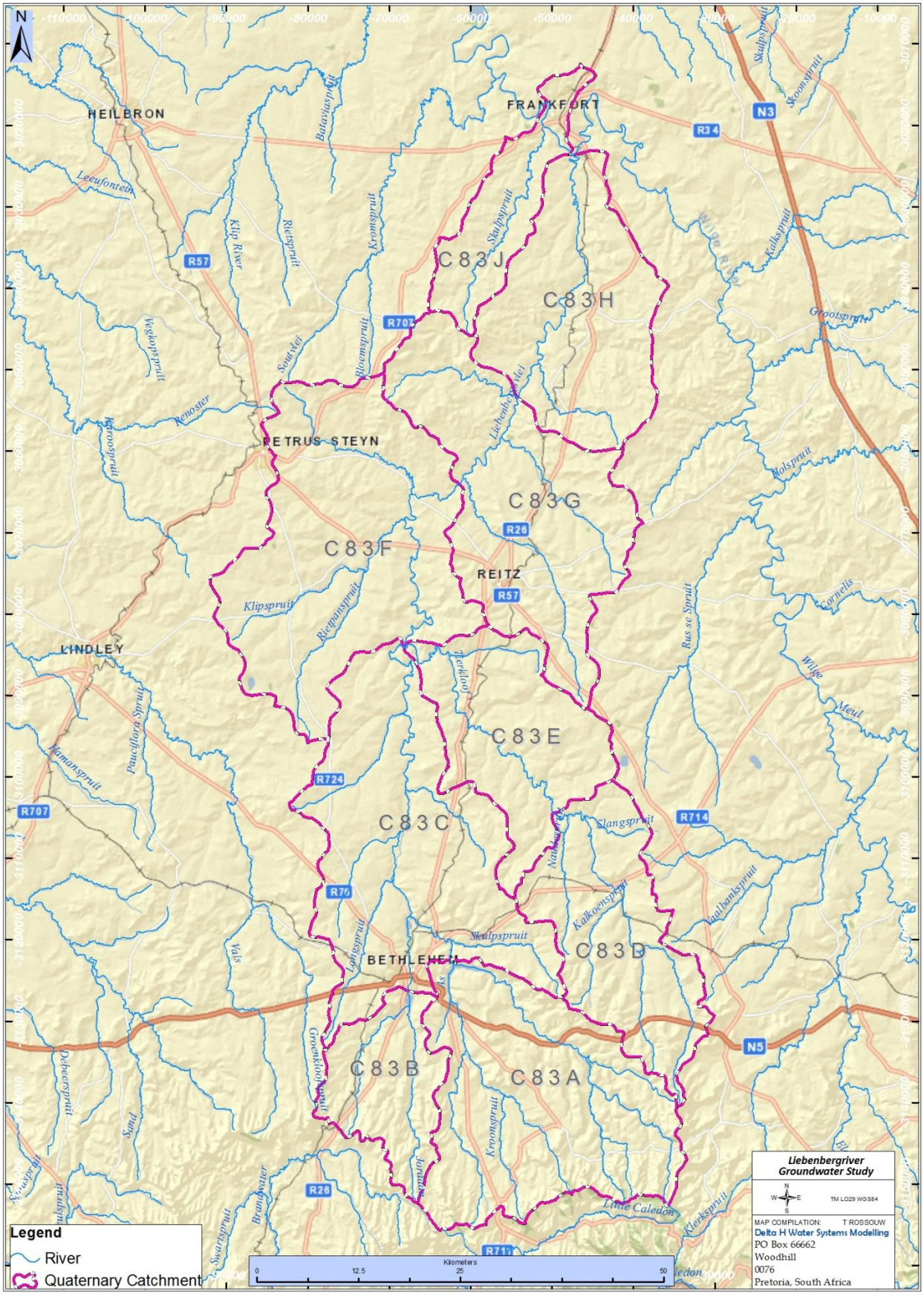

Figure 44: Upper Vaal groundwater model domain.

The finite-element model was set-up as a three-dimensional groundwater flow model. In view of the capabilities of the used software to simulate outcropping layers, the layers were arranged to represent the conceptual model, i.e. the weathered, alluvial and fractured aquifers. The layer used to represent the alluvial sediments is therefore only present along the main surface water courses and not present throughout the model domain (***Figure 45***).

Figure 45: Example of vertical grid layout with a separate discontinuous layer (indicated in red) representing alluvial aquifers.

The model domain was spatially discretized into 128 617 nodes on four node layers, which make up three element layers with 169 043 elements (triangles and quadrangles) each. The horizontal element size (side length) varies from a minimum of 15 m along certain river sections to a maximum of 300 meters (*Figure* ***46***) further away from areas of expected steep groundwater gradients. The spatially variable lateral and vertical discretization of the finite-element model domain allows to accurately incorporate the surface water courses as well as the accompanying alluvial aquifers in the regional Upper Vaal groundwater flow model.

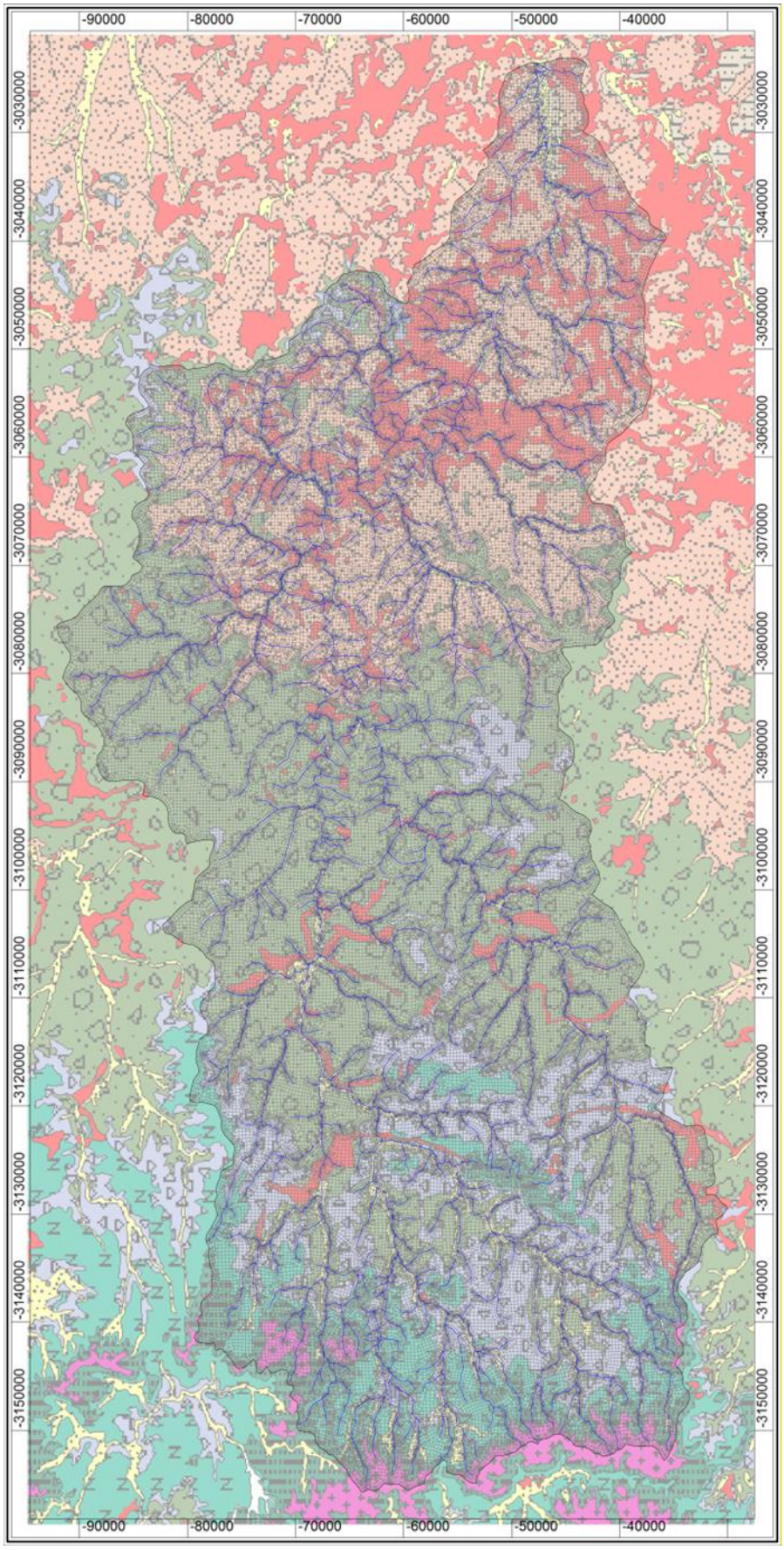

Figure 46: Mesh layout for the Upper Vaal groundwater flow model.

3.5 GROUNDWATER ELEVATIONS AND FLOW DIRECTIONS

One hundred seven (107) water levels were collated from boreholes over the study area, which includes monitoring data from the 2015 hydrocensus by the project team as well as data from the National Groundwater Archive (NGA). Water levels range from 1 mbgl to 55 mbgl, with an average of only 16.2 mbgl, suggesting that most of the boreholes measure the upper weathered aquifer. A plot of the groundwater table against surface elevation data for all boreholes (*Figure **47***) shows a correlation of 98% (Pearson product moment correlation coefficient R^2 = 0.98), indicating that the shallow regional water levels mimic surface topography within the study area and groundwater flows from higher lying ground towards lower lying ground and potentially into drainage systems (natural streams).

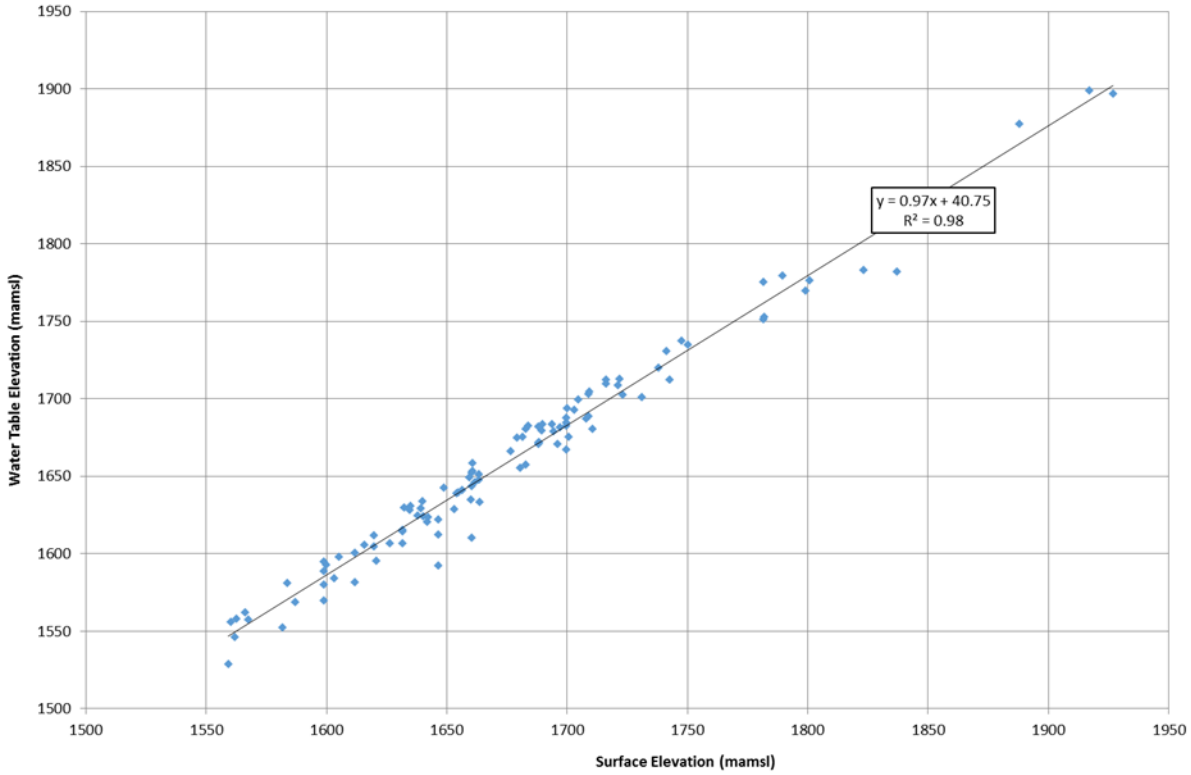

Figure 47: Correlation between surface topography and groundwater elevation in the Upper Vaal study area.

The observed correlation is used to improve the interpolation of initial water levels for the numerical model in data scarce environments by applying co-kriging based on known topography (Bayesian interpolation). A groundwater piezometric map was interpolated from the collated measured shallow water levels using Bayesian interpolation, based on the established correlation between surface topography and groundwater levels. The Bayesian interpolation method uses correlated data to improve the spatial interpolation of the unknown variable, in this case the groundwater level. As a Universal Kriging algorithm, it relies on a mathematical description of the change (or variance) of a variable with distance, i.e. to what extent neighboring observations are spatially correlated. Such correlation is expressed in a semi-variogram, as depicted in the empirical semi-variogram for the Upper Vaal study area below (*Figure **48***) with the fitted Bayesian

model used for the interpolation. The semi-variogram model is then used in combination with the knowledge of the surface elevation and its correlation to the groundwater elevation as a qualified guess to improve the spatial interpolation of water levels.

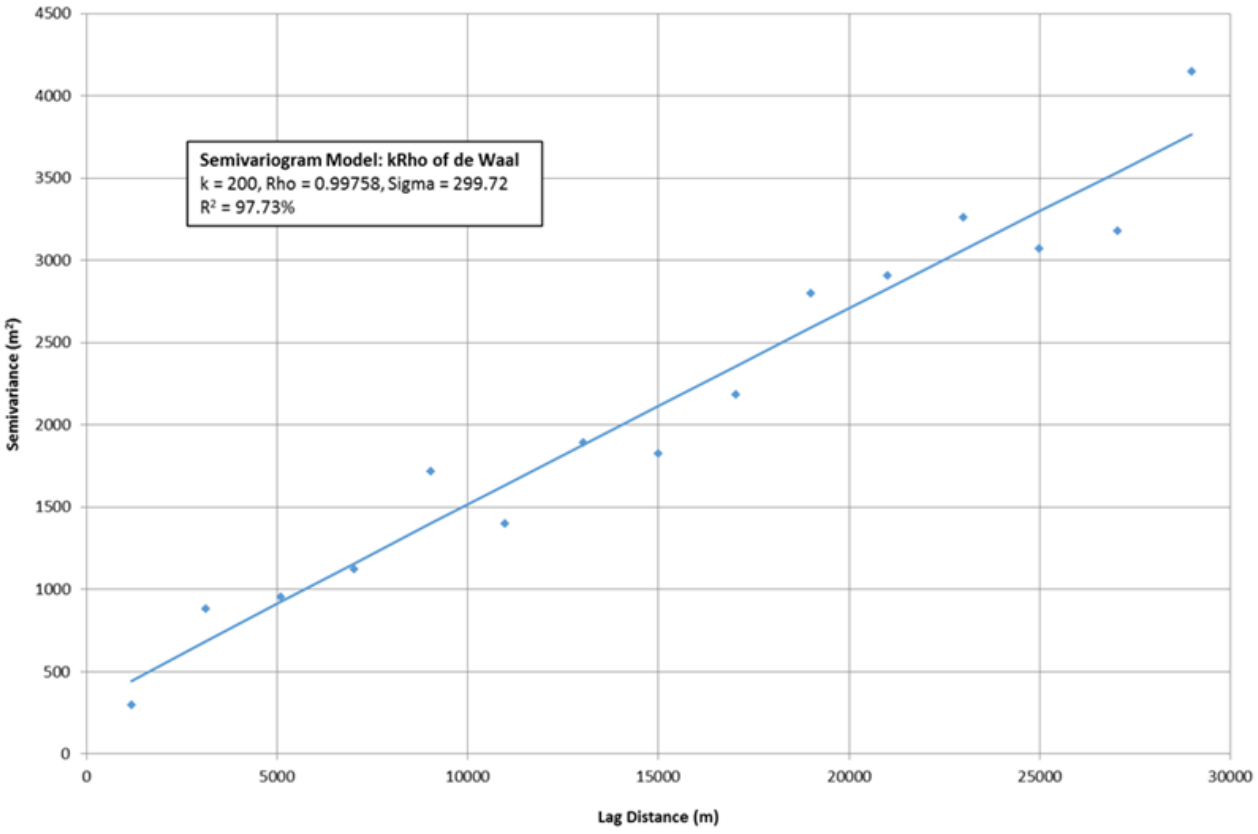

Figure 48: Empirical semi-variogram and fitted Bayesian model for the Upper Vaal study area.

The interpolated (unconfined) groundwater piezometric map using Bayesian interpolation (with the model parameters given above) is shown in *Figure **49*** and was subsequently used as initial heads for the model calibration. It must be noted that initial heads only accelerate the mathematical convergence of a steady-state model, but do not change the outcome of the model i.e. the calculated steady-state heads.

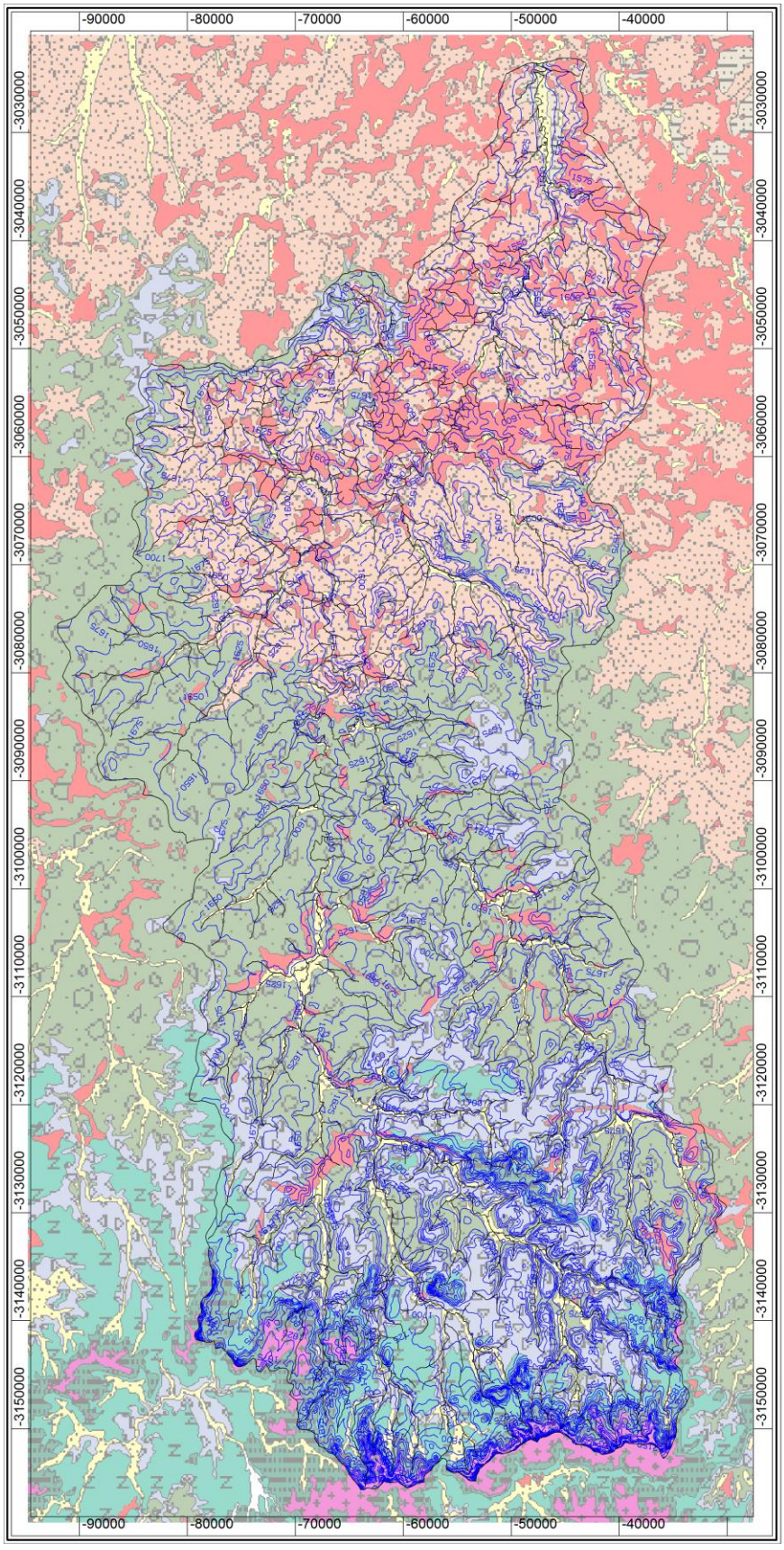

Figure 49: Initial water levels for the Upper Vaal study area.

3.6 SOURCES AND SINKS

3.6.1 GROUNDWATER RECHARGE

The groundwater recharge rates, as estimated by the hydrological working group of the GRAII project by the Department of Water Affairs and Sanitation (Table 10, column "Recharge") were assigned to the top layer of the different quaternary catchments of the model domain. The rates were considered fixed for the calibration of the model.

3.6.2 GROUNDWATER ABSTRACTIONS

Groundwater abstractions of 30 boreholes as registered in the WARMS database (Table 11) were assigned in the model setup. In the absence of verified abstraction rates, it was assumed that the registered use represents actual use.

Table 11: Registered groundwater abstractions (source: WARMS database)

Register No	X-Coord	Y-Coord	WU_Sector	Type	Date	Volume (m^3/a)
10002597	-50949.8	-3146206	AGRICULTURE: WATERING LIVESTOCK	BOREHOLE	2002-04-01	4000
10002837	-69408.8	-3112531	AGRICULTURE: IRRIGATION	BOREHOLE	2002-04-01	18616
10003836	-62827.5	-3126589	AGRICULTURE: IRRIGATION	BOREHOLE	2002-04-01	5604
10004764	-68690.9	-3113973	AGRICULTURE: WATERING LIVESTOCK	BOREHOLE	2002-04-01	2900
10004906	-62197.7	-3129175	AGRICULTURE: IRRIGATION	BOREHOLE	1980-01-01	5750
10004960	-69405.6	-3112537	AGRICULTURE: IRRIGATION	BOREHOLE	2002-04-01	46973
10005353	-56539.2	-3027264	AGRICULTURE: IRRIGATION	BOREHOLE	2002-04-01	200500
10005399	-50047	-3050805	INDUSTRY (URBAN)	BOREHOLE	2009-04-01	1095
10006352	-43662.4	-3054297	AGRICULTURE: IRRIGATION	BOREHOLE	2002-04-01	121500
10010891	-41218.7	-3046901	AGRICULTURE: IRRIGATION	SPRING/EYE	2002-04-01	213487.6
10015388	-47754.2	-3059852	AGRICULTURE: IRRIGATION	BOREHOLE	2002-04-01	6100
10015798	-46847.1	-3046152	INDUSTRY (NON-URBAN)	BOREHOLE	2002-04-01	12775
20001908	-62368	-3096547	INDUSTRY (NON-URBAN)	BOREHOLE	2010-01-01	1825
20003087	-72062.9	-3051784	AGRICULTURE: IRRIGATION	BOREHOLE	2002-04-01	12200
20003915	-50538.3	-3114960	AGRICULTURE: IRRIGATION	BOREHOLE	2002-04-01	13950
20013478	-48239	-3014572	INDUSTRY (NON-URBAN)	BOREHOLE	2002-04-01	1825
20016144	-76981.7	-3119103	AGRICULTURE: IRRIGATION	BOREHOLE	2008-10-01	12253
20020790	-68764.4	-3127876	INDUSTRY (NON-URBAN)	BOREHOLE	2002-04-01	1825
20021245	-64964.6	-3117492	INDUSTRY (NON-URBAN)	BOREHOLE	2002-04-01	5810
20030093	-82795.7	-3063950	INDUSTRY (URBAN)	BOREHOLE	1969-01-01	21900
20037899	-34231.9	-3145256	INDUSTRY (URBAN)	BOREHOLE	2007-07-01	5760

20038807	-60497.8	-3129996	INDUSTRY (NON-URBAN)	BOREHOLE	2002-04-01	277
20039129	-50802.5	-3047228	INDUSTRY (URBAN)	BOREHOLE	2002-04-01	263
20042268	-60295.2	-3059329	INDUSTRY (URBAN)	BOREHOLE	2006-01-01	1153
20042366	-63044.1	-3146164	INDUSTRY (NON-URBAN)	BOREHOLE	2007-03-01	335
20042918	-39127.9	-3037492	INDUSTRY (URBAN)	BOREHOLE	2011-06-01	21600
20043025	-50610.4	-3077943	INDUSTRY (NON-URBAN)	BOREHOLE	2012-11-01	10950
20044159	-39836	-3042006	INDUSTRY (URBAN)	BOREHOLE	2012-03-01	3600
20044239	-47838	-3050444	INDUSTRY (NON-URBAN)	BOREHOLE	2012-03-01	3600
20044809	-57325.6	-3078761	INDUSTRY (NON-URBAN)	BOREHOLE	2012-11-01	2250

3.6.3 SURFACE WATER

Water leaves the model domain via numerous perennial and non-perennial rivers. A river or 3rd type (Cauchy) boundary condition was assigned to the streams and river courses within the model domain, whereby the leakage of groundwater into the river (or vice versa) depends on the prevailing gradient. Furthermore, using the river network mass balance approach built into SPRING, losses of downstream river stretches are limited to upstream groundwater baseflow or artificial discharge (e.g. Ash River outlet) into the river network. By preventing unrealistic water losses from individual river stretches, the approach ensures a dependable mass balance for surface water courses in the model domain.

Based on estimated baseflow rates for the catchments of interest (chapter 6.4), the streams/rivers were generally classified as potentially gaining streams/rivers with limited leakage of surface water into the aquifer respectively the model domain allowed along the perennial river stems. With the chosen approach no water losses occur from the non-perennial rivers into the model domain, but groundwater on either side of the river/drainage might discharge into it as a function of the calculated gradients. In the absence of site specific data, leakage of groundwater into the rivers/streams was initially assumed to be not constricted by semi-pervious layers in the river bed and a leakage coefficient equivalent to the aquifer permeability assigned to the river. The final leakage coefficients for the main river systems were then calibrated based on estimated baseflow values (see Table 10).

A uniform incision of 4 meters below the surrounding topography was assumed for the hydraulic active river bed for all rivers in the model domain.

As for the surface water model, the following additional discharges into or abstractions from surface water courses were considered in the groundwater flow model (Table 12):

Table 12: Registered surface water discharges and abstractions (source: WR2012 and municipal data 2009)

Quaternary catchment	Long	Long	Annual inflow (+)/abstraction (-) (Mm3/a)	Comment
C83A	-28.43917	28.39722	+683 (average 1999 to 2009)	Tunnel outlet

C83a	Upstream of Sol Plaatje Dam		-7.69	Bethlehem Town Supply 2009
C83C	-28.213615	28.31139	+4.50	Bethlehem Discharge 2009
C83G	Upstream of Roodekraal		-0.96	Reitz Abstraction

3.6.4 REGIONAL GROUNDWATER FLOW

While the shallow groundwater levels follow generally surface topography (*Figure **49***) and shallow groundwater and surface water catchments therefore likely to correspond, the same is not proven and likely to be true for the deeper fractured groundwater flow system. This is attributable to the heterogeneity of the fractured aquifers as well as the depth of such flow systems, where recharge and discharge areas can be substantial distance apart based on the geological, structural and topographic setting.

Especially deeper regional groundwater outflows from the model domain are important for the overall water balance of the model, as they allow water to leave the model domain without discharging into surface water courses, i.e. If no deeper groundwater outflows are assumed, the assigned groundwater abstractions and the river boundaries represent the only sinks available for water recharged over the model domain. So any recharged water not abstracted from boreholes would then have to report to surface water courses to comply with the water balance and artificially inflate the groundwater contribution to baseflow in the quaternary catchments.

Unfortunately, the absence of deep monitoring boreholes (beyond 60 meters below ground level) in the study area precludes the understanding or quantification of deeper groundwater flow systems.

3.7 BOUNDARY CONDITIONS

An overview of the physical features and assigned boundary conditions used in the Upper Vaal groundwater flow model is given in Table 13

Table 13: Boundary conditions assigned in the Upper Vaal Groundwater Model

Boundary	Element layer	Natural feature	Assigned boundary condition
Top	I	Land surface	Rainfall recharge, see Table 10
Top	I	Surface water courses	River network, losses limited to upstream gains
E, S, W	I - III	Quaternary catchment boundary, topographic high	No-flow
N	II - III	Deeper groundwater flow	Specified head
Internal	I-II	Groundwater abstractions	Abstraction rates, see Table 11
Internal	I	Surface water abstractions/discharges	Abstraction/discharge rates, see Table 12

3.8 MODEL CALIBRATIONS

3.8.1 CALIBRATION TARGETS

The average groundwater levels (in meters above mean sea level) measured in 67 boreholes within the immediate model domain were used as targets for the steady-state calibration. It is

obvious that the water levels, measured several years to decades (water levels measured between 1980 and today were considered) apart and potentially only as a once off in a single season are far from ideal for calibration purposes. The water levels were nevertheless utilized to increase the number of calibration targets (sic. monitoring points) and to ensure a regional spread of calibration targets, instead of only using the most recent water level measurements along the Liebenbergsvlei. However, more emphasis was placed on fitting the water levels measured during the 2015 hydrocensus by the project team.

To avoid errors associated with different elevation measurements or estimates in the data set, the water levels as measured in meters below ground level were converted into meters above mean sea level based on the digital elevation model used in the groundwater model for the purpose of calibration.

Secondary calibration targets were provided the estimated groundwater baseflow values per quaternary catchment as provided in Table 10. The leakage rates of the main river systems per quaternary catchment were for this purpose manually altered until a reasonable agreement of the baseflow values was achieved. Since the groundwater baseflow values provided in Table 10 are also outcomes of mathematical models with significant variability amongst the applied models, no further effort was placed on an exact match thereof.

The calibration was done by manually altering assigned hydraulic conductivity values until a best fit between observed and simulated water levels was achieved. As modeled groundwater levels are directly related to the assigned recharge rates and strata hydraulic conductivities, the estimated recharge rates were fixed during calibration to arrive at a potentially unique solution of the model. Similarly, to avoid the introduction of another set of unknown calibration parameter, vertical hydraulic conductivities were fixed at 5% of the horizontal conductivities.

3.8.2 INITIAL CONDITIONS

The initial conditions specified in the steady state flow model were as follows:

- Starting heads for the aquifers were interpolated from measured shallow water levels using Gaussian interpolation and used as initial heads for the steady-state simulations (*Figure **49***).
- Horizontal hydraulic conductivities of 1E-06 m/s for the weathered and 1E-07 m/s for the fractured aquifer.
- Vertical hydraulic conductivities were set at 10% of the horizontal conductivities.
- Porosity values do not influence the outcome of the steady-state flow model, but only the transient model results. The effective porosity values were specified as 12% for the weathered and alluvial aquifer and 5% for the fractured aquifer.

3.8.3 NUMERICAL PARAMETERS

SPRING uses an efficient preconditioned conjugate gradient (PCG) solver for the iterative solution of the flow and transport equation. The closure criterion for the solver, i.e. the convergence limit of the iteration process was set at a residual below 1e-06. The Picard iteration, used for the iterative computation of the relative permeability for each element as a function of the relative saturation respectively capillary pressure, used a damping factor of 0.3 and was limited to 7 iterations. The relative difference between the two computed potential heads or capillary pressures after 8 iterations was generally below an acceptable 0.1 m.

3.8.4 STEADY STATE CALIBRATION

Groundwater levels measured in 67 boreholes within the model domain were assumed to be representative of the "more recent", average aquifer conditions and used as the primary calibration targets. The baseflow estimates in Table 10 were used as broad secondary calibration targets to enable the calibration of leakage coefficients and the derivation of reasonable baseflow values.

Since the modelled groundwater levels are directly related to the assigned recharge rates and hydraulic conductivities, an independent estimate of one or the other parameter is required to arrive at a potentially unique solution of the model. The estimated recharge rates were therefore considered fixed during the calibration and only hydraulic conductivities varied. Similarly, no attempt was made to change hydraulic conductivity values within different geological units, so as to achieve representative uniform aquifer parameters for these.

The original model was run with the initial conditions and the hydraulic conductivities and leakage coefficients of the river courses adjusted using sensible boundaries until a best fit between measured and computed values was achieved (*Figure **50***).

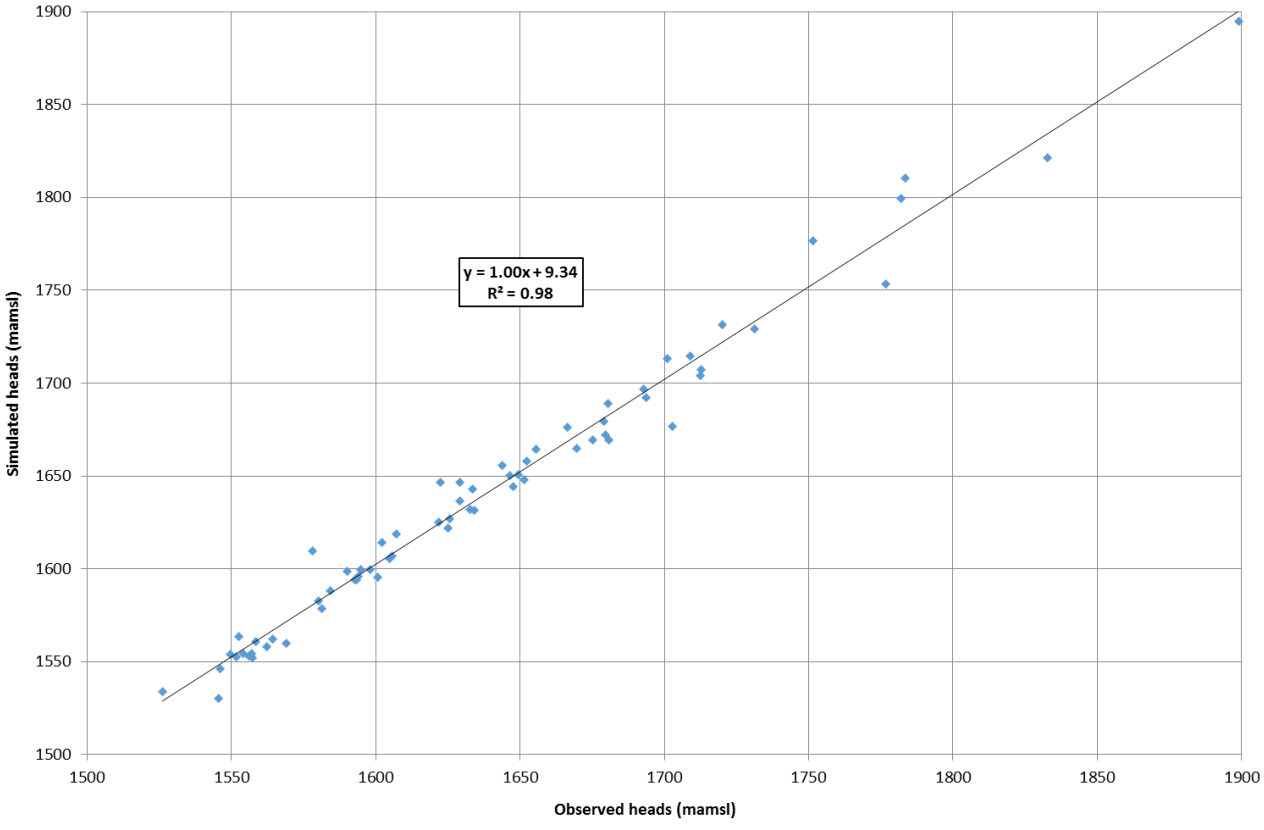

Figure 50: Steady-state calibration of the Upper Vaal Groundwater Flow Model.

The steady-state model calibration (*Figure **50***) achieved a 98% correlation (R^2 = 0.98) between observed and modeled heads. No obvious bias of simulated heads, i.e. no systematic deviation towards too high or too low simulated heads in comparison to observed heads (even distribution

of data points around regression line in *Figure **50*** and confirmed by the unit slope of the regression line (y = 1x + 9.34).

The root mean square error (RMSE) respectively the normalised root mean square error (NRMSE) were used as additional quantitative indicators for the adequacy of the fit between the 67 (=*n*) observed (h_{obs}) and simulated (h_{sim}) water levels:

$$RMSE = \sqrt{\frac{\sum(h_{obs} - h_{sim})^2}{n}}$$

$$NRMSE = \frac{RMSE}{h_{max} - h_{min}}$$

The normalised root mean square error scales the error value to the overall range of observed heads within a model domain (here $h_{max} - h_{min}$ =1899 mamsl - 1526 mamsl = 373 m), with values lower than 10% considered acceptable.

Despite the intended constraint of uniform hydraulic conductivity values for the different geological units, a root mean square error of RMSE = **8.77** and normalised root mean square error of NRMSE = **2.35 %** was achieved during the steady-state calibration of the Upper Vaal groundwater flow model are is considered more than adequate.

A comparison of observed (or rather estimated based on hydrological models) and simulated baseflow values for the different quaternary catchments is given in Table 14. Without any significant alterations to the leakage coefficients (reflecting the hydraulic conductivity of alluvial sediments, i.e. the absence of any clayey colmation layer), the simulated baseflow values show a very good agreement to especially the estimates by Hughes as referenced in the GRAII dataset.

In other words, the consideration of surface - groundwater interaction in the numerical groundwater flow model appears to replicate baseflow figures as put forward in the surface water run-off model, increasing the confidence in these values.

Table 14: Estimated (GRAII) and simulated baseflow values in the Upper Vaal Groundwater Model.

Quaternary catchment	Baseflow Estimates (Mm^3/a)				
	Schultz	Pitman	Hughes	GRAII	Model
C83A	3.65	8.13	13.02	12.64	13.42
C83B	1.15	2.31	3.72	3.65	3.54
C83C	3.48	7.45	10.95	10.69	11.67
C83D	1.96	3.77	6.11	5.97	6.54

Quaternary catchment	Baseflow Estimates (Mm^3/a)				
	Schultz	Pitman	Hughes	GRAII	Model
C83E	1.74	3.62	5.29	5.21	5.50
C83F	2.25	7.53	10.74	9.34	11.55
C83G	1.88	6.32	9.33	8.06	9.29
C83H	1.47	4.87	7.31	6.27	7.32

The general acceptable fit of observed heads and estimate baseflow values confirms the suitability of the model to predict average regional water levels and baseflow rates towards the surface water courses and the calibrated hydraulic conductivity values (Table 15) were subsequently used for the predictive model runs.

Table 15: Calibrated hydraulic conductivities of the Upper Vaal Groundwater Model.

Aquifer / Formation	Hydraulic conductivity	
	(m/s)	(m/d)
Alluvial aquifers	2E-05	1.7
Weathered Karoo – Molteno & Elliot	2.1E-06	0.18
Weathered Karoo – Tarkastad	2.2E-06	0.19
Weathered Karoo – Normandien	1.5E-06	0.13
Fractured Karoo – Molteno & Elliot	5E-08	0.004
Fractured Karoo – Tarkastad	9E-08	0.008
Fractured Karoo – Normandien	3.5E-08	0.003
Fractured Drakensberg F.	1E-08	0.001

3.9 PREDICTIVE SIMULATIONS

The solution of the calibrated steady-state groundwater model was subsequently used for the predictive model simulations. Based on the general scope of work, the conceptual and numerical models were used to:

1. Derive groundwater protection zones to limit potential quality impacts of groundwater pollution on receiving surface water courses
2. Derive groundwater protection zones to limit potential impacts of groundwater abstractions on receiving surface water courses
3. Estimate the potential impact of reduced discharges from the Lesotho Highland Water Scheme on groundwater gradients and baseflow towards the Liebenbergsvlei and Ash Rivers.

The objective of the first two model applications is the delineation of buffer zones along significant surface water courses, in which land use activities (with the risk of groundwater pollution) or groundwater abstractions should be limited to maintain the quality or quantity of the surface water

resources in the Upper Vaal. The theoretical background for the derivation of the quality and quantity protection zones is provided in the respective chapters below. While both methods use the hydraulic properties of the different aquifers as derived by the numerical model calibration, the delineation of the quality protection zones uses a reversed groundwater flow field (achieved by reversal of head gradients in the flow equation) to derive travel times towards surface water courses under consideration of advective-dispersive transport (i.e. transport according to the average pore water velocity and the variability thereof),

The delineation of the quantity protection zone is on the other hand based on dimensionless stream flow depletion factors, which were derived within the modeling package, but could as well be calculated using GIS software.

The objective of the third model application or scenario is on the other hand an assessment of the behavior of the groundwater system under a set of changing parameters, in this case changes in surface water discharges into the Ash River. The model scenario entails therefore changes to the boundary conditions, assigned in the numerical model to the upper reach of the Ash River. By changing the discharges into the river, the model scenarios simulate essentially the change to or from natural conditions, in other words how the system behaved pre-development of the Lesotho Highland Scheme (without any discharges) and how it is likely to behave if these conditions are re-established. Since the changes in discharge and thereby surface water elevation will mostly affect changes in bank and alluvial aquifer storage, the scenario investigates the influence of groundwater release from storage within the alluvial aquifers on groundwater baseflow and the "new" or pre-development groundwater gradients towards the Ash River and Liebenbergsvlei downstream of its confluence.

The theoretical background and results of the different model applications are described in detail below.

3.10 GROUNDWATER QUALITY PROTECTION ZONES

3.10.1 APPROACH

In many countries there is no policy that directly addresses the protection of groundwater used for drinking water. However, a wide variety of techniques can be used to determine protection zones for boreholes, varying from simple analytical methods to complex numerical transport models
(EPA, 1993). The size and shape of the borehole protection zone depends on the hydrogeological characteristics of the aquifer system, and the design and operational characteristics of the structure(s) used to pump water from the aquifer system.

Since the contaminant transport processes governing the derivation of these borehole protection zones is equivalent for groundwater baseflow to surface water courses (with surface water courses representing the point or rather lines of discharge), the same concept is applied here for the protection of the groundwater baseflow quality.

Numerical simulations of the surface-groundwater interaction offer in either case, i.e. boreholes or surface water courses, the best available analysis of the flow system and the best available

delineation of the zone of contribution for a given well or receiving surface water course. In this study, the Upper Vaal groundwater flow model was used to delineate commonly used protection zones to achieve the following levels of protection (Jolly and Reynders, 1993; Chave et al, 2005), see *Figure* ***51***.

- *A Wellhead Operational Zone immediately adjacent to the site of the borehole or wellfield to prevent rapid ingress of contaminants or damage to the borehole (also referred to as the 'Accident Prevention Zone')* → *Not applicable for groundwater baseflow to surface water courses as it represents the river course and banks itself.*

1. An Inner Protection Zone based on the time expected to be needed for a reduction in pathogen presence to an acceptable level (often referred to as the 'Microbial Protection Area').
2. An Outer Protection Zone based on the expected time required for dilution and effective attenuation of slowly degrading substances to an acceptable level. A further consideration in the delineation of this zone is sometimes also the time needed to identify and implement remedial intervention for persistent contaminants.

- *The Total Capture Area, covering essentially the total catchment area of a particular abstraction area where all water will eventually reach the abstraction point or surface water course. This is equivalent to the quaternary catchment area and would aimto avoid long term degradation of quality.*

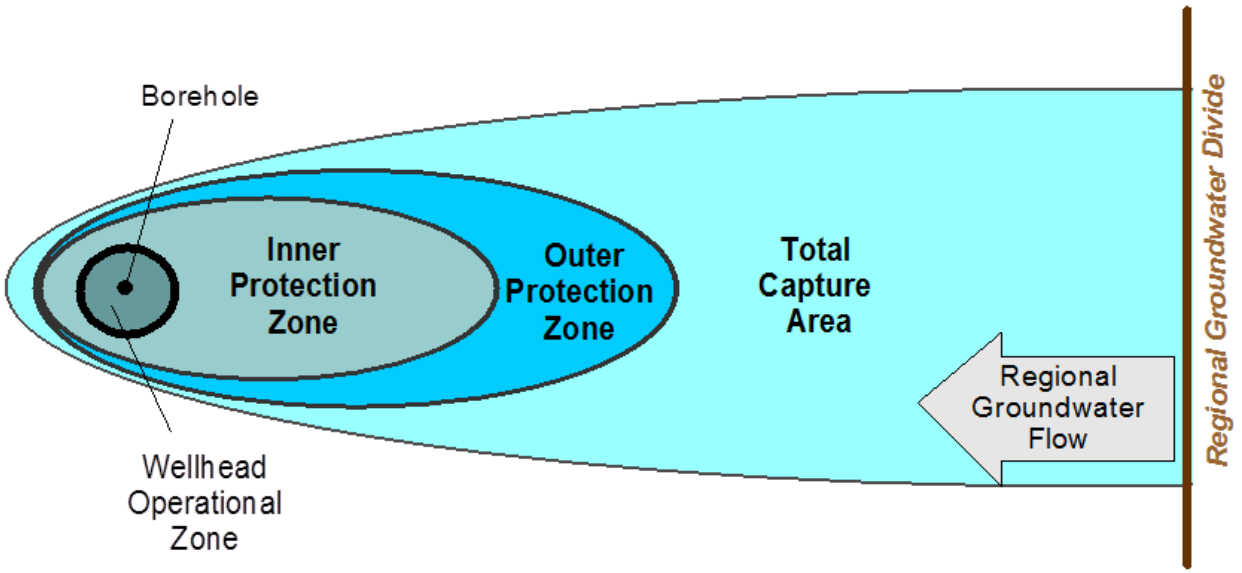

Figure 51: Common protection areas delineated around drinking water supplies (DWAF, 2008).

The developed Upper Vaal groundwater flow model was used to delineate the capture zone of all major surface water courses in the area of interest. The groundwater flow field was for this purpose "reversed", a unit source concentration assigned to the river courses and the advective-dispersive transport subsequently calculated to delineate the time-of-travel based capture zones of surface water courses. The following time-of-travel capture zones towards the river courses were used to rank the degree of risk based on the contaminant travel time to reach the surface water course:

1. Inner protection zone – 50 day travel time:

- Based on the information that enteric viruses survive in water.
- Includes the time required to ensure natural, appreciable reduction in microbiological organisms, which is 50 days (EPA, 1993).

2. Outer protection zone – 1 year time-of travel:
   - Based on expected time needed to implement remedial intervention for alluvial aquifers.

3.10.2 RESULTS

Based on the simulated time-of-travel for each river stretch, the protection zones (*Figure **51***) were captured by delineating the end points of the simulated flow/transport paths (travel lines), representing the surface origins of pollutants that would eventually reach the surface water courses. The travel lines considered the full depth of three dimensional flow system of water and associated pollutants, i.e. also the vertical transport time components in the unsaturated zone.

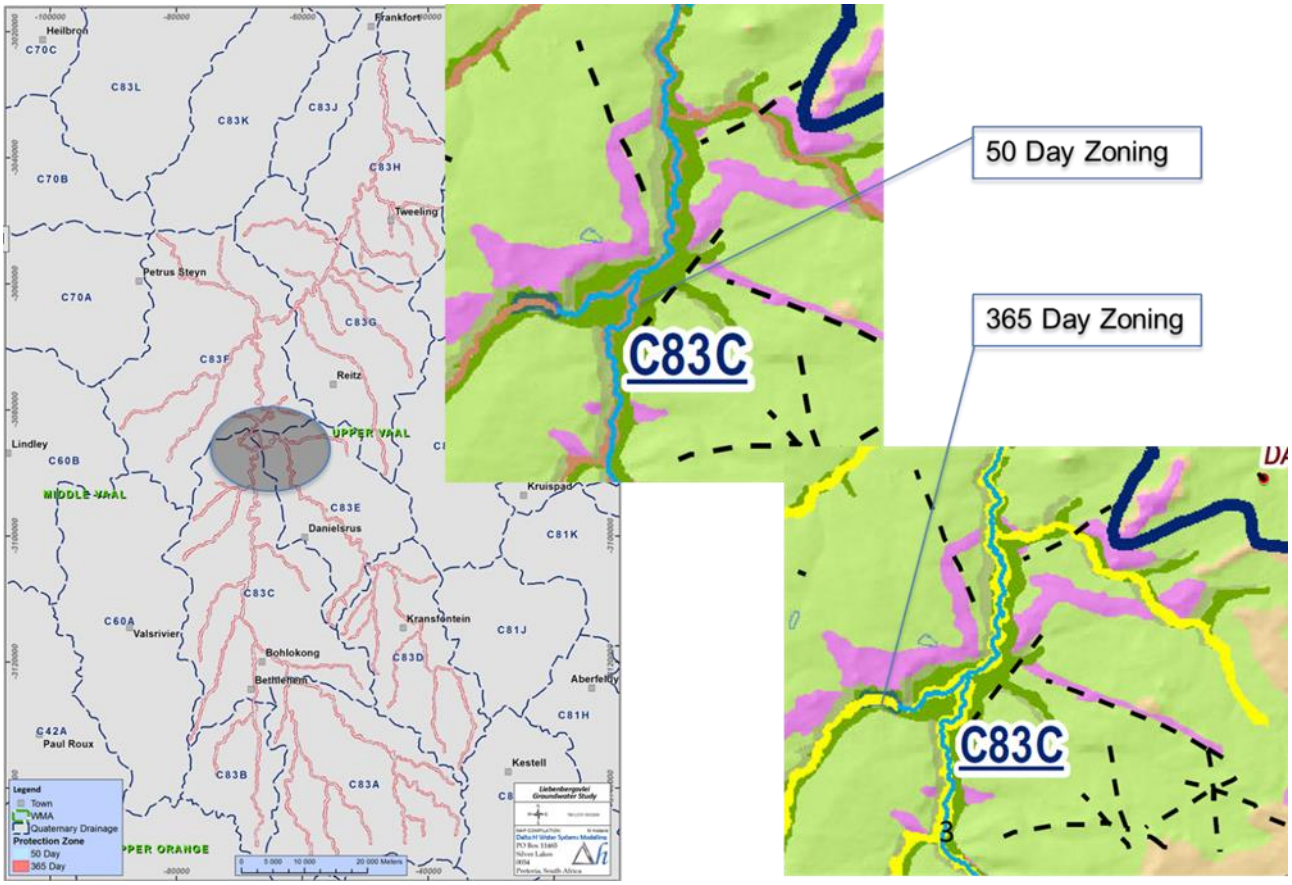

Figure 52: Water quality protection zones of major river courses within the Upper Vaal Groundwater Model domain.

While difficult to identify in *Figure **52*** due to scale, the protection zones comprise predominantly the alluvial aquifer along the river courses, and transgress only partially into the neighboring and underlying weathered and/or fractured aquifer.

To overcome the scale issues of the inherently regional nature of map outputs of the Upper Vaal project, the protection zones will be supplied as digital shape files to the client.

3.11 GROUNDWATER QUANTITY PROTECTION ZONES

3.11.1 APPROACH

The impacts of groundwater abstractions on surface water courses (*Figure **53***), termed streamflow depletion, can be grouped into the (1) Interception of ambient groundwater flow, which would have otherwise contributed to groundwater baseflow into the river and (2) Induced recharge due to a reversal of the hydraulic gradient towards a well. Depending on the topographic setting, the latter impact requires typically a well in closer proximity to the surface water course and often a substantial abstraction rate so that the drawdown in the borehole induces a gradient from the river towards the borehole.

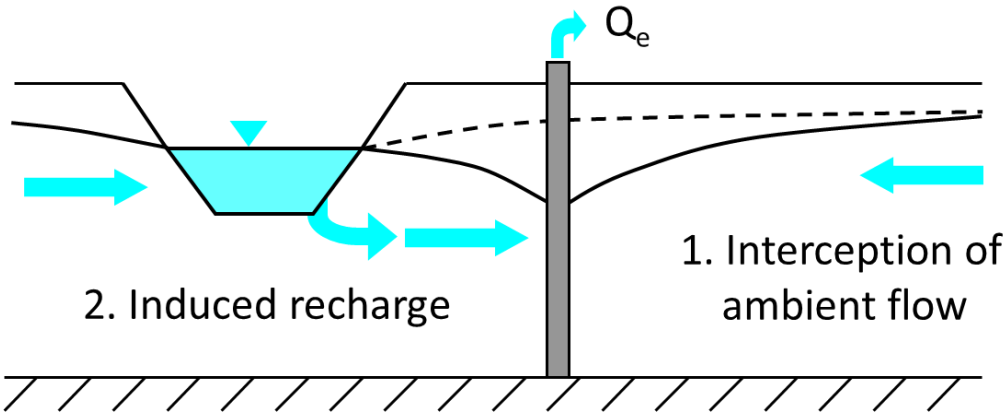

Figure 53: Impacts of groundwater abstractions on surface water courses.

The degree of streamflow depletion by groundwater abstractions depends generally upon the:

- aquifer diffusivity, i.e. the ratio of transmissivity and storativity of an aquifer, which determines the rate at which a cone of dewatering propagates(similar to waves on a lake if you throw a stone),
- pump rate and distance of the well field(s) to the river,
- clogging layers (e.g. clay) in the streambed, which limit the hydraulic interaction (act as flow boundary),
- bank storage, which provides a separate aquifer system along a river course and acts as a buffer to both, surface and groundwater,
- geometry of the streambed (flat/wide or deep/narrow, determines the contact area),
- properties of the vadose zone (hydraulic connectivity), and
- flow duration in the river (Ash and Liebenbergsvlei are in permanent in "flood condition" due to releases),

There are numerous analytical and numerical solutions with variable degrees of complexity available to assess the impact of single abstractions on streamflow (see DWAF 2006 for an

overview of methods).

While these methods are generally applied to individual (or aggregated) abstractions, the underlying conceptual understanding can also be applied to delineate water quantity protection zones along river courses, which aim to limit the potential impact of future abstractions on surface water courses.

It is obvious that individual pump rates or distances of boreholes towards a river cannot be considered in the derivation of quantity protection zones for several quaternary catchments, as the essentially unlimited ratio of pump rates and distances along the river stretches would preclude any reasonable computation effort. While their influence can therefore not be directly considered, the response time (i.e. the time period after which the impact starts to materialize) and relative rate (i.e. in relation to an abstraction rate) of streamflow depletion is largely determined by the hydraulic diffusivity of the underlying aquifer(s).

Assuming an infinitely long river penetrating the entire homogeneous, isotropic semi-infinite aquifer, a fully penetrating well pumping at a constant rate, no drawdown in the river or in the aquifer due to previous pumping (i.e. a constant transmissivity and no regional gradient) and an instantaneous release of water from storage, Glover & Balmer (1954) derived for example a simple solution for the relative streamflow depletion:

$$\frac{\Delta Q}{Q_{abs}} = erfc\left(\sqrt{\frac{Sd^2}{4Tt}}\right) \qquad \text{(Eq. 1)}$$

where ΔQ is the stream depletion rate or leakage, Q_{abs} the constant (from $t = 0$ to $t = \infty$, i.e. continuous) abstraction rate at the well, S the aquifer storage coefficient or specific yield, T the aquifer transmissivity, t the time and d the shortest distance between the well and the stream.

Using the analytical solution above, Jenkins (1968) proposed the widely applied concept of stream depletion factors (*sdf*):

$$sdf = \frac{d^2 S}{T} \qquad \text{(Eq. 2)}$$

The *sdf* has the unit of time and depends on the aquifer diffusivity (T/S) as well as the perpendicular distance between the well and the stream. The *sdf* describes essentially the aquifer

and thereby river response time to abstractions and Jenkins (1968) gave several dimensionless plots of volumes and rates of stream depletion versus *sdf* and time.

Following this concept, the conceptual understanding of the river setting (*Figure **54***) in combination with the hydraulic diffusivities of the respective aquifers along river stretches can therefore be used to derive protection zones, which limit groundwater abstractions where their impact would translate into an almost direct (i.e. within a short time frame) streamflow depletion at the same rate as the abstraction.

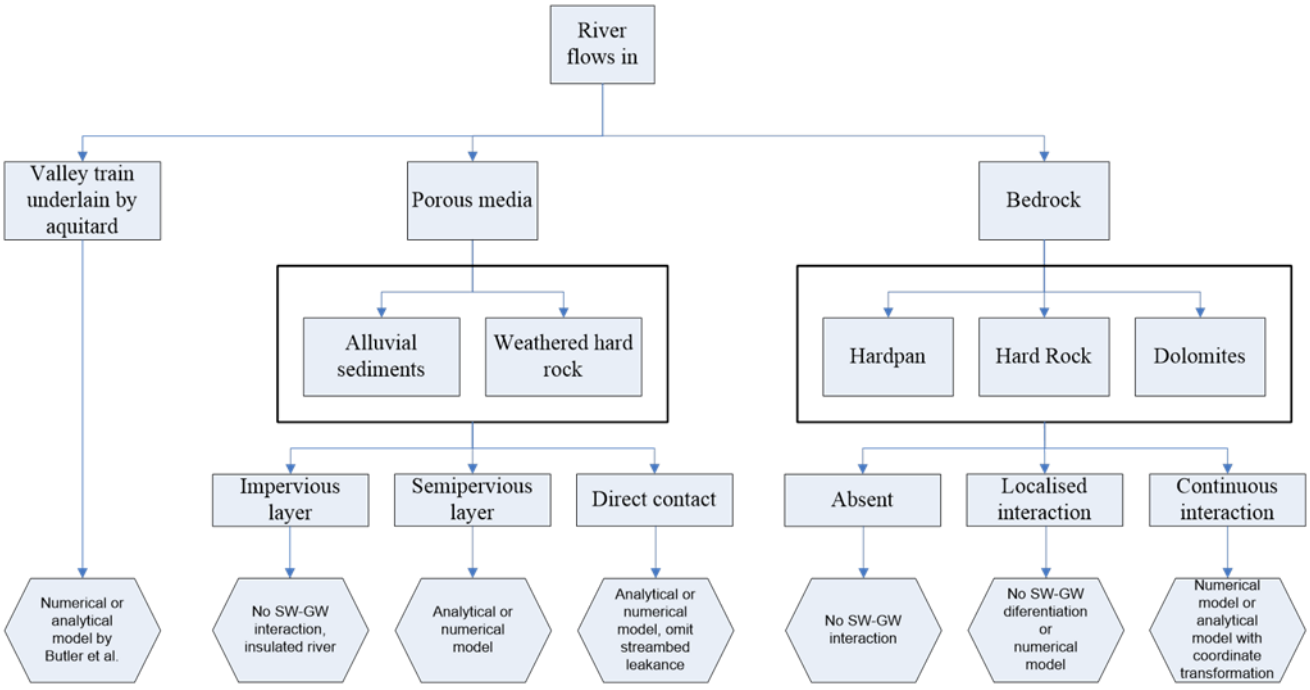

Figure 54: Aquifer classification for the quantification of surface - groundwater interaction (DWAF 2006).

3.11.2 RESULTS

Considering the aquifer classification in *Figure **54***, the Liebenbergsvlei and Ash River can predominantly be classified as

a. Rivers flowing in porous media (alluvial sediments or weathered hard rock), with direct contact, and
b. For a few sections as rivers flowing on bedrock with absent (dolerite sills) or localized (fractured sand stone and interface to dolerite) interaction

The dominant setting for the catchments of interest is direct contact between the rivers with the alluvial aquifers, which form so called "valley train" aquifers (Environmental Agency 2002) or a Bank Storage System of variable width and thickness. The alluvial aquifers along the Liebenbergsvlei and Ash River have by far the highest hydraulic diffusivity (in comparison to the underlying fractured and weathered Karoo aquifer), which determines the rate at which changes in head propagate within an aquifer. Abstractions from the alluvial aquifers are therefore likely to impact directly on stream flow.

Abstractions from the regional Karoo aquifer (of moderate diffusivity) are on the other hand likely to only impact delayed and in a subdued manner on stream flow, with additional buffering provided by water storage within the alluvial aquifers. While this is true for the general regional setting, there might be exemptions. For example, abstractions from a borehole targeting a dolerite dyke contact zone, which extends underneath the river course, might also impact directly on stream flow. However, the localized nature and scale of such interactions makes it impossible to identify as part of a regional assessment, as it would be similar to finding a needle in a haystack.

B*Figure 55*ased on the regional aquifer classification above, the stream depletion factors (*sdf*) for the Liebenbergsvlei and Ash River were calculated using the hydraulic conductivity values as calibrated in the numerical model (Table 15, resulting in effective transmissivities of 30 and 5.8 m^2/d for the alluvial and fractured aquifer, respectively), in other words regionally adopted hydraulic parameters. Since no experimentally determined storativity values of the alluvial and fractured aquifers were available in the area of interest, literature values of storativity for alluvial and Karoo aquifers (0.15 and 0.01) were used in the determination of the SDF. A raster map (grid size $10x10m^2$) of calculated SDF values was then generated for the fractured bedrock aquifer, before this was overlain by the SDF map for the areas covered by alluvium. The two SDF raster files were then combined before a contour map of SDF values with specified cut-off values (see legend *Figure 55* for bin sizes) was generated.

The groundwater quantity protection zones based on a SDF up to 325 days for the Upper Vaal groundwater model domain is shown in *Figure 55*, with an enlarged section (only contour lines of SDF) for better contextualisation. Groundwater abstractions within areas of low SDF values are likely to translate quickly into a surface water depletion of similar magnitude, whereas abstractions from areas with a high SDF are likely to only show a delayed and subdued impact on surface water.

As for the water quality protection zones, the regional scale of the map outputs of the Upper Vaal project precludes a meaningful visualization within the A4 report and the protection zones will therefore be supplied as digital shape files to the client.

The SDF zoning correlates expectedly with the developed conceptual model of an Alluvial (River Flood Plain) Aquifer System underlain by a moderate diffusivity fractured Karoo aquifer for the Liebenbergsvlei and Ash River in the Upper Vaal catchment. The largest impacts of groundwater abstractions on surface water may take place within the alluvial aquifer (low SDF), with diminishing impacts once abstractions move upslope onto the fractured aquifer beyond the flood plains. The zones of low SDF values along the river courses correlate therefore well with the delineated water quality protection zones (see *Figure 56* below).

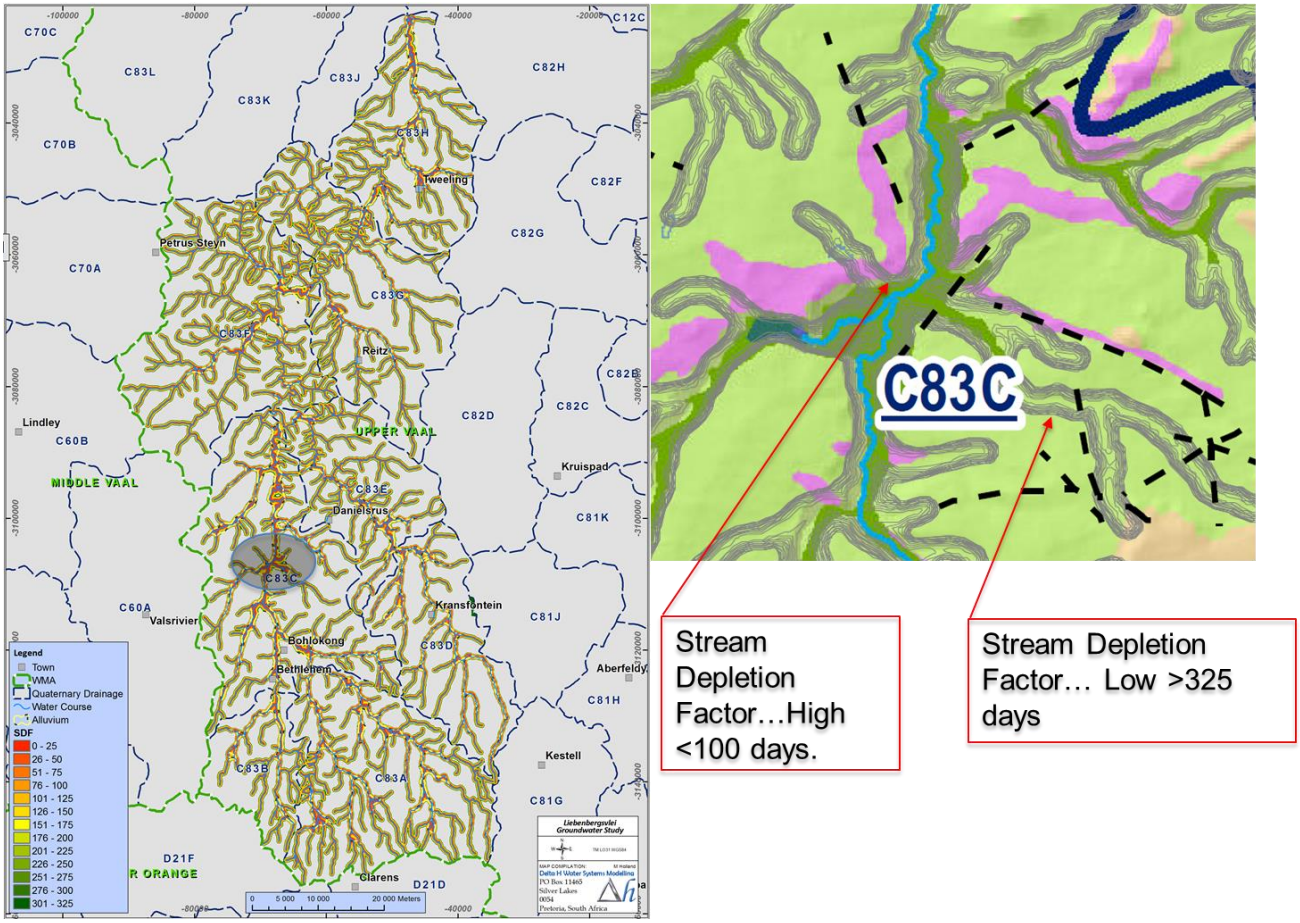

Figure 55: Water quantity (SDF) protection zones of major river courses within the Upper Vaal Groundwater Model domain.

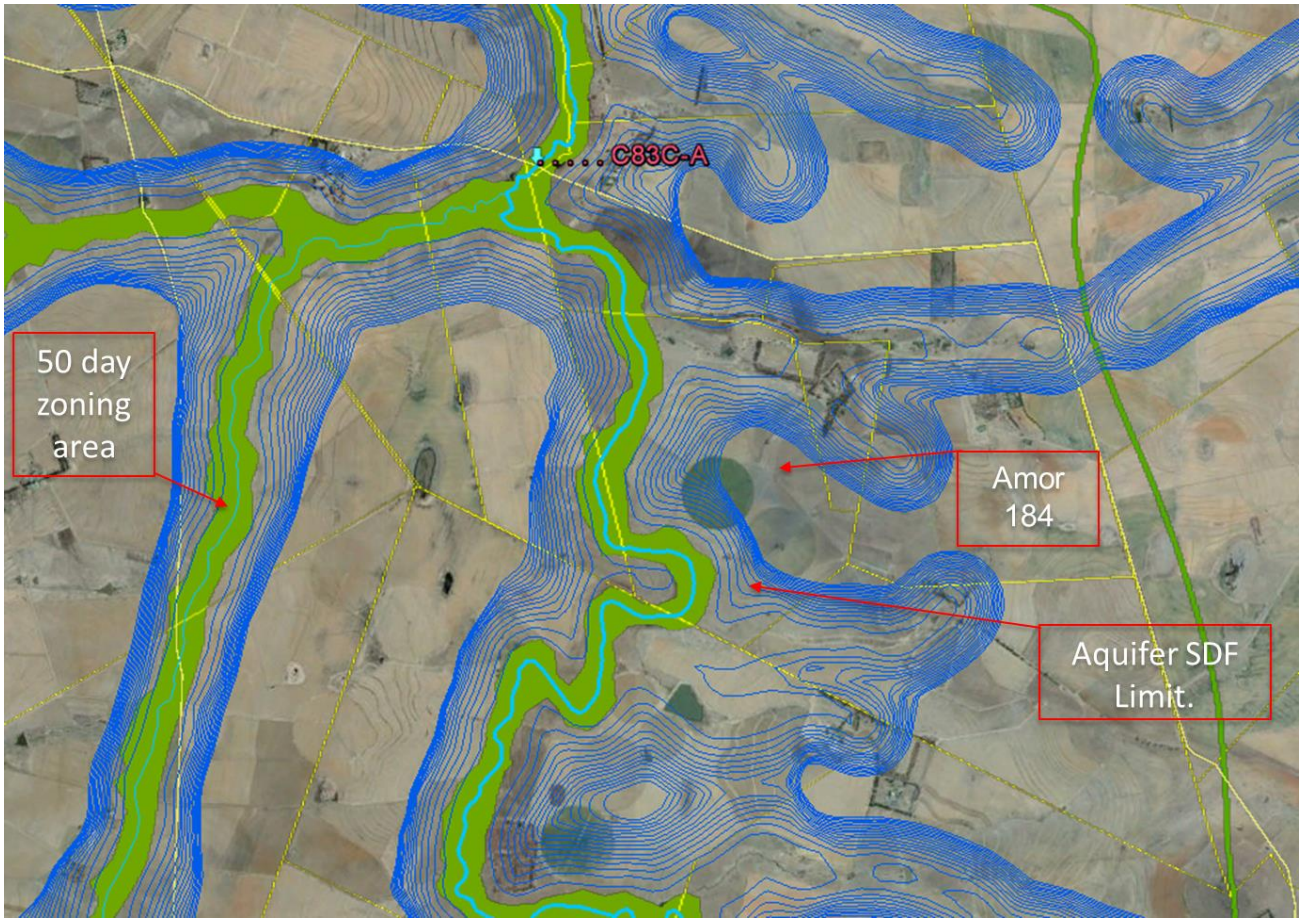

Figure 56: Example of water quality (green zone indicates 50 day protection zone) and quantity (blue SDF contour lines) protection zones within the Upper Vaal Groundwater Model domain.

It must be noted that the derived regional water resource protection zones (quality and quantity) are based on regionally adopted aquifer parameter and poor geological mapping (in the context of spatial coverage, not necessarily mapping quality itself) of the river flood plain alluvial deposits along the main stem system and its tributaries. The derived resource protection zones should therefore be seen as being regional in context and utilized for e.g. high level screening processes, but not as a local decision tool. The developed methodology is however applicable for both scale and the zones can be updated based on local parameters if significant groundwater abstractions or land use changes (with pollution potential) are proposed.

3.11.3 UPDATED RESULTS

As stated above, the derived water resource protection zones are burdened by a poor geological mapping of the river flood plain alluvial deposits along the main stem system. In order to overcome this limitation of the regional study, the project team combined the outcomes of the applied surface and groundwater model. This was achieved by updating the river flood plain alluvial deposits considered in the numerical groundwater flow and transport model based on the outcomes of the surface water (HECRAS) model.

The flood plains inundated by a 50-year rainfall event (to be confirmed) were for this purpose imported into the groundwater model and the mapped alluvial aquifer boundaries updated (including aquifer parameters) if the inundated areas exceeded these. The rationale behind the approach is that low laying and subsequently inundated areas along the river courses (as

identified by the rainfall-runoff model) are likely to represent the flood plain alluvial aquifer.

The water quality and quantity protection zones were subsequently re-calculated using the updated alluvial aquifer boundaries. While the differences are for obvious reasons not identifiable on the regional map due to scale, small scale differences in the extent of the protection zones are evident and confirm the necessity for accurate geological mapping of the alluvial aquifers.

4. SYNOPSIS: HYDROLOGICAL MONITORING PROGRAMME/NETWORK

The current hydrological monitoring network consists of the DWS gauging stations situated along the Main Stem System of the study area, i.e. the Ash and Liebenbergsvlei Rivers (see discussion in 2.2 above). The monitoring attributes varies from continuous logging, i.e. water level eLoggers installed at most of the gauging structures and bi-weekly interval water sampling/water quality analyses).

No surface water flow and/or water quality monitoring network is operational on the major tributaries, i.e. the Tierkloof River, the Langspruit (including its secondary tributaries) and the western Klipspruit drainage systems.

In terms of groundwater monitoring, no time series water level monitoring are currently operational, although groundwater level monitoring were done at the larger towns (i.e. Bethlehem, Reits and Tweeling) in the past to support the local municipal water supply schemes. These towns are currently linked to the surface water resources, thus the groundwater monitoring network programmes have been discontinued.

In terms of groundwater quality monitoring, one long-term operational water quality monitoring site exists in the area which is part of the DWS's National Groundwater Quality Monitoring Programme and is situated at Bethlehem.

To conclude having a monitoring network/programme available to support future requirements for this study area, it is required that a specific programme/network needs to be designed/implement.

This monitoring network will have to be close to one of the surface water gauging structures for reference with the surface water component. A proposed surface water – groundwater monitoring network, including one of the DWS surface water gauging stations are illustrated in ***Figure 57*** below.

Several borehole configurations are required boreholes for reporting the groundwater conditions in the following aquifer systems:

- The a shallow alluvial aquifer system in the river flood plain alluvial aquifer system (blue dotted sites);
- An deeper aquifer zone (viz. fractured systems) underlying the river flood plain alluvial aquifer system (brown dotted site next to main stem);
- An upper, shallow aquifer in the fractured and weathered Karoo aquifer system intercepting the direct rainfall recharged component (green dotted sites);
- A back ground deep water bearing formation control to evaluate the basement aquifer quality and quality and indications of the general groundwater flow pattern on the river valley side (up to 500 m from the main stem, brown dotted sites).

It is envisaged that the average distances between the borehole positions should not exceed 150-200 m.

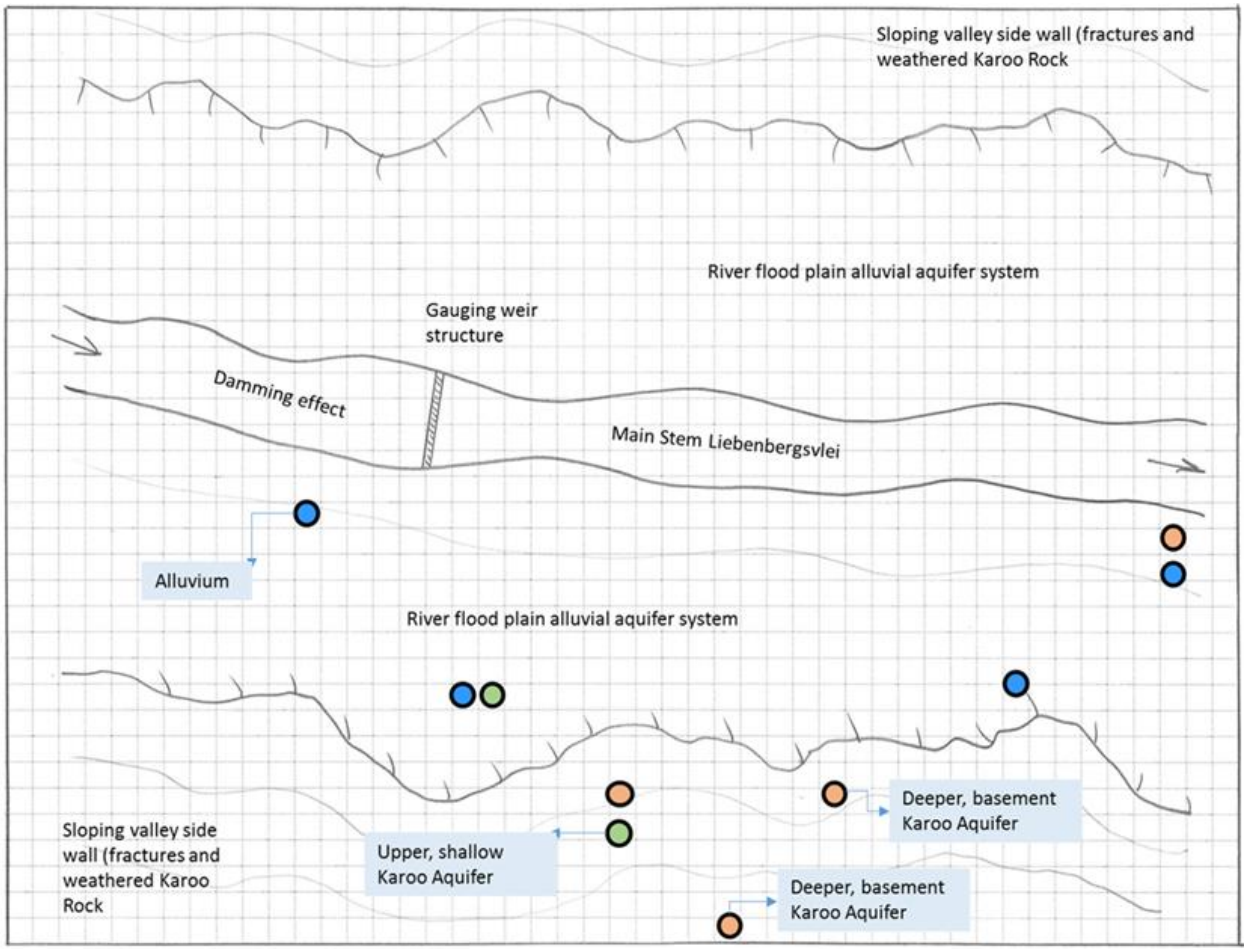

Figure 57: Schematic illustration of an integrated surface water – groundwater monitoring network for the Main Stem Liebenbergsvlei.

5. EXAMPLE OF A WATER RESOURCES PROTECTION ZONING APPLICATION

The results of the surface water – groundwater interaction study based on the quality and quality principle through the integration of the groundwater-numerical and the surface water modelling is based on a GIS coverage.

An illustration of the GIS presentation (through dotKMZ files for use on the Google Earth Pro GIS facility) where the user can see the different zonings as well as the local land owner/farm information for the industrial development on the Farm Violet 660 (see ***Figure 58*** below).

Interpretation of the illustration would be as follows:

- The green patched area maps the 50 day water quality protection zoning, indicating that microbial pollution within this zone could impact of the river water source as the bacteria could reach the river water within a 50 day period. The 50 day period is the international limit for bacteriological life cycle in the absence of the host; and

- The blue coloured contouring indicates Stream Depletion Factor based on the general hydraulic characteristics of the surrounding fractured and weathered hard rock to limit the effect of groundwater abstraction within these areas. It indicates that groundwater abstraction within the inner zone of the contoured area, could impact the alluvial aquifer within 25 days and abstraction within the outer zone of the contoured zone, more than one hydrological cycle (>365 days).

In terms of water quality protection for the surface water resource at this industrial site, there should be a concern for local pollution of the shallow aquifer system and ultimately impacting on the main stem surface water resource, and in terms of the stream depletion factor, abstraction from local shallow groundwater should be outside the 365 day zoned area – unless specific site investigation proof otherwise.

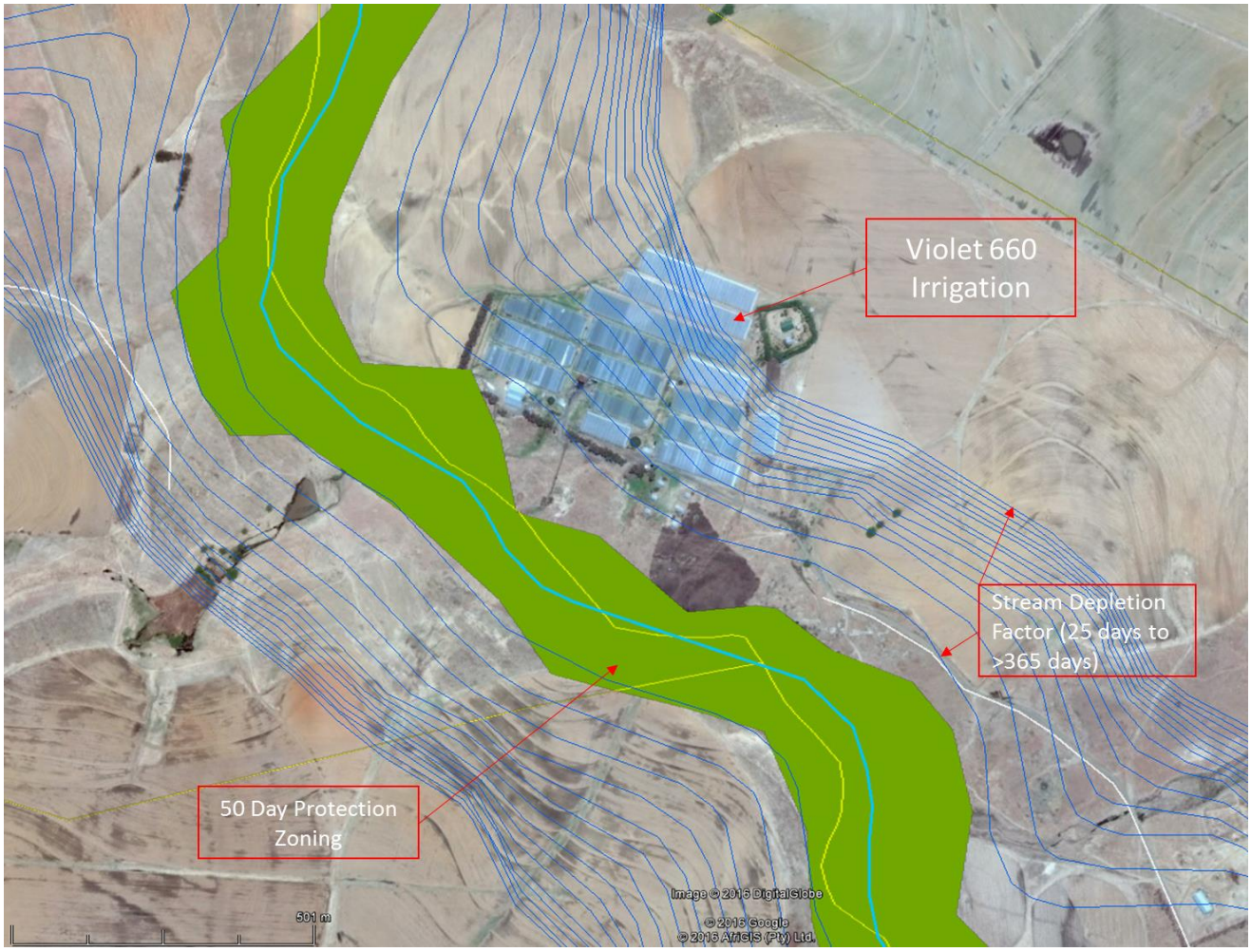

Figure 58: Illustrating the Water Resources Protection Zoning for water quality (green section) and stream depletion factors (contouring).

6. CONCLUSION

Conclusions relating to the surface water – groundwater interaction study are as follows:

- Historical hydrological datasets are available, however, due to calibration issues surface flow data from only 1999 to 2009 could be used for the surface water modelling phase;
- Discharge from the Sol Plaatje Dam seems to have been producing inaccurate data from

approximately October 2008, thus data for the last year's should be excluded;

- No surface water flow or water quality from the major tributary drainages is monitored – the 27 Bridges Monitoring Network provided data for the 2015-2016 hydrological season's "dry cycle", but it is only a "Life of Project" programme;
- Due to the current dry spell in southern Africa, no flow conditions prevails for the major tributaries – up to date, no "wet cycle" flows occurred and surface water quality could be collected. A monitoring run in April 2016, indicated only sporadic flows in some sections of the major tributaries and high-lights the fact if these tributaries could be non-perennial systems that only drive intermittent base flow releases following above-normal rainfall events in the upper head waters regions;
- The surface water quality assessment indicate that the water quality data from the DWS gauging stations suggest minimal changes along the main stem reach as well as insignificant seasonal changes, this data is not sensitive enough to be used to aid in the understanding of the system from a mass balance perspective, i.e. applying the mass balance analytical model. This aspect has been confirmed during the Diurnal and 27 Bridges Monitoring Network Runs;
- The analytical modelling methodology has therefore been omitted due to the high volume of fresh mountain water "flooding" the main stem channel and the large variation between on-site diurnal water quality ranges (observed as C83C-A) and the main stem channel water quality variation over the 220 km flow distance;.
- The numerical model has been developed and calibrated against water levels, base flow estimates and estimated recharge rates;
- Water resources protection zoning are based on the extend and occurrences the river flood plain alluvial aquifer system based on the local and internationally recommended hydraulic parameter applications (viz. a 50 and 356 day flow path and the stream depletion factor approach); and
- The river flood plain alluvial aquifer system has been identified as an interface between the main stem channel (surface water resource) and the surrounding hard rock (intergranular and fractured groundwater resource) and will represent the primary system (or unit) for the purpose of water resources protection and management.
- The actual hydrogeological characteristics of the river flood plain alluvial aquifer system is not specifically known and is merely based on a conceptual model as made up from a few meagrely boreholes placed along the 220 km stretch of the main stem. Although the width can be correctly visualised, the depth/thickness/medium is generalised based on the baseline geological knowledge of alluvial aquifers.

7. RECOMMENDATIONS

The following recommendations are proposed:

- Update/re-calibration of the surface water gauging weirs;
- The current hydrological monitoring programme, which addresses mainly the Main Stem Liebenbergsvlei system needs to be expanded to include the groundwater component. It is therefore recommended that an integrated monitoring network is designed and implemented consisting of a gauging station and a configuration of specially designated monitor boreholes

- In terms of monitoring equipment infrastructure, each of the groundwater monitoring boreholes should be specifically designed for either alluvium, shallow upper fractured & weathered aquifer and the "virtually unknown" deeper Karoo Aquifer System(s) (including the secondary Karoo/Dolerite Contact Aquifer Systems); and
- Groundwater level measurements in a specific group of boreholes close to the main stem and major tributaries should be measured at specific intervals over a prescribed period (say 5 years, using water level eLoggers). Boreholes identified during the November 2015 Hydrocensus Survey should be used; although the hydrological monitoring infrastructure proposed in section 4 should be implemented
- Increase the accuracy of the water resources protection zoning application (viz. Stream Depletion Factors in terms of the hydraulic characteristics of the local aquifer systems) based on the quantity zoning (i.e. how close to the main stem should one allow groundwater abstraction based on the actual hydraulic parameters of the local aquifer systems); and
- Apply a general "Controlled Activity" principle on the alluvial aquifers along the Ash-Liebenbergsvlei Main Stem as well as the major perennial tributaries
- In terms of the surface water monitoring infrastructure, some engineering design should be applied to capture the water "lost" through the hydro-electric power station at the dam site.
- The contributions (flows) from the main tributaries should be used for regional water quality status monitoring. This required a well-planned monitoring programme that not only includes sampling at specific sites on the main tributaries, but also include water quality sampling close to the downstream discharge areas of the Quaternary Catchments, i.e. by optimizing the 27-Bridges Monitoring Network/Programme.
- Mapping of alluvial deposits along the Main Stem System and Main Tributaries (width and thickness of alluvial aquifer) where land use changes or groundwater abstractions are expected. Such mapping could be done in cooperation with universities or technikons.
- Hydraulic testing of alluvial aquifer (pumping tests with separate observation borehole(s) to enable reliable estimation of specific yield/storativity values); and
- Recalculation of local protection zones based on local aquifer parameter if significant groundwater abstractions or land use changes are proposed.

8. REFERENCES USED IN THIS HYDROCENSUS REPORT

The following references were consulted:

1. Chave P., Howard G., Schijven J., Appleyard S., Fladerer F. and Schimon W. (2005): Groundwater protection zones. In Schmoll O., Howard G., Chilton J (eds) Protecting Groundwater for Health. World Health Organisation, IWA Publishing, London.
2. Duncan, R.A., Hooper, P.R., Rehacek, J., March, J.S., and Duncan, A.R., 1997. *The timing and duration of the Karoo igneous event, southern Gondwana.* In: Journal of Geophysical Research, Vol. 102, No. B8, 18,127-18,138, August 10, 1997.
3. [DWAF] Department of Water Affairs and Forestry (2008). Feasibility Study towards the Policy Development on Aquifer Protection Zoning. Directorate: Water Resources Information Programme, Pretoria.

4. [DWAF] Department of Water Affairs and Forestry (2006). Surface-groundwater interaction methodologies – literature study by K.T. Witthüser, K.T. Planning reference No. 14/14/2/3/8/1, SD:PS Ref. No. Study 18, Pretoria.
5. Glover, R.E. & Balmer, C.G. (1954). River depletion from pumping a well near a river. American Geophysical Union Transactions 35(3): 468 – 470.
6. Jenkins, C.T. (1968): Techniques for computing rate and volume of stream depletion by wells. Ground Water 6(2): 37 – 46.
7. Jolly J.L. and Reynders A.G. (1993). The protection of Aquifers: A proposed classification and protection zoning system for South African conditions. An international Groundwater convention entitled 'Africa Needs Groundwater' at the University of the Witwatersrand,
8. Johanson M.R., C.J. Van Vuuren, J.N.J. Visser, D.I Cole, H.de.V.Wickens, A.D.M. Christile, D.L. Roberts and G. Brandi (2006). Sedimentary Rocks of the Karoo Supergroup. In the Geology of South Africa (Johnson, M.R., C. R. Anhaeusser and R.J. Thomas, Edits). The Geological Society of South Africa and Council for Geosciences.
9. König, C. (2011). SPRING; Simulation of Processes in Groundwater. User Manual delta h Ingenieurgesellschaft mbH, Witten, Germany.
10. Moseki, M.C., 2013. Surface water – Groundwater interactions: Developments of methodologies suitable for South African conditions. Ph.D. Thesis, Faculty of Natural Sciences and Agriculture, Institute for Groundwater Studies, University of the Free State, Bloemfontein,
11. [US EPA] US Environmental Protection Agency, 1993: Guidelines for delineation of wellhead protection areas EPA 440/5-93-001.
12. Woodford, Ac. And Chevallier L. (2002). Hydrogeology of the Main Karoo Basin. Current Knowledge and Future research Needs. Water research Commission (WRC) report No. TT179/02
13. Voss, C.I. (1984). SUTRA: A finite-element simulation model for saturated-unsaturated fluid-density-dependent ground-water flow with energy transport or chemically-reactive single-species solute transport, U.S. Geol. Surv. Water Resour. Invest., 84-4369.
14. Chave P., Howard G., Schijven J., Appleyard S., Fladerer F. and Schimon W. (2005): Groundwater protection zones. In Schmoll O., Howard G., Chilton J (eds) Protecting Groundwater for Health. World Health Organisation, IWA Publishing, London.
15. [DWAF] Department of Water Affairs and Forestry (2008). Feasibility Study towards the Policy Development on Aquifer Protection Zoning. Directorate: Water Resources Information Programme, Pretoria.
16. [DWAF] Department of Water Affairs and Forestry (2006). Surface-groundwater interaction methodologies – literature study by K.T. Witthüser, K.T. Planning reference No. 14/14/2/3/8/1, SD:PS Ref. No. Study 18, Pretoria.
17. Environment Agency (2002). Impact of groundwater abstractions on river flows: Phase 2 – "A numerical modelling approach to the estimation of impact" (IGARF II). Report prepared by Parkin, G., Birkinshaw, S., Rao, Z. Murray, M. & Younger, P.L., R&D Project Record W6-046/PR, Environment Agency, Bristol.
18. Glover, R.E. & Balmer, C.G. (1954). River depletion from pumping a well near a river. American Geophysical Union Transactions 35(3): 468 – 470.
19. Jenkins, C.T. (1968): Techniques for computing rate and volume of stream depletion by wells. Ground Water 6(2): 37 – 46.

20. Jolly J.L. and Reynders A.G. (1993). The protection of Aquifers: A proposed classification and protection zoning system for South African conditions. An international Groundwater convention entitled 'Africa Needs Groundwater' at the University of the Witwatersrand, Johannesburg, South Africa, 6-8, September 1993.
21. König, C. (2011). SPRING; Simulation of Processes in Groundwater. User Manual delta h Ingenieurgesellschaft mbH, Witten, Germany.
22. [US EPA] US Environmental Protection Agency, 1993: Guidelines for delineation of wellhead protection areas EPA 440/5-93-001.
23. Voss, C.I. (1984). SUTRA: A finite-element simulation model for saturated-unsaturated fluid-density-dependent ground-water flow with energy transport or chemically-reactive single-species solute transport, U.S. Geol. Surv. Water Resour. Invest., 84-4369.